



# Techno-Economic Analysis and Market Potential of Geological Thermal Energy Storage (GeoTES) Charged With Solar Thermal and Heat Pumps

Dayo Akindipe,<sup>1</sup> Joshua McTigue,<sup>1</sup> Patrick Dobson,<sup>2</sup>  
Trevor Atkinson,<sup>3</sup> Erik Witter,<sup>1</sup> Ram Kumar,<sup>2,3</sup>  
Eric Sonnenthal,<sup>2</sup> Mike Umbro,<sup>4</sup> Jim Lederhos,<sup>4</sup>  
Derek Adams,<sup>5</sup> and Guangdong Zhu<sup>1</sup>

*1 National Renewable Energy Laboratory  
2 Lawrence Berkeley National Laboratory  
3 Idaho National Laboratory  
4 Premier Resource Management  
5 EarthBridge Energy*

**NREL is a national laboratory of the U.S. Department of Energy  
Office of Energy Efficiency & Renewable Energy  
Operated by the Alliance for Sustainable Energy, LLC**

This report is available at no cost from the National Renewable Energy Laboratory (NREL) at [www.nrel.gov/publications](http://www.nrel.gov/publications).

Contract No. DE-AC36-08GO28308

**Technical Report**  
NREL/TP-5700-91225  
October 2024



# Techno-Economic Analysis and Market Potential of Geological Thermal Energy Storage (GeoTES) Charged With Solar Thermal and Heat Pumps

Dayo Akindipe,<sup>1</sup> Joshua McTigue,<sup>1</sup> Patrick Dobson,<sup>2</sup>  
Trevor Atkinson,<sup>3</sup> Erik Witter,<sup>1</sup> Ram Kumar,<sup>2,3</sup>  
Eric Sonnenthal,<sup>2</sup> Mike Umbro,<sup>4</sup> Jim Lederhos,<sup>4</sup>  
Derek Adams,<sup>5</sup> and Guangdong Zhu<sup>1</sup>

*1 National Renewable Energy Laboratory*

*2 Lawrence Berkeley National Laboratory*

*3 Idaho National Laboratory*

*4 Premier Resource Management*

*5 EarthBridge Energy*

## **Suggested Citation**

Akindipe, Dayo, Joshua McTigue, Patrick Dobson, Trevor Atkinson, Erik Witter, Ram Kumar, Eric Sonnenthal, Mike Umbro, Jim Lederhos, Derek Adams, and Guangdong Zhu. 2024. *Techno-Economic Analysis and Market Potential of Geological Thermal Energy Storage (GeoTES) Charged With Solar Thermal and Heat Pumps*. Golden, CO: National Renewable Energy Laboratory. NREL/TP-5700-91225. <https://www.nrel.gov/docs/fy25osti/91225.pdf>.

**NREL is a national laboratory of the U.S. Department of Energy  
Office of Energy Efficiency & Renewable Energy  
Operated by the Alliance for Sustainable Energy, LLC**

This report is available at no cost from the National Renewable Energy Laboratory (NREL) at [www.nrel.gov/publications](http://www.nrel.gov/publications).

Contract No. DE-AC36-08GO28308

**Technical Report**  
NREL/TP-5700-91225  
October 2024

National Renewable Energy Laboratory  
15013 Denver West Parkway  
Golden, CO 80401  
303-275-3000 • [www.nrel.gov](http://www.nrel.gov)

## NOTICE

This work was authored in part by the National Renewable Energy Laboratory, operated by Alliance for Sustainable Energy, LLC, for the U.S. Department of Energy (DOE) under Contract No. DE-AC36-08GO28308. Funding provided by U.S. Department of Energy Office of Energy Efficiency and Renewable Energy Geothermal Technologies Office. The views expressed herein do not necessarily represent the views of the DOE or the U.S. Government.

This report is available at no cost from the National Renewable Energy Laboratory (NREL) at [www.nrel.gov/publications](http://www.nrel.gov/publications).

U.S. Department of Energy (DOE) reports produced after 1991 and a growing number of pre-1991 documents are available free via [www.OSTI.gov](http://www.OSTI.gov).

*Cover Photos by Dennis Schroeder: (clockwise, left to right) NREL 51934, NREL 45897, NREL 42160, NREL 45891, NREL 48097, NREL 46526.*

NREL prints on paper that contains recycled content.

## Acknowledgments

This report is based upon work supported by the U.S. Department of Energy, Office of Energy Efficiency and Renewable Energy (EERE), Geothermal Technologies Office, under Contract No. DE-AC36-08GO28308 with the National Renewable Energy Laboratory, Contract Number DE-AC07-05ID14517 with Idaho National Laboratory, and Contract Number DE-AC02-05CH11231 with Lawrence Berkeley National Laboratory. The views expressed herein do not necessarily represent the views of the DOE or the U.S. Government.

The authors acknowledge the technical contributions, reviews, and strategic guidance of Jeff Winick, Kevin Kitz, and Andy Adams of the U.S. Department of Energy Geothermal Technologies Office (GTO). We also appreciate participants who attended and contributed to discussions at our project workshops and consultations afterwards that have helped shaped our project work and this report, including Sean Porse, Jeffrey Bowman, Jerry Carr, Timothy Steeves (DOE-GTO), Gustavo Perez (EarthBridge Energy), Amanda Kolker, Whitney Trainor-Guitton, Zhiwen Ma, Juliet Simpson, Hyunjun Oh, Jonathan Ho, Tara Wertz (NREL), Daniel Wendt (INL), Justin Birdwell, Jeffrey Pepin (USGS), Yingqi Zhang (LBNL), Greg Rhodes (Fervo), Simon Webbison (Ormat), Kristie McLin (ConocoPhillips), Clare Falcon (Louisiana Geological Survey), Emilie Gentry (Teverra), and Eric Peterson (Honua Resources).

## List of Acronyms

ATES	aquifer thermal energy storage
BOE	barrel of oil equivalents
BOEPD	barrel of oil equivalents per day
BOPD	barrel of oil per day
BRACS	Brackish Resources Aquifer Characterization System
BWPD	barrel of water per day
CalGEM	California Geologic Energy Management Division
CAPEX	capital expenditures
CB	Carnot battery
CB-GeoTES	Carnot battery coupled with geological thermal energy storage
COP	coefficient of performance
CSP	concentrating solar power
CST	concentrating solar thermal
CST-GeoTES	concentrating solar thermal coupled with geological thermal energy storage
DOE	U.S. Department of Energy
GTO	U.S. Department of Energy Geothermal Technologies Office
FCR	fixed charge rate
GeoTES	geological thermal energy storage
GETEM	Geothermal Electricity Technology Evaluation Model
GIS	geographic information system
HT-ATES	high-temperature aquifer thermal energy storage
INL	Idaho National Laboratory
ITC	investment tax credit
LBNL	Lawrence Berkeley National Laboratory
LCOE	levelized cost of energy
LCOH	levelized cost of heat
LCOS	levelized cost of storage
LDES	long-duration energy storage
NPV	net present value
NREL	National Renewable Energy Laboratory
MMBO	million barrels of oil
MMBOE	million barrels of oil equivalents
MS-TES	molten-salt thermal energy storage
NATCARB	National Carbon Sequestration Database
OPEX	operational expenses
O&M	operation and maintenance
POR	Point of Rocks
PRM	Premier Resource Management
RSAT	Resource Size Assessment Tool
SAM	System Advisor Model
TDS	total dissolved solids
TEA	techno-economic analysis
TES	thermal energy storage
USGS	United States Geological Survey
VRE	variable renewable energy

## Executive Summary

Geological thermal energy storage (GeoTES) is a technology that can potentially enable vast amounts of storage of thermal energy within multiple sedimentary formations across the United States. GeoTES provides long-duration storage of solar thermal energy and excess renewable electricity at hourly and seasonal scales. GeoTES can be paired with a concentrating solar thermal (CST) system as a primary storage unit or as a secondary storage unit that is paired with a surface-based thermal storage tank. It can also be paired with a Carnot battery (CB) system to enable storage of excess, curtailed, or behind-the meter renewable electricity as thermal energy.

In this project, we developed a techno-economic analysis (TEA) model that can be used to evaluate the viability of a proposed GeoTES design. This MATLAB-based model integrates distinct subsystem models for the reservoir, wells, power cycle, and solar field to capture their distinct characteristics. It applies this approach in simulating GeoTES storage and dispatch operations for durations ranging from hourly to seasonal. Using cases studies based on GeoTES designs provided by industry partners—Premier Resource Management (PRM) and EarthBridge Energy—we validated the TEA model estimations of system performance and costs (such as thermal and electrical power/energy inflow and outflow, capital costs, and levelized costs of energy and storage) for both CST and CB pairings with GeoTES (CST-GeoTES and CB-GeoTES).

For the CST-GeoTES case, the model was validated against the proposed system designed by PRM. It showed good agreement with PRM's estimations when well and pump costs derived from PRM's estimations were used. When costs based on the Geothermal Electricity Technology Evaluation Model (GETEM) were used, the capital cost and operations cost both increased, leading to a 60% increase in estimated levelized cost of energy (LCOE) due to GETEM's project/site-agnostic assumption of these costs. From a sensitivity analysis perspective, the LCOE of the CST-GeoTES case was most sensitive to well flow rate and the charging temperature. An optimal design scenario resulted in an LCOE of 0.11 \$/kWh<sub>e</sub> for a system that reliably delivers power for 8 hours per day, year-round. Input to achieve this value requires the application of a 40% Investment Tax Credit, optimistic cost assumption for the CST field of 125 \$/m<sup>2</sup>, and good well flow rates of 80 L/s to minimize the number of wells. In this scenario, the solar field accounts for 40% of the LCOE, the power cycle for 28%, the geothermal wells for 11% and O&M for 21%. CST-GeoTES can also provide a source of heat to meet seasonal demands. With 12-hour and 24-hour levelized cost of heat (LCOH) of 0.018 \$/kWh<sub>th</sub> and 0.022 \$/kWh<sub>th</sub>, respectively, CST-GeoTES could be competitive in the California market with an average industrial price of natural gas in California of 0.041–0.047 \$/kWh<sub>th</sub>. The levelized cost of storage (LCOS) for CST-GeoTES depends on the energy storage duration. Although the LCOS is relatively higher for shorter durations (e.g., ~0.50 \$/kWh<sub>e</sub> for 1 hour of storage), it is an order of magnitude lower (0.06 \$/kWh<sub>e</sub>) for longer storage durations and competitive with lithium-ion batteries (beyond 12 hours of storage) and molten-salt thermal energy storage (beyond 32 hours).

The CB-GeoTES model was validated against the proposed design developed by EarthBridge Energy. Three options were explored and applied to the EarthBridge case study: (1) a CB design using R125 working fluid with both hot and cold storage; (2) a CB design using R125 working fluid with only hot storage; and (3) a CB using a commercially available heat pump with carbon

dioxide (CO<sub>2</sub>) working fluid and hot storage only. The CB-GeoTES with cold storage only had a slight (round-trip) efficiency advantage over the system without (43.4% vs. 42.8%). This is because the cold storage is limited by the freezing point of water, so the cold storage is not much colder than the environment. The system using commercially available technologies was the least efficient—partly because different cycles were used in the heat pump (CO<sub>2</sub>) and heat engine (binary cycle) which leads to some inefficiencies. Using the commercially available design, the levelized cost of energy LCOS from the model (0.10 \$/kWh<sub>e</sub>) was higher than that estimated by EarthBridge (0.068 \$/kWh<sub>e</sub>). This is because of the low round-trip (38.7%) efficiency of the commercially available design. Sensitivity analysis reveals that the model is most sensitive to electricity price. Including electricity price in the TEA for CB-GeoTES leads to an increase in LCOS from the base value to 0.25 \$/kWh<sub>e</sub>.

To determine storage sites suitable for GeoTES, we gathered and analyzed geological, petrophysical, and geophysical data of oil and gas reservoirs and aquifers in California and Texas. We down-selected possible sites based on cut-off values for site characteristics (e.g., reservoir temperature, formation thickness, permeability, porosity, depth, and brine salinity) and preliminary costs. Using this approach, the Carrizo-Wilcox, Yegua-Jackson, and Dockum brackish aquifers in Texas were identified as having the highest suitability. Similarly, in the central California region, the White Wolf, Belridge South Tulare, and Belridge South Reef Ridge were the most suitable. Going further, we assessed the storage potential in the selected sites. To do this we developed distributions of reservoir characteristic data and applied a Monte Carlo-based analysis to account for intrinsic uncertainty in the acquired data. The analysis revealed that the Carrizo-Wilcox aquifer had the highest storage potential with a mean capacity of 554 TWh<sub>th</sub> (i.e., 63 TWh<sub>e</sub>). The estimated capacity serves as an upper limit of storage potential given that not all fields in the basin will be developed.

We participated in multiple outreach activities including conference presentations, panel session discussions, and the facilitation of a GeoTES workshop (at the National Renewable Energy Laboratory's South Table Mountain campus). These forums served as platforms to engage with stakeholders and to gauge industry knowledge and perspectives on the technical, commercial, and social/environmental justice aspects of developing GeoTES. These forums also served as an avenue for the team to share our ongoing work. We received constructive questions and suggestions from geothermal and oil and gas industry experts. As applicable, we have incorporated some of the feedback into our modeling work and appropriated others in our determination of potential areas for future research.



# Table of Contents

<b>Executive Summary</b> .....	<b>v</b>
<b>1 Project Overview</b> .....	<b>1</b>
1.1 Introduction .....	1
1.2 Project Objectives .....	2
<b>2 The GeoTES Techno-Economic Analysis Model</b> .....	<b>4</b>
2.1 CST-GeoTES Design Configuration.....	4
2.2 Carnot Battery-GeoTES Design Configuration.....	5
2.3 Model Definition .....	8
2.4 Model Implementation .....	9
<b>3 GeoTES Potential Estimation</b> .....	<b>11</b>
3.1 Candidate GeoTES Reservoir Selection.....	11
3.1.1 Depleted Oil and Gas Reservoirs .....	11
3.1.2 Shallow Aquifers.....	15
3.2 GeoTES Storage Potential Estimation Analysis.....	16
3.2.1 Methodology .....	17
3.2.2 Assumptions.....	18
3.2.3 Data Sources.....	20
3.2.4 Results .....	21
3.2.5 Future Work .....	23
<b>4 Premier Resource Management CST-GeoTES Demonstration</b> .....	<b>25</b>
4.1 Project Overview.....	25
4.2 Subsurface Reservoir.....	26
4.3 Surface Plant .....	29
4.4 System Operation .....	30
4.5 PRM Pilot Demonstration Techno-Economic Analysis.....	30
4.6 PRM Demo TEA Case Study Validation.....	31
4.6.1 TEA Validation .....	31
4.6.2 Improving CST-GeoTES Performance and Cost Using Insights From the TEA Model	34
4.6.3 CST-GeoTES LCOS as a Function of Storage Duration .....	41
4.7 Non-Technical Hurdles to PRM’s GeoTES Demonstration .....	43
<b>5 EarthBridge Energy CB-GeoTES Demonstration</b> .....	<b>44</b>
5.1 Project Overview.....	44
5.2 Subsurface Reservoir.....	45
5.3 Surface Plant .....	47
5.4 System Operation .....	48
5.5 EarthBridge Pilot Demonstration Techno-Economic Assessment.....	49
5.6 EarthBridge Demo Techno-Economic Analysis Case Study Validation .....	49
5.6.1 TEA Validation .....	49
5.6.2 Improving CB-GeoTES Performance and Cost Using Insights From the TEA Model	52
5.6.3 CB-GeoTES LCOS as a Function of Discharge Duration .....	55
<b>6 Project Outcomes and Plan for Future Work</b> .....	<b>57</b>
6.1 Project Outcomes .....	57
6.2 Suggestions for Future Work .....	58
<b>References</b> .....	<b>61</b>



# List of Figures

Figure 1. Electricity generation from variable renewable sources in California over several years..... 1

Figure 2. Illustration of the CST-GeoTES system design..... 4

Figure 3. Energy flows between components in a CST-GeoTES system within a (a) standalone vs. (b) combined cycle plant design ..... 5

Figure 4. High-efficiency design configuration of the CB-GeoTES during (a) charging and (b) discharging operations. The design assumes sufficient reservoir volume to accommodate both cold and hot storage. The well geometry shown in the figure is vertical. However, actual systems may utilize wells with laterals for better heat sweep in thin beds..... 6

Figure 5. Schematic of a CB with geological thermal storage during charge (top) and discharge (bottom) 7

Figure 6. Flow chart of the CST-GeoTES techno-economic assessment model showing interdependencies between surface and subsurface system models and integration of these model outputs in MATLAB..... 9

Figure 7. California oil and gas fields (left) and Texas oil and gas districts (right) ..... 12

Figure 8. Pressure vs. depth for all reservoirs in central California. Hydrostatic pressure vs. depth is plotted as a solid line. Temperature vs. depth is plotted in an orange color, and solid lines represent temperature at 50°C and 80°C..... 13

Figure 9. Permeability and porosity for all oil pools in central California. Dashed line at x=10 represents porosity cut-off, and y=100 represents permeability cut-off at 100 millidarcy. .... 13

Figure 10. Salinity (ppm) and average thickness (m) for all oil pools in central California. Blue solid line represents 30,000 ppm salinity and orange solid line represents 50 m thickness. .... 14

Figure 11. A flow chart for site characterization approach for GeoTES applications ..... 14

Figure 12. Preliminary evaluation of BRACS (Brackish Resources Aquifer Characterization System) aquifers in Texas (top) and California (bottom) in terms of their cost per capacity and steady-state self-discharge rate. Note that we use the self-discharge rates at year 10 as an approximation of steady-state self-discharge rates by assuming the aquifers are in thermal equilibrium with ambient temperatures. .... 16

Figure 13. (Top) Thermal storage capacity results with inputs reflecting all fields. .... 22

Figure 14. (Top) Thermal storage capacity results with inputs reflecting only depleted fields..... 23

Figure 15. (Top) Contiguous U.S. saline reservoirs from NATCARB database (Bauer et al., 2018). ..... 24

Figure 16. PRM’s proposed CSP-GeoTES design..... 25

Figure 17. The geological section of the Kreyenhagen Formation showing the structural features and lithologies within PRM’s lease area. The POR sandstone is up to 3,000 ft thick and has a shale-type top (Kreyenhagen shale and Tulare clay) and bottom (Canoas shale) confining layers. .... 27

Figure 18. Example of seven-spot well arrangement with producers shown in green and injectors shown in red ..... 29

Figure 19. Thermal energy flows for the 15-MW demonstration PRM CSP-GeoTES system ..... 33

Figure 20. Quantity of energy stored in the GeoTES throughout the year for the Demonstration 15-MW system ..... 33

Figure 21. Thermal energy flows for the 199-MW demonstration PRM CSP-GeoTES system ..... 34

Figure 22. Tornado chart illustrating sensitivity of CSP-GeoTES LCOE to design parameters ..... 36

Figure 23. Bar chart showing path to reduced LCOE for CSP-GeoTES ..... 36

Figure 24. CSP-GeoTES energy capacity for the 199-MW nominal case with 6 hours dispatch per day. The red area indicates the net increase in energy capacity over the course of 1 year. .... 37

Figure 25. Thermal energy flows in August with solar curtailment illustrated in red areas. Left: Solar multiple = 1.25. Right: Solar multiple = 2.5. .... 38

Figure 26. Thermal energy flows in August for a solar multiple of 2.5 for a system with additional charging wells to reduce curtailment ..... 39

Figure 27. Thermal energy flows for a combined CST-GeoTES system with high-temperature storage and power cycle .....	40
Figure 28. LCOS of CSP-GeoTES, Li-ion and molten-salt thermal energy storage as a function of storage duration. Shaded areas indicate the effect of efficiency on the LCOS.....	43
Figure 29. EarthBridge Energy’s CB-GeoTES concept. Showing a subsurface system with three wells connected to surface system that mainly consists of a heat pump and heat engine .....	45
Figure 30. Line diagram of the surface unit showing the components in the heat pump (left) and the heat engine (right). The heat pump consists of a compressor, turbo expander, and two heat exchangers. The heat engine comprises a turbo pump, turbine-generator, and heat exchangers. The black flow line represents working fluid flow in the closed loop. The blue, brown, and red lines represent chilled, cooled, and heated water, respectively.....	48
Figure 31. Temperature-entropy diagram of a recuperated heat pump using R125 working fluid. The heat pump heats one set of production fluids up to 162°C and another set of fluids are cooled to 5°C. The hot and cold fluid streams are then reinjected to separate regions of the GeoTES to create hot and cold storage.....	50
Figure 32. Bar chart showing three Carnot Battery designs applied to the EarthBridge 10-MW case study. Results are evaluated using fixed costs suggested by EarthBridge (marked “EB”) and also by using GETEM. ....	52
Figure 33. Tornado chart illustrating sensitivity of CB-GeoTES LCOS to design parameters .....	53
Figure 34. Tornado chart illustrating sensitivity of CB-GeoTES LCOH to design parameters .....	55
Figure 35. LCOS as a function of storage duration and efficiency for CB-GeoTES, Li-ion batteries, and MS-TES .....	56

## List of Tables

Table 1. Criteria for Shortlisting Oil and Gas Reservoirs in California and Texas for Hot Geothermal Energy Storage.....	12
Table 2. Summary of Data Sources Used for GeoTES Storage Capacity Analysis.....	20
Table 3. Physical Properties of the Reservoir Rock and Fluid Within the POR Reservoir .....	28
Table 4. Field Development and Expansion Plan for Wells in PRM’s Lease Area.....	28
Table 5. PRM’s Financial Model Output Parameters .....	31
Table 6. Techno-Economic Results for Two CSP-GeoTES Case Studies.....	32
Table 7. Sensitivity Parameters for CSP-GeoTES Analysis.....	35
Table 8. Effect of Increasing Solar Multiple on Dispatch Hours, Spare Capacity, and System Cost.....	38
Table 9. Techno-Economic Results for a Combined CST-GeoTES System With High-Temperature Storage and Power Cycle .....	40
Table 10. LCOH of CSP-GeoTES Systems Delivering Either 12h or 24h Heat per Day .....	41
Table 11. Reservoir Brine Composition, Total Dissolved Solids, Hardness, and Specific Conductivity...	46
Table 12. Physical and Thermal Properties of the Reservoir Rock and Fluid .....	46
Table 13. EarthBridge's TEA Model Input and Output Parameters.....	49
Table 14. Technical Performance of Three Carnot Batteries Considered for the 10-MW EarthBridge Case Study .....	51
Table 15. Sensitivity Parameters for the CB-GeoTES Analysis.....	52
Table 16. Performance Details of Three Available Heat Pumps .....	54

# 1 Project Overview

## 1.1 Introduction

Energy storage is increasingly necessary as variable renewable energy (VRE) technologies replace emissions-intensive fossil fuels for electricity generation and thermal applications. Many energy storage solutions are being developed to address short discharge durations. This suggests that there is a significant gap in long-duration energy storage to compensate for significant diurnal and seasonal variations in VRE generation and electricity consumption.

As an example, consider the energy generation characteristics in California—namely, the observation of the daily and seasonal variations in energy produced by solar photovoltaics, wind, and hydro-electric. Figure 1 indicates that these electricity sources exhibit considerable seasonal variability, with the average energy generation in summer months roughly 75% greater than that in winter months. Furthermore, the so-called “duck curve” phenomenon is a well-known feature of the Californian electricity system that describes daily energy supply and demand; in particular, late afternoons in the spring and summer are characterized by the requirement for power generation to ramp rapidly while there is decreasing solar generation as the sun sets (California ISO, 2020; Rothleder, 2022; EIA, 2023). Thus, energy storage technologies that provide both daily and seasonal storage capabilities could add value to the Californian grid.

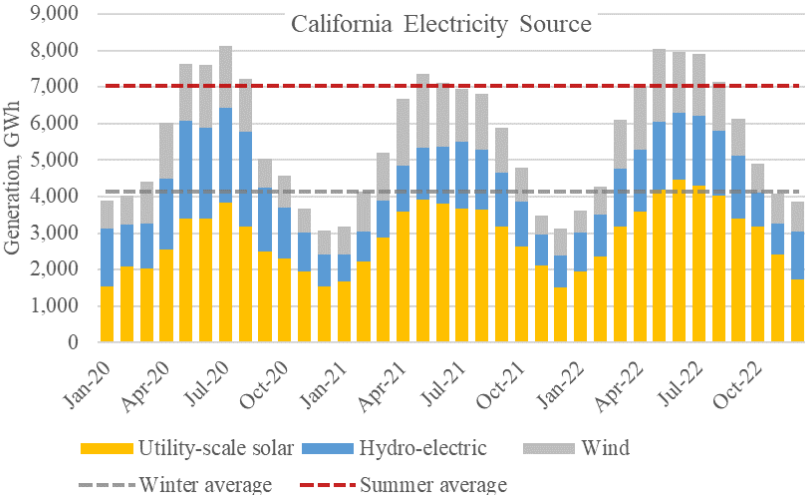


**Figure 1. Electricity generation from variable renewable sources in California over several years**

Data from <https://www.eia.gov/opendata>.

Seasonal energy storage can shift renewable energy generation from the summer to the winter, but these technologies must have extremely large energy capacities and need to be cost competitive over the project life cycle. Long-Duration Energy Storage (LDES) is typically defined as having a discharge duration over 10 hours, and LDES technologies include compressed air energy storage, hydrogen, and gravity storage. We propose **Geological Thermal Energy Storage (GeoTES)** as an LDES system to provide a solution for daily and seasonal energy storage. Excess thermal energy can be stored in permeable reservoirs such as non-potable aquifers and depleted hydrocarbon reservoirs for several months. Sharan et al. (2021) determined

that storing thermal energy from a concentrating solar thermal (CST) unit in a GeoTES reservoir provides a constant and low levelized cost of storage (LCOS) over both short and long durations compared to the commonly used molten-salt thermal energy storage (TES), batteries and hydrogen technologies (Sharan et al., 2021).

GeoTES can utilize various types of reservoirs such as shallow aquifers and depleted oil/gas fields—the latter actually presents a substantial impact to resilience of energy sectors and energy transition of carbon-intensive industries. There are a few demonstration projects of GeoTES in shallow aquifers in the United States and western Europe for low-temperature (<50°C) building and district heating applications (Fleuchaus et al., 2018). However, there are currently no operational commercial thermal storage projects in depleted oil reservoirs, although plans for demonstration projects are ongoing in Germany as part of the Deepstor project for the Karlsruhe Institute of Technology campus (Schill et al., 2024). California-based Premier Resource Management (PRM)—in collaboration with the National Renewable Energy Laboratory (NREL), Ramsgate Engineering, and Gossamer Space Frames—has recently been awarded \$6 million in federal funds by the U.S. Department of Energy Solar Energy Technologies Office to construct a 100 kW<sub>e</sub> demonstration system at PRM’s lease in Bakersfield, California (DOE, 2024). This demonstration will involve the drilling of eight wells, a 2 MW<sub>th</sub> CST system, and a 100 kW<sub>e</sub> power plant. This will be a first-of-a-kind commercial-scale demonstration of high-temperature GeoTES in the United States.

Significant barriers to the deployment of GeoTES for seasonal storage exist. For example, there is a lack of grid impact and market potential analysis to recognize the value of flexible long-term storage systems to various electric grids and markets. Another challenge is obtaining and evaluating suitable geological data in a standardized way. Geological data from sedimentary basins may be void of thermophysical and geochemical fluid/rock characteristics, which can be highly site-specific. Furthermore, the economic feasibility of GeoTES depends heavily on the interaction of the reservoirs with the surface equipment that generates and utilizes the heat. These barriers can be addressed by developing standards and guidelines for site suitability assessments, as well as developing methods to couple reservoir models into full system models to enable evaluation of techno-economic viability. In this project, we advance the state of the art in GeoTES technology development by research and analyses that address technical aspects of these barriers.

## 1.2 Project Objectives

In this project, we develop a techno-economic analysis (TEA) model to evaluate the commercial feasibility of GeoTES systems charged with two energy sources—solar thermal and renewable electricity. This TEA model will take in inputs from specialized subsystem physical models such as those for power cycle design and optimization and dynamic reservoir modeling. The TEA model will also be capable of determining GeoTES hourly, diurnal, and seasonal dispatch operations in response to power demand for simple market operations (e.g., arbitrage and capacity payments). Through a complementary geological and geophysical property data gathering effort, we identify and assess suitable non-potable shallow aquifers and oil and gas reservoirs that could be suitable for GeoTES in California and Texas. These will inform further research on the development of supply (cost versus capacity) curves for GeoTES that can be

useful for grid planning and capacity expansion. The team also engaged in several outreaches to GeoTES stakeholders. Discussions during the outreach activities are presented in Appendix A.

## 2 The GeoTES Techno-Economic Analysis Model

### 2.1 CST-GeoTES Design Configuration

CST technologies harness the radiative thermal energy from the sun through (a) parabolic solar troughs, (b) linear Fresnel mirrors, (c) parabolic mirrors, or (d) heliostats, which concentrate this energy to flow lines filled with high-boiling-point organic fluids (a and b), heat-engine receivers (c only), or power towers (d only). CST technology is not new; multiple plants are in operation in the United States and globally. The dominant thermal energy storage system for CST technologies has been insulated steel tanks containing molten salts (e.g., sodium nitrate and potassium nitrate) capable of storage temperatures of up to 700°C (Islam et al., 2018). However, deployed concentrating solar power (CSP) plants operate at temperatures 300°–550°C, generating electricity using steam cycles and providing flexibility by using thermal energy storage. The CST coupled with GeoTES (CST-GeoTES) design shown in Figure 2 comprises a parabolic trough solar collector that uses an organic oil-based working fluid to exchange heat with subsurface fluids for energy storage and discharge. Apart from the solar collectors, the surface system consists of heat exchangers, fluid separators, and a power block (typically steam turbine-generator or other high-temperature cycles).

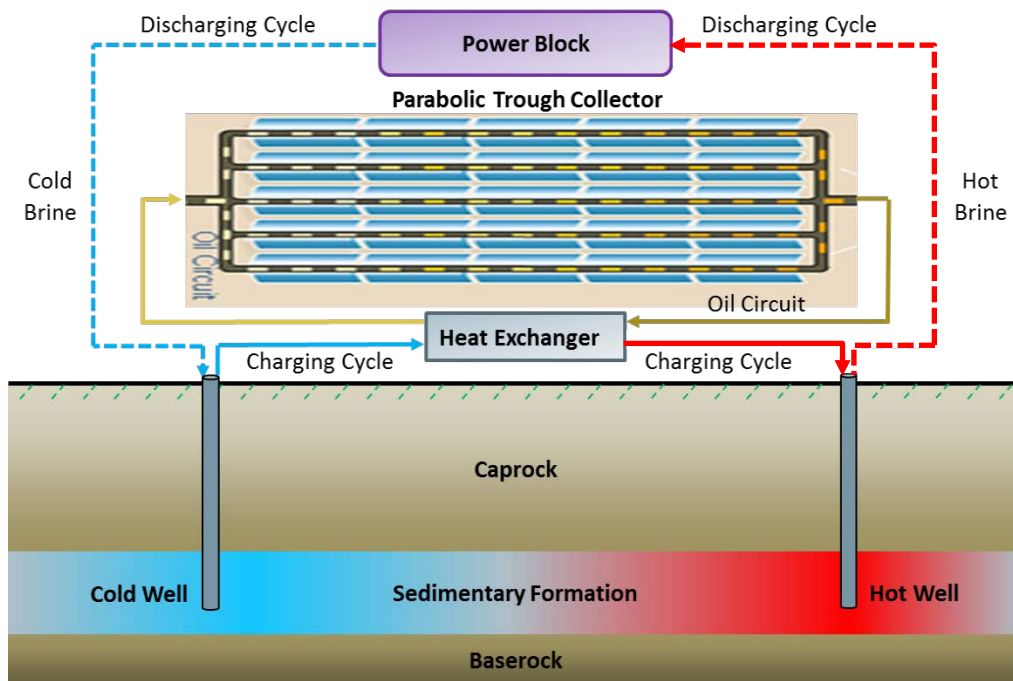


**Figure 2. Illustration of the CST-GeoTES system design**

Figure from (Sharan et al., 2021)

The CST-GeoTES system configuration used in this project comprises a concentrating solar field that concentrates sunlight to generate heat using parabolic trough collectors at 200°C. The heat is either converted directly into electricity using an air-cooled organic Rankine cycle or stored in the GeoTES, as illustrated in Figure 3. The CST-GeoTES cycle can serve as a bottoming cycle to an existing high-temperature CST topping power cycle (i.e., a combined cycle plant) or a standalone system. In this project, we have considered both a standalone (McTigue et al., 2023)

and combined cycle designs with a simple dispatch approach. For the standalone design, whenever there is excess solar heat that cannot be absorbed by the organic Rankine cycle, the GeoTES is charged. The GeoTES is discharged whenever solar heat is less than the design heat input to the organic Rankine cycle (McTigue et al., 2023). For the combined cycle design, the heat discharged from the topping high-temperature cycle is used to drive the organic Rankine cycle and the excess is stored in the GeoTES.

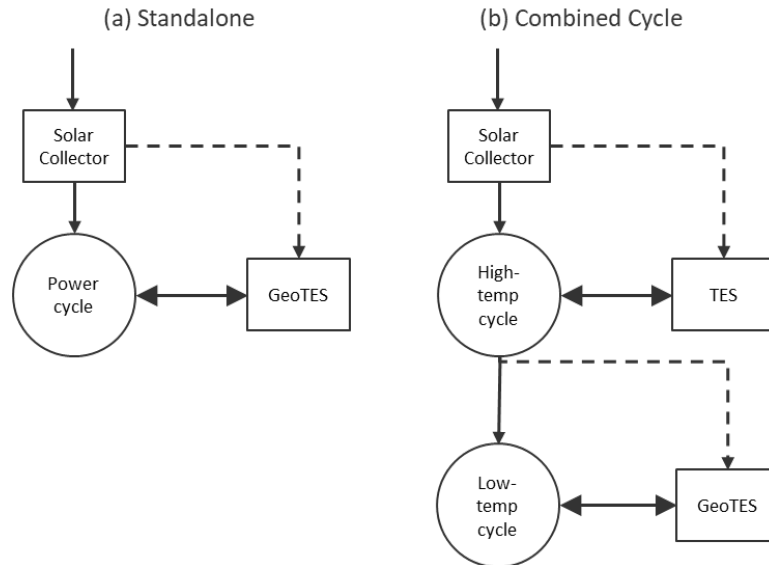


**Figure 3. Energy flows between components in a CST-GeoTES system within a (a) standalone vs. (b) combined cycle plant design**

Figure from (McTigue et al., 2023)

## 2.2 Carnot Battery-GeoTES Design Configuration

Carnot batteries (CBs) work on a thermodynamic principle that converts electricity into thermal energy via a heat pump. The heat pump primarily extracts thermal energy from a low-temperature heat source (e.g., the air, ground, surface water, groundwater) and upgrades the extracted energy to higher temperatures by adding work (electricity) to the system and finally delivering the higher temperature energy to a heat sink (i.e., a storage reservoir). The stored thermal energy is later converted back into electricity on demand using a heat engine. CBs typically use a contained volume for the cold reservoir. This enables cold storage at temperatures lower than the environment (which improves efficiency and energy density) and also reduces the impact of ambient temperature variations. Previous work has demonstrated that by using thermal energy storage media, CBs can achieve low marginal costs of electricity storage capacity, especially for longer duration storage (McTigue et al., 2022). However, very large durations of storage (e.g., weekly to seasonal storage) would require impracticably large containment volumes. One solution is to create thermal reservoirs in the subsurface, i.e., GeoTES, to achieve low-cost, long-duration storage.

The CB coupled with GeoTES (CB-GeoTES) system design is shown in Figure 4. The surface design consists of an industrial-scale water-source heat pump and a similar scale heat engine. A suitable working fluid must be chosen for the heat pump and heat engine, and candidates include



carbon dioxide (CO<sub>2</sub>) and R125. The subsurface system consists of a shallow aquifer for cold storage, a relatively deep aquifer for hot storage, and a set of four wells: (1) cold, (2) tepid, (3) warm, and (4) hot. Wells 1 and 2 are drilled into a shallow aquifer and Wells 3 and 4 are completed in a deep aquifer. The shallow reservoir is assumed to be at a lower temperature compared to the deeper reservoir. The initial temperature difference between these reservoirs will depend on the site-based pre-GeoTES subsurface thermal gradient. Although, the wells in Figure 4 are vertical in geometry, they are so only for illustrative purposes. A simpler CB-GeoTES design will accommodate only hot storage, and cooler water exchanged within the heat pump and heat engine could be surface-sourced or from a shallow water well. The heat pump may also be an air-sourced unit. This will mean two wells (Wells 3 and 4 as a doublet) per section of acreage instead of four.

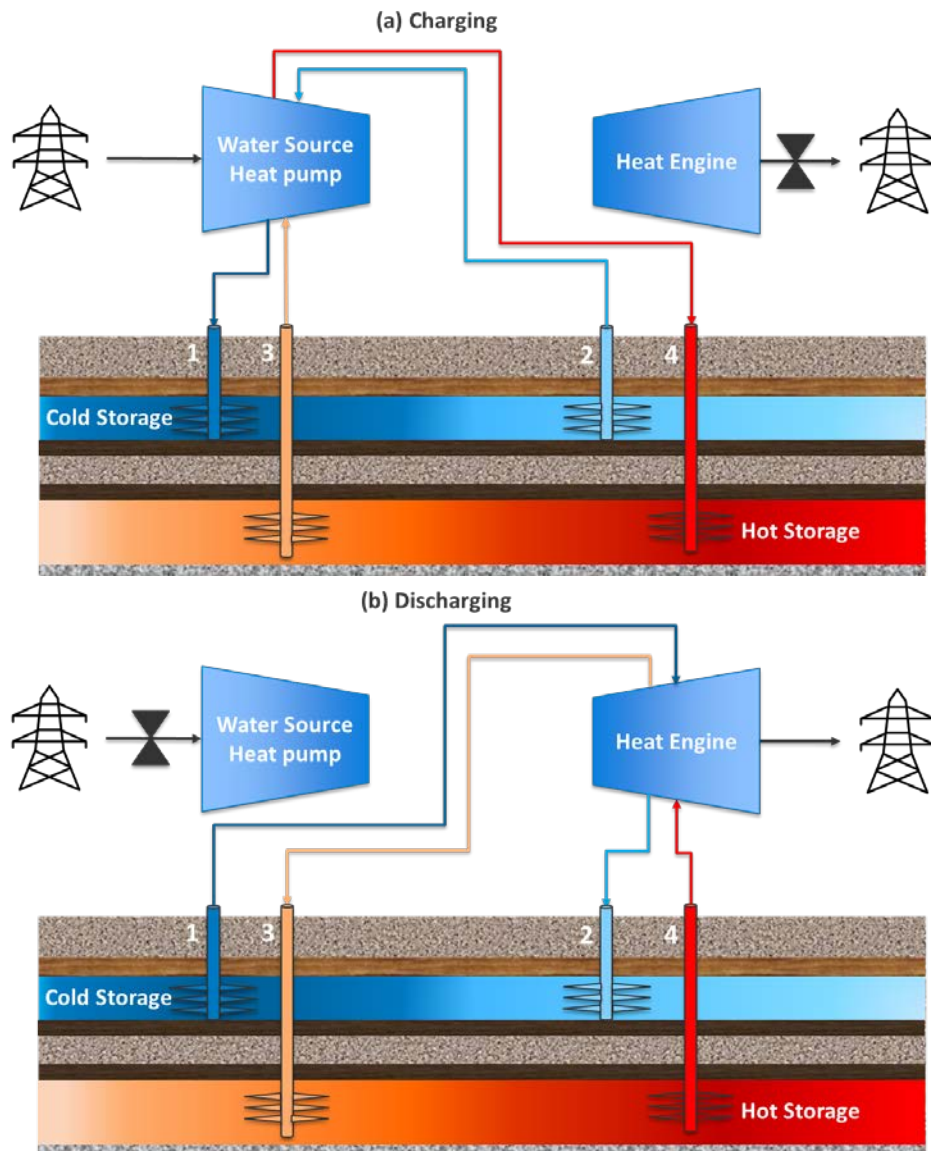


**Figure 4. High-efficiency design configuration of the CB-GeoTES during (a) charging and (b) discharging operations. The design assumes sufficient reservoir volume to accommodate both cold and hot storage. The well geometry shown in the figure is vertical. However, actual systems may utilize wells with laterals for better heat sweep in thin beds.**

For cost-optimized performance, we describe a three-well CB-GeoTES system illustrated in Figure 5. Fluid is produced from one reservoir (point 1g. on Figure 5) and used as both the heat source and sink for the heat pump: The production fluids are split, and one fraction is heated up by the hot side of the heat pump before being reinjected into another formation that will become the hot reservoir (2g.). The other fraction of production fluids is cooled in the heat pump evaporator and then reinjected into a separate formation, which becomes the cold storage (3g.).

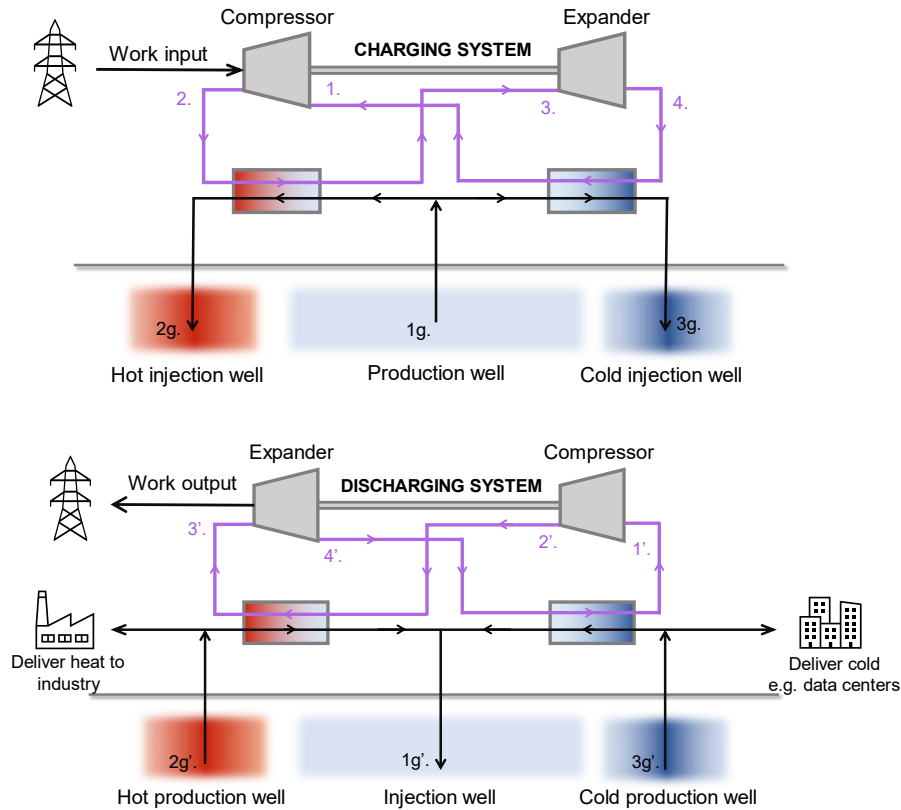


**Figure 5. Schematic of a CB with geological thermal storage during charge (top) and discharge (bottom)**

Figure from (McTigue et al., 2023).

To discharge the system, the flow direction of each process is reversed. Hot fluid is produced from the hot geothermal reservoir (2g'.) and used as the heat source in a heat engine. Heat engines conventionally reject heat to the environment, but in this case, cold fluid produced from the cold reservoir (3g'.) is used. Because the cold reservoir is at temperatures below the average ambient temperature, the heat engine should achieve higher efficiencies than a conventional heat engine operating between the hot reservoir and the environment.

Continued steady-state operation of the CB imposes several constraints on the system design. First, fluid must be returned to its original temperature at the end of discharge—i.e., hot fluid must be cooled to its original temperature, and cold fluid must be heated to its original temperature by the heat engine before it is reinjected to the original reservoir. This ensures that the temperature of the reservoirs do not change over time (which could compromise system

performance). Secondly, the hot and cold reservoirs should be discharged at the same rate. If one reservoir is discharged more quickly than the other, then the full energy potential of the system cannot be exploited.

These constraints can be simplified by using the atmosphere as the cold reservoir instead of the geological formation. Then, only the hot fluid would be subject to temperature constraints, and there would be more flexibility in the system design. The cost of the cold wells and pumps must be balanced against the cost of moving large volumes of air instead. Furthermore, cold storage will provide some efficiency advantages and decouple the plant power output from ambient temperature variations. Such comparisons will be made in Section 5.

## 2.3 Model Definition

The GeoTES TEA model implements an algorithm that follows a top-down approach to estimating the performance and cost of generic and customized systems. It is a MATLAB-based integrator that comprises several distinct subsystems (such as the reservoir, wells, power cycle, and solar field) that each require detailed modeling to capture their distinct characteristics (McTigue et al., 2023). As shown in Figure 6, the CST system is designed and modeled using NREL’s System Advisor Model (SAM) (*System Advisor Model (SAM)*, 2022). Specifically, SAM is used to define the geometry and optical properties of the parabolic trough collectors and to calculate the hourly thermal power generated on an annual basis. The power cycles are modeled using the flow-sheeting tool IPSEpro (*IPSEpro: Process Simulation and Heat Balance Software*, 2022), which allows the off-design behavior to be obtained. The methodology for estimating subsurface development and equipment requirements is based on the Geothermal Electricity Technology Evaluation Model (GETEM). This is used to calculate parameters relating to exploration, drilling (corrected to account for sedimentary formations), production and injection pump costs and power requirements, and operations and maintenance costs. We assume that the reservoirs are charged and discharged by injecting and producing fluid from the same location in the reservoir. This is similar to a “huff and puff” operation in cyclic thermal injection systems. This can be achieved by operating each well in a bidirectional push/pull mode with a capability of serving as both an injection and production well depending on whether the GeoTES system is charging or discharging. We also model separate wells for injection and production but assume the wells are drilled to the same depth. The model is also capable of using outputs of discharge temperature and heat from reservoir models (e.g., TOUGH).

The outputs of the individual models are combined in MATLAB, and the performance and cost of the full system are subsequently calculated (McTigue et al., 2023). (Uncertainty and sensitivity can also be evaluated in the integrated MATLAB model). Figure 6 shows a flow diagram of the algorithm implementation. For CST-GeoTES, the electrical power output and relative solar field size are first defined. MATLAB calls SAM and calculates the solar field size to deliver the required thermal input given the individual properties of the location and solar collector design. The thermal energy is then calculated for each hour of the year based on the solar collector optical properties and the solar resource at the chosen location. A simple dispatch model is then used to determine whether thermal energy drives the heat engine or is injected or produced from the GeoTES. Once the thermal input to the power cycle is known, then the electrical output is calculated by interpolating the off-design performance map generated from IPSEpro. The energy flows are calculated over the course of a year, and subsequently the annual

energy production is evaluated, and economic metrics such as the levelized cost of electricity (LCOE) are calculated.

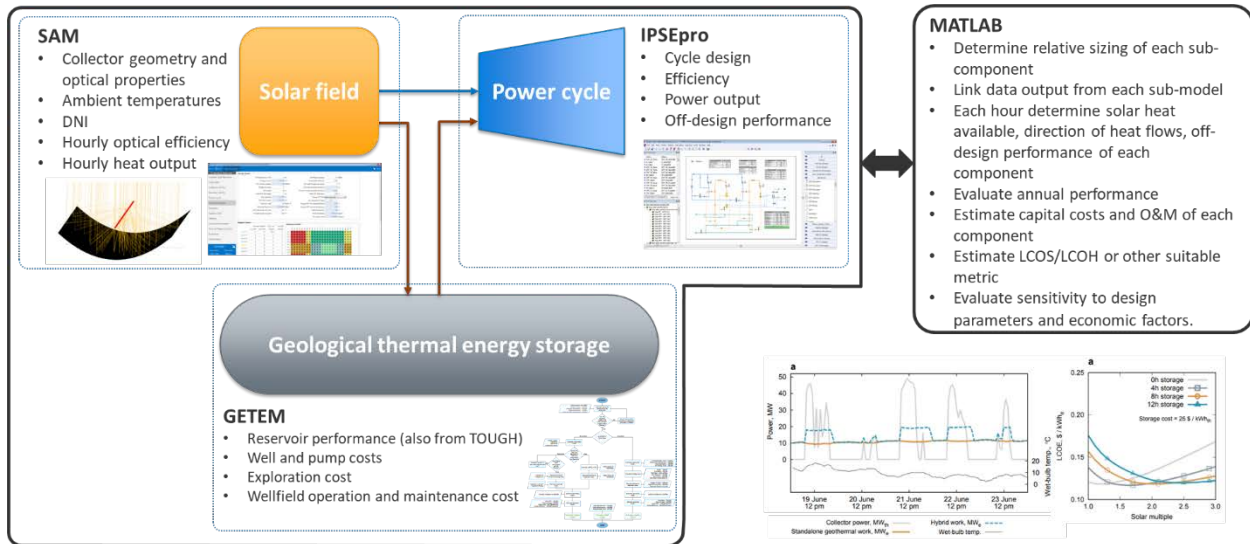


**Figure 6. Flow chart of the CST-GeoTES techno-economic assessment model showing interdependencies between surface and subsurface system models and integration of these model outputs in MATLAB**

## 2.4 Model Implementation

To initiate the simulation, the GeoTES is assumed to be fully discharged in order to closely represent the native state (e.g., initial temperature and pressure) of the reservoir. An initial charging operation is then implemented until steady-state conditions are achieved. The attainment of steady state depends on reservoir properties and the outcome of the reservoir simulation. The initial charging time will differ based on the reservoir geometric and thermophysical properties and the defined steady-state criteria (i.e., full reservoir charging or near-wellbore charging). Afterwards, multiple charging and discharging cycles for several years are simulated based on operational demand (e.g., diurnal or seasonal). Once multiyear operations are achieved, the annual energy production is evaluated, and economic metrics are calculated. The solar field and power cycle costs are estimated using simple per unit values (e.g., dollars per unit area and dollars per electrical power output) based on our previous analysis and discussion with industry representatives (McTigue et al., 2023). Annual operations and maintenance (O&M) costs for the surface systems are evaluated as a percentage of the total capital cost. Subsurface capital costs (for the wells, pumps, and flow lines) and O&M costs are calculated using assumptions and methods from GETEM.

Having estimated the total energy output and both capital and O&M cost, the levelized cost is evaluated using the Fixed Charge Rate (FCR) method (Short & Packey, 1995). The FCR requires assumptions about the project lifetime, debt fraction and interest rate, inflation rate, tax rate, and depreciation.

$$\text{LCOE (or LCOH)} = \frac{\text{FCR} \cdot \text{Capital cost} + \text{O\&M} + \text{Fuel cost}}{\text{Energy output}} \quad (1)$$

Fuel cost accounts for any electricity that is purchased to run the GeoTES. This is significant for the CB-GeoTES as electricity is used to drive the CB. The “Energy output” term may be the total electricity output or total thermal energy output. For CST-GeoTES, the system is being used for energy generation; therefore, either the LCOE as \$/MWh<sub>e</sub> or levelized cost of heat (LCOH) as \$/MWh<sub>th</sub> are calculated, depending on whether the system delivers electricity or thermal energy as the output. For CB-GeoTES, the system provides electricity storage, so the appropriate term is levelized cost of storage (LCOS) as \$/MWh<sub>e</sub>, although the denominator of the LCOS equation is the annual electricity output. To calculate the LCOS for the CST-GeoTES, only the reservoir storage system (e.g., wells and pumps) is accounted for. This is to avoid double counting since without storage, the CST is already coupled with a power cycle for electricity generation. Therefore, the expression for the CST-GeoTES LCOS is:

$$\text{LCOS}_{\text{CST-GeoTES}} = \frac{(\text{Wells} + \text{pumps}) \cdot \text{FCR} + \text{Pump O\&M}}{\text{Electricity due to GeoTES discharge}} \quad (2)$$

The analysis with the TEA model can include subsidies, such as investment tax credits or production tax credits, and other incentives that will introduce significant system cost savings and impact the calculated levelized costs. Throughout this work, we assume an Investment Tax Credit (ITC) of 40%, which is available to organizations who meet certain criteria, such as having sufficient domestic manufacturing content, or being part of an energy community or low-income community.

## 3 GeoTES Potential Estimation

In this project, we have evaluated several sedimentary basins in California and Texas to determine their potential and suitability for GeoTES. Our primary focus is on depleted oil and gas fields that have surpassed their economic life and shallow brackish aquifers unsuitable for potable water use.

### 3.1 Candidate GeoTES Reservoir Selection

#### 3.1.1 Depleted Oil and Gas Reservoirs

Oil and gas fields in central California and east Texas were analyzed as potential candidate formations for GeoTES. Reservoir data such as porosity, permeability, thermal conductivity, temperature, pressure, mineralogy, depth and thickness of the formation, brine salinity, and productive area were gathered from the California Geologic Energy Management Division (CalGEM) database, California Department of Conservation, Division of Oil, Gas, and Geothermal Resources (1998), Railroad Commission of Texas, and the Texas Bureau of Economic Geology (Figure 7). The data for 568 oil and gas fields in central California (Zone I), and 198 abandoned reservoirs in Railroad Commission of Texas Districts 1 through 6 have been characterized for hot geothermal storage. These zones/districts were selected based on their high levels of historical oil and gas activities compared to others within the states. To shortlist the formations for hot geothermal storage, we determined a cut-off value for reservoir properties (Table 1) (Glassley et al., 2013). Pressure and temperature data are plotted in Figure 8, porosity and permeability data are plotted in Figure 9, and Figure 10 shows salinity and thickness of the formation. Based on the criteria listed in Table 1, oil and gas formations in central California and east Texas have been screened, prioritized, and shortlisted. A detailed thermal-hydraulic-mechanical-chemical modeling approach is recommended for the shortlisted formations on a case-by-case basis. This is an integral input to the final investment decision on its application for hot geothermal storage. A decision flow chart for evaluating and selecting a candidate formation is outlined in Figure 11.

It is important to note here that although this research did not include an analysis of lower temperature reservoirs that can be used for cold water storage, the potential exists for other applications of the same principle. For example, lower thermal areas might be good candidates for use in industrial cooling or refrigeration applications. Researchers at Lawrence Berkeley National Laboratory (LBNL), NREL, and Idaho National Laboratory (INL) also have evaluated the use of subsurface fluids for data center cooling as well (Zhang et al., 2024). A similar analysis as is shown in this report could be performed to identify candidates for these types of applications as well.



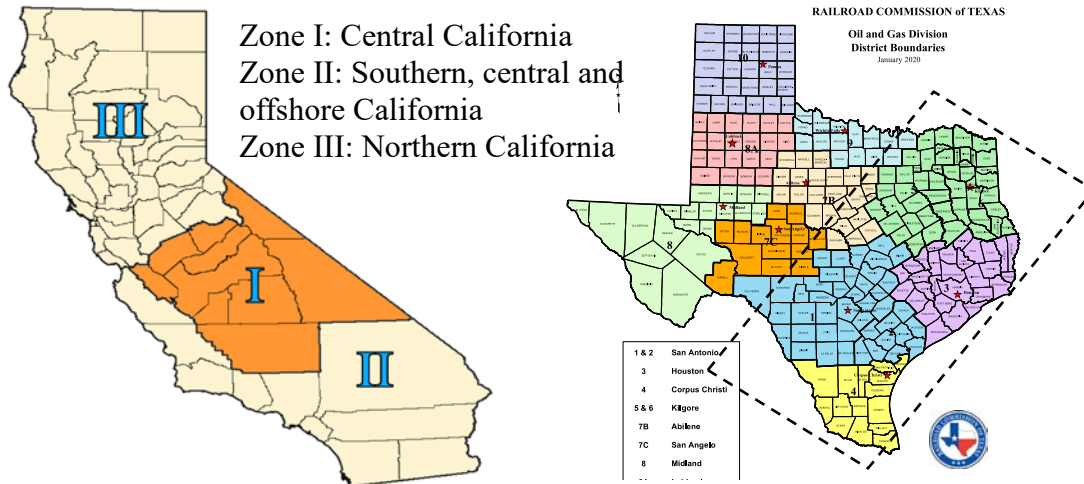


**Figure 7. California oil and gas fields (left) and Texas oil and gas districts (right)**

Source: California Department of Conservation, Division of Oil, Gas, and Geothermal Resources (1998); Railroad Commission of Texas (2020)

**Table 1. Criteria for Shortlisting Oil and Gas Reservoirs in California and Texas for Hot Geothermal Energy Storage**

Reservoir Properties	Cut-Off Value
Temperature	>50°C
Pressure	bar; <i>depth dependent (regressed from the compiled data)</i>
Average thickness of the formation	>150 ft or 50 m
Average depth	>1,500 ft
Porosity	>10%
Permeability	>100 millidarcy (md)
Salinity	<30,000 parts per million (ppm)
Productive area	>100 acres



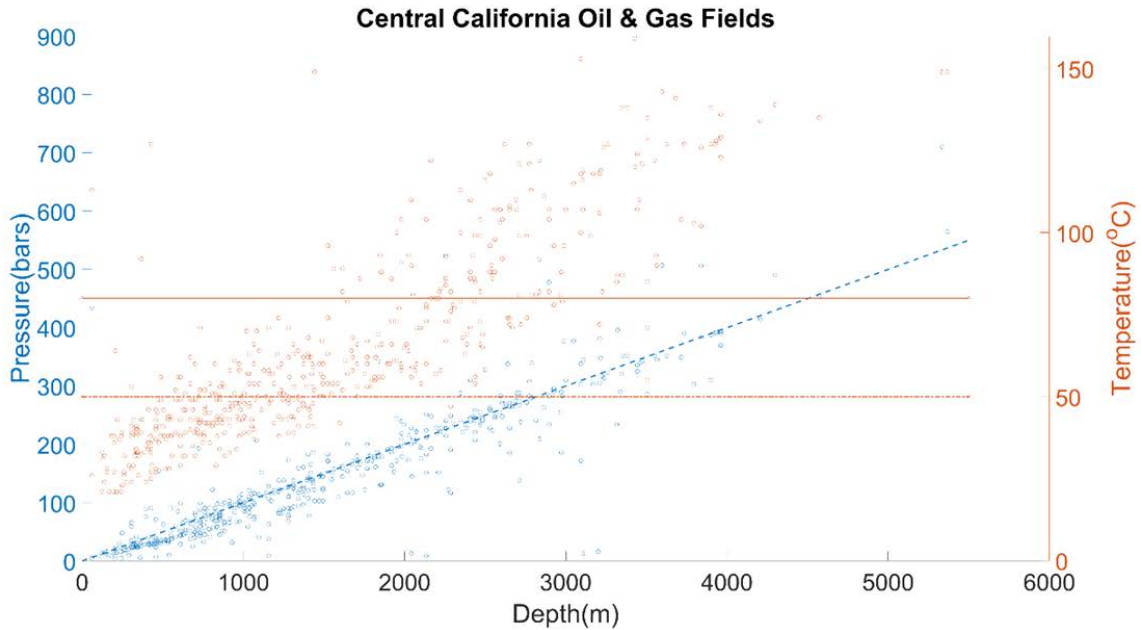


**Figure 8. Pressure vs. depth for all reservoirs in central California. Hydrostatic pressure vs. depth is plotted as a solid line. Temperature vs. depth is plotted in an orange color, and solid lines represent temperature at 50°C and 80°C.**

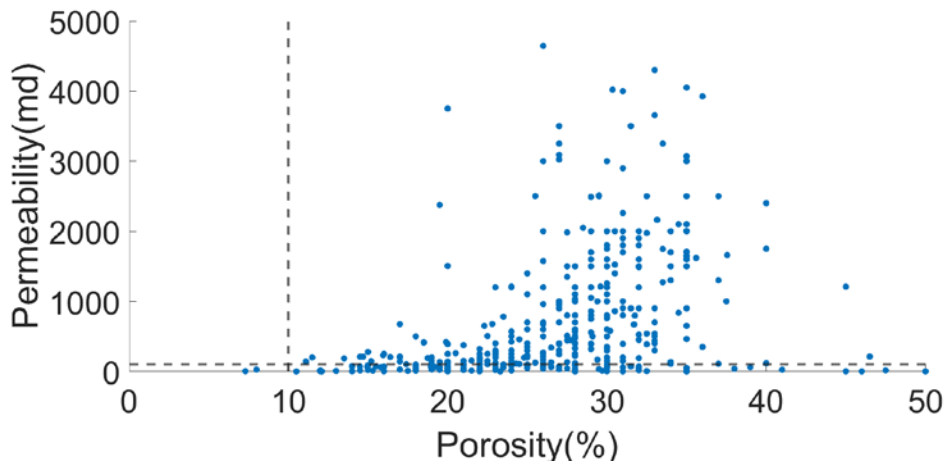


**Figure 9. Permeability and porosity for all oil pools in central California. Dashed line at x=10 represents porosity cut-off, and y=100 represents permeability cut-off at 100 millidarcy.**

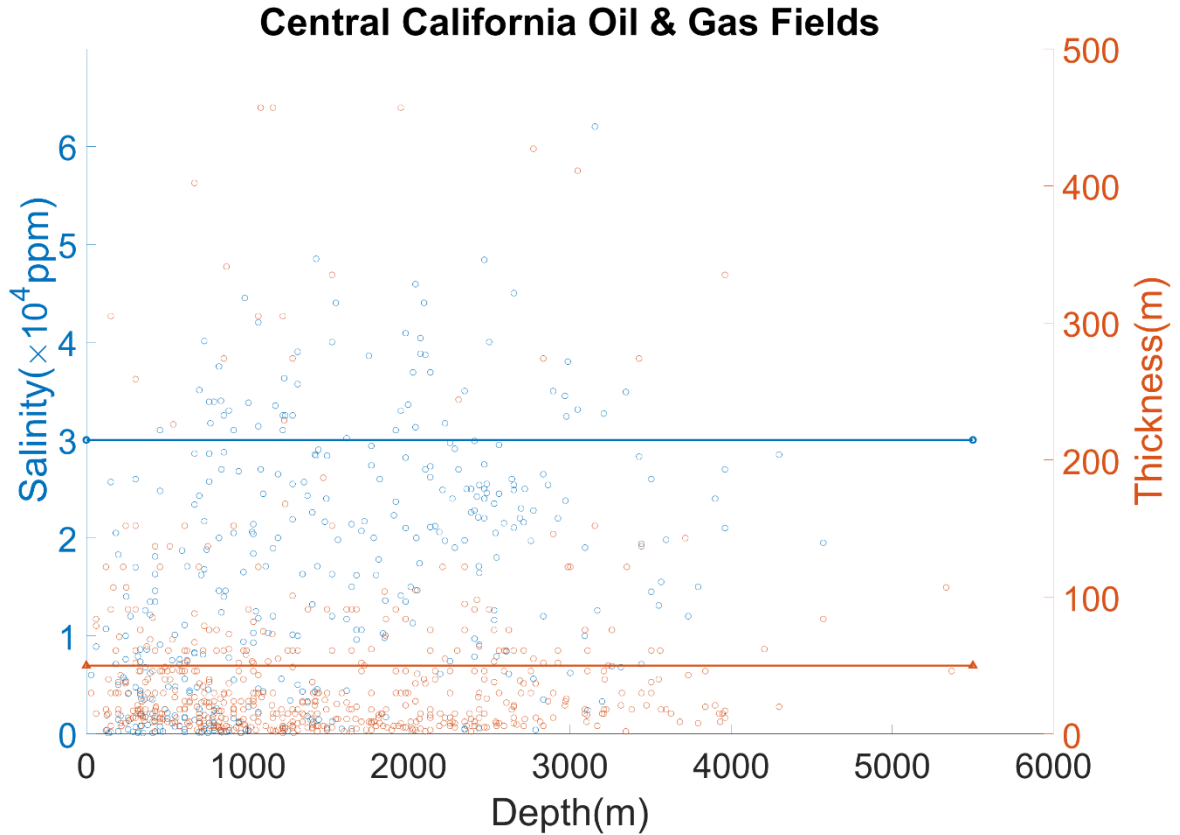


**Figure 10. Salinity (ppm) and average thickness (m) for all oil pools in central California. Blue solid line represents 30,000 ppm salinity and orange solid line represents 50 m thickness.**

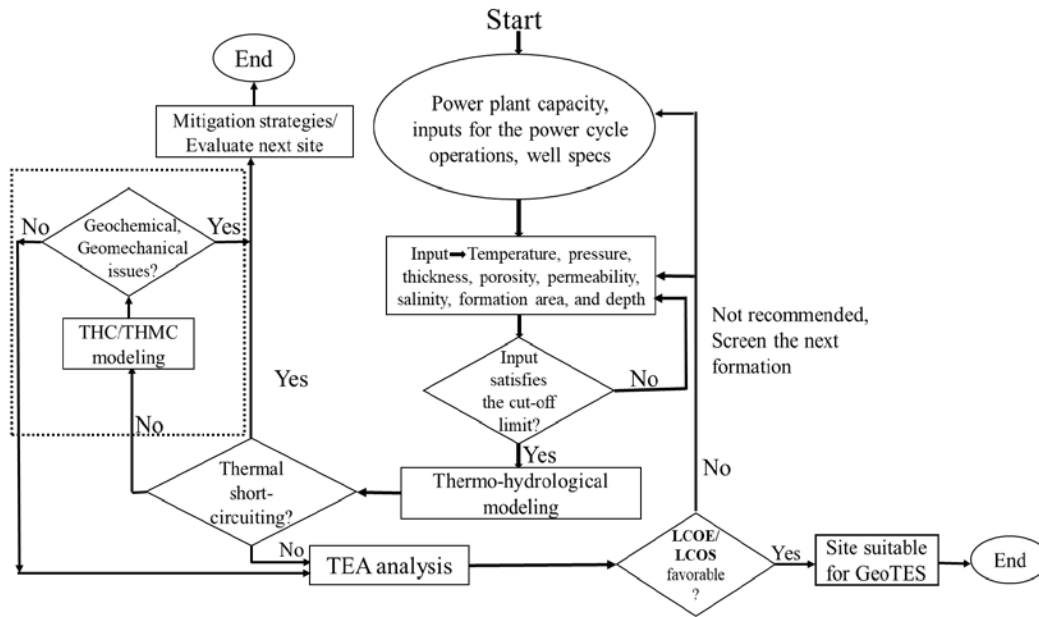


**Figure 11. A flow chart for site characterization approach for GeoTES applications**

### 3.1.2 Shallow Aquifers

GeoTES systems that comprise several vast subsurface reservoirs are key to the success of a GeoTES project. This requires favorable subsurface characteristics such as porosity, permeability, geochemistry, formation thickness, temperature, etc. Depth also plays a substantial role in the economics of the project, as in most cases increasing depth brings higher drilling costs. For this reason, we evaluated shallow reservoirs (<1,500 ft) and aquifers for their feasibility of heat for seasonal or on-demand use in Texas and California. Although horizontal wells could play an important role in improving heat extraction, this analysis only considered vertical wells as the main well configuration.

State and national datasets were analyzed to understand the various reservoirs and aquifers that could potentially be used for GeoTES. In Texas, 15 brackish aquifers (Meyer et al., 2020) were identified as potential GeoTES reservoirs because they (1) are shallow compared to deep depleted oil fields, (2) contain low-quality fluids (brackish) that will not be used for potable water sources, and (3) cover large areas within the state. Similarly, 53 shallow reservoirs in the central California region (California Department of Conservation & Division of Oil, Gas, and Geothermal Resources, 1998) were evaluated to understand which reservoirs have the highest potential for GeoTES operations.

By using formation depth, estimated drilling costs, and storage capacity assumptions, aquifer properties such as permeability, porosity, mass, density, thermal conductivity, and specific heat capacity were translated into preliminary techno-economic parameters to down-select the top-performing shallow reservoirs. Specifically, these aquifer properties were translated into two parameters: cost per storage capacity (i.e., the ratio of total capital cost over total capacity) and steady-state self-discharge rate. Because drilling cost is the largest cost driver, we modeled the total capital cost as a function of aquifer depth (Daniilidis et al., 2022). The total capacity was determined based on aquifer thickness and bulk specific heat. The self-discharge rate of an aquifer was defined as the ratio of its annual heat loss over its storage capacity. We estimated the self-discharge rates of all aquifers by considering heat loss by thermal conduction, following similar models as in Pepin et al. (2021) and Burns et al. (2020). We then pinpoint all aquifers on a two-dimensional plane to evaluate their overall performance (Figure 12). In this preliminary evaluation, the Carrizo-Wilcox, Yegua-Jackson, and Dockum brackish aquifers were identified as having the highest potential for further investigation in Texas. Similarly, the White Wolf, Belridge South Tulare, and Belridge South Reef Ridge exhibit the highest potential for further study in the central California region. Future work will focus on these reservoirs and aquifers to perform higher level TEA and inform economic feasibility under a variety of operational scenarios.

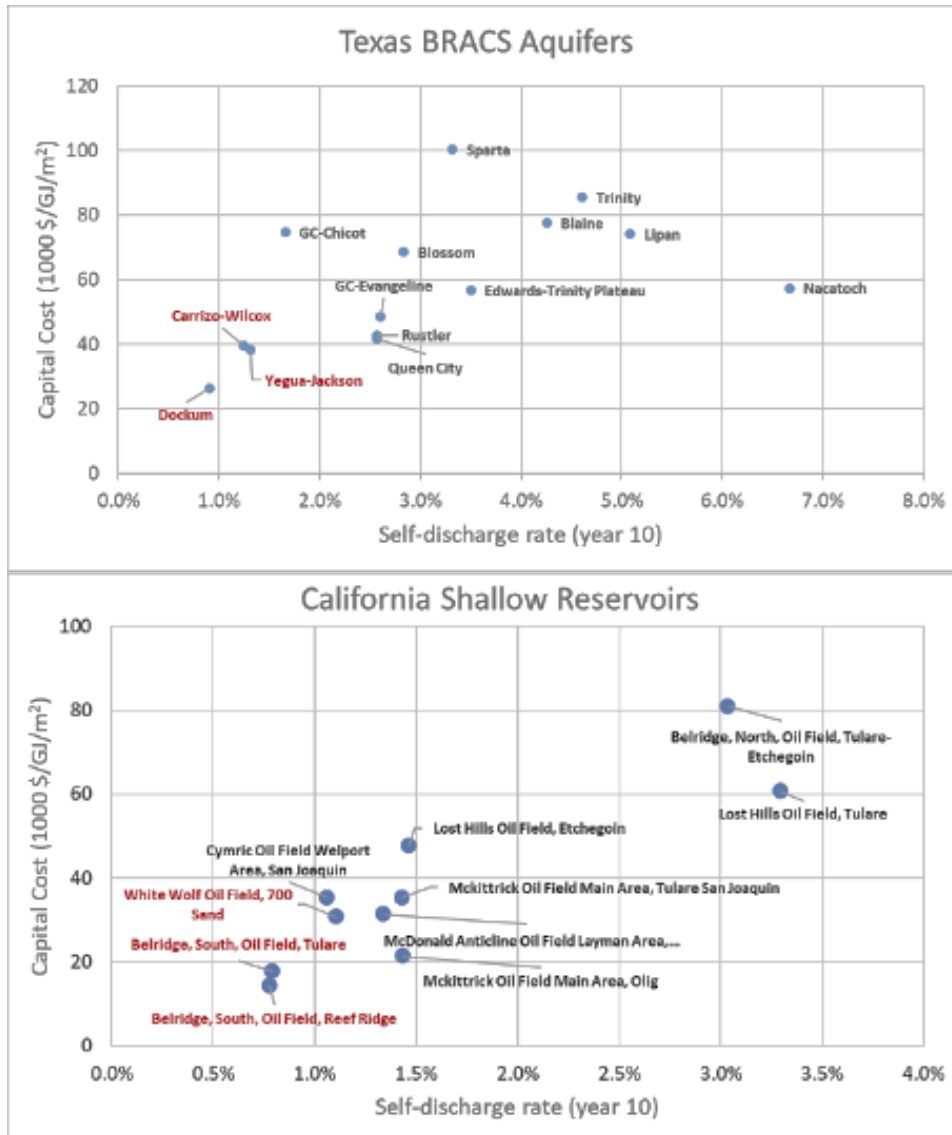


**Figure 12. Preliminary evaluation of BRACS (Brackish Resources Aquifer Characterization System) aquifers in Texas (top) and California (bottom) in terms of their cost per capacity and steady-state self-discharge rate. Note that we use the self-discharge rates at year 10 as an approximation of steady-state self-discharge rates by assuming the aquifers are in thermal equilibrium with ambient temperatures.**

### 3.2 GeoTES Storage Potential Estimation Analysis

Estimating the storage potential of GeoTES candidate reservoirs is a crucial step in site selection and technology valuation. The diverse characteristics of the target formation and surrounding subsurface create a complex and dynamic environment, necessitating detailed, site-specific characterization for precise modeling and assessment. However, a high-level estimation of a reservoir’s storage capacity can provide valuable data and insights for early reservoir comparison and site selection. Previous capacity estimation efforts have focused on low-temperature reservoir thermal energy storage and geothermal systems (Burns et al., 2020; Esposito et al., 2012; Pepin et al., 2021; Stricker et al., 2020) and heavily influence the following effort. This

section outlines the development of a high-level energy storage capacity estimation tool, detailing the assumptions built into the model, and its application to potential GeoTES formations in California and Texas. The formations were selected based on the potential estimation work outlined previously and are the Antelope Hills and Belridge South depleted oil fields in California and the Yegua-Jackson and Carrizo Wilcox aquifers in Texas. This tool is currently in development, and assumptions and values may evolve as GeoTES technology advances, and more data become available. This effort establishes the foundation for future work in estimating the grid-scale potential of GeoTES.

### 3.2.1 Methodology

An Excel-based tool was developed at NREL to assess the storage potential of a candidate GeoTES reservoir. The GeoTES model uses the structure of the pre-existing geothermal Resource Size Assessment Tool (RSAT) (Rubin et al., 2022). The RSAT was altered to apply to GeoTES formations, mirroring the methods used for reservoir thermal energy storage capacity estimation in Burns et al. (2020) and Pepin et al. (2021), which present the following equation to calculate the thermal energy storage capacity per unit area ( $E'_{th}$ ):

$$E'_{th} = bn\rho_w c_w \Delta T \left[ \frac{J}{m^2} \right] \quad (3)$$

in which  $b$  is the formation thickness,  $n$  is the porosity,  $\rho_w$  is the density of the liquid,  $c_w$  is the specific heat of the liquid, and  $\Delta T$  is the difference between the reservoir outlet and return temperatures. This equation can be altered to include the heat stored in the solid phase of the reservoir, as seen in Equation 4.

$$E'_{th} = b((1 - n)\rho_s c_s + (n\rho_w c_w))\Delta T \left[ \frac{J}{m^2} \right] \quad (4)$$

in which  $\rho_s$  is the density of the solid and  $c_s$  is the specific heat of the solid. The model calculates  $E'_{th}$  for the liquid phase and solid phase alone, as well as liquid storage capacity + four levels of solid phase storage ranging from 25% to 100% in 25% increments. This range of estimated values represents the idea that a GeoTES system may recover a varying amount of thermal energy from the solid phase of its reservoir, depending on operation schemes and subsurface characteristics. This concept is explored further in the Assumptions section (see next page); however, the results presented here represent the storage capacity of only the liquid stored in the reservoir. A geothermal recovery factor ( $R_{th}$ ) is applied, representing the amount of thermal energy that can be recovered from the reservoir after reinjection (see Section 3.2.2.3 for details). Additionally, the subsurface area ( $A$ ) represents the area of the sample reservoir based on the collected data. These samples do not represent the entire area of the target storage reservoir. As GeoTES systems can supply thermal energy or electricity to customers, the recoverable electrical storage capacity of the reservoir is also calculated using a conversion efficiency ( $\eta_e$ ). Equations 5 and 6 represent the recoverable thermal energy storage capacity and the recoverable electrical energy storage capacity (all based on Equation 3), respectively.

$$E'_{th} = bAn\rho_w c_w \Delta T R_{th} [Wh] \quad (4)$$

$$E'_e = bAn\rho_w c_w \Delta T R_{th} \eta_e [Wh] \quad (5)$$

The user provides values for each of these parameters along with a desired probability distribution type. Distribution types include triangular, normal, lognormal, uniform, and constant and each type requires the user to input different values for each parameter. For example, a triangular distribution requires the user to enter the minimum, maximum, and most likely/mean values, while a normal distribution requires most likely/mean and standard deviation values. Monte Carlo simulation is then used to calculate the P90, P50, P10, and mean thermal and electrical storage capacities of the reservoir. By presenting these statistical metrics instead of a single value estimation, we hope to address the uncertainty implicit in subsurface characterization and that which is introduced by the following assumptions.

### 3.2.2 Assumptions

As a high-level preliminary estimation, this model incorporates several assumptions that influence the results. The most significant assumptions pertain to reservoir heterogeneity, reservoir characteristics, and the GeoTES system's operation schedule.

#### 3.2.2.1 Homogeneity

Homogeneity is assumed for the rock density and the specific heat capacity of both the liquid and rock, consistent across all reservoirs. This mirrors the assumptions in Burns et al. (2020) and Pepin et al. (2021) and is primarily due to the lack of site-specific data, but should be adjusted when such data become available. We understand that both rock density and specific heat can vary with temperature; however, we have not considered temperature dependence on their properties in our analysis. Another constant value is the liquid density, calculated for each formation based on its reported TDS content using the equation from Bradley (1987):

$$\rho_w = 1 + TDS \times 0.695 \times 10^{-6} \left[ \frac{g}{cm^3} \right] \quad (7)$$

#### 3.2.2.2 Monte Carlo Simulation: Addressing Variability and Uncertainty

Monte Carlo simulations help to address the variability of input parameters, though the data used to create these inputs may have their own uncertainties, which propagate into the model. For example, the input values for a reservoir's thickness, including most likely/mean and standard deviation values, may be based on a relatively small number of data points. Furthermore, while the subsurface area of a reservoir, such as those selected aquifers in Texas, may be vast, only a fraction of this area may possess all the favorable characteristics required for GeoTES. The data used in this analysis are a set of undefined sample areas within the target storage reservoir. These areas span different formations and do not represent the entire reservoir in their sum. Nevertheless, the vast available area supports potential project expansion and grid-scale systems.

The selection of an appropriate probability distribution type significantly influences the outcomes of Monte Carlo simulations, ensuring more accurate and reliable results. Reservoir area and thickness data often suggest a lognormal distribution due to the prevalence of smaller volumes and a few outliers with much larger values. However, these outliers can result in disproportionately large capacity estimates, skewing the overall results. This issue has previously been addressed using different methodologies according to the resource and geology being assessed. Williams et al. (2008) recommended the use of triangular probability distributions instead of lognormal distributions when assessing geothermal resource volume. Alternatively, Charpentier & Klett (2005) suggest the use of a "truncated shifted lognormal distribution for



accumulation size” for conventional O&G resource assessments. This analysis follows the approach of Williams et al. (2008), using triangular distributions to mitigate the impact of outliers and achieve more balanced and realistic capacity estimations, although future work in the evaluation of thermal energy storage reservoirs may shift this assumption.

### *3.2.2.3 Conversion Efficiency and Recovery Factor*

The conversion efficiency of each GeoTES system is assumed to be the same across all formations, characterized by a triangular probability distribution. This distribution is defined based on a worldwide review of geothermal plant efficiencies by Zarrouk & Moon (2014), which reports a minimum efficiency of 1% (Chena Hot Springs, Alaska), a maximum efficiency of 20.7% (Darajat, Indonesia), and a worldwide average efficiency of 12%. The conversion efficiency reflects the infrastructure’s ability to convert thermal energy into electricity, and accounts for non-condensable gas content, parasitic loads, heat loss, turbine efficiency, and generator efficiency. These values encompass all geothermal plant types, including binary, single, double, and triple flash, dry steam, and hybrid systems. Although flash systems are generally more efficient, GeoTES will primarily employ binary power cycles to avoid operational challenges such as calcite precipitation and fluid loss through cooling towers.

Similarly, the geothermal recovery factor is given a triangular probability distribution that is consistent across all formations. This recovery factor ranges from a minimum of 0.7 to a most likely/mean value of 0.8, and a maximum of 0.9. While this is significantly higher than the recovery factor typically observed in conventional geothermal plants (usually 0.1–0.25) (Williams et al., 2008), similar system operations align GeoTES more closely with the recovery factors observed in high-temperature aquifer TES (HT-ATES) systems (Atkinson et al., 2023). This alignment is further supported by the GeoTES analysis presented in Sharan et al. (2021). Like an HT-ATES system, GeoTES will often recover energy from the reinjection of hot fluids in a “huff and puff” operation, as opposed to the conventional geothermal method of mining pre-existing heat. This cyclic reinjection and production of liquid utilize preferential flow pathways, resulting in exceptionally high recovery factors. While external energy loss may occur from ambient groundwater flow, background geothermal heat flux, nearby pumping, or conductive energy losses at the storage plume boundary, it is assumed to be relatively low due to the thermal insulation provided by pre-charging the GeoTES reservoir (Sharan et al., 2021).

### *3.2.2.4 Impact of Dispatch Schedules and Storage Zone Characteristics*

GeoTES can operate on various dispatch schedules, from diurnal cycling to seasonal storage. The timescale at which a system operates, as well as the characteristics of the storage zone, will influence the thermal insulation of the pre-charged storage zone and the amount of heat recovered from the solid phase of the reservoir. Sharan et al. (2021) simulated a GeoTES system in diurnal operation, finding that on short time scales, whether diurnal or hourly, the system will not have sufficient time to extract heat from the rock in the storage zone, instead drawing heat almost exclusively from the liquid during the discharge phase. This leads to the temperature of the storage zone remaining essentially constant, provided there has been any amount of pre-charging, and maintaining a high recovery factor as discussed above. As the storage zone does not change temperature on this timescale, there is no thermal gradient to drive heat transfer out of the rocks. While this scenario results in an extremely high recovery factor due to the thermal insulation, the storage capacity only includes the energy produced from the liquid in the



reservoir. Conversely, a system operating for seasonal storage will likely have a relatively long discharge cycle. Over this extended period, the liquid phase will become depleted of thermal energy creating a substantial thermal gradient between the rock and the liquid. This induces conductive heat transfer between the solid phase and the liquid phase at the phase and convective heat transfer within the flow liquid phase, allowing for heat recovery. Seasonal operation can significantly increase the storage capacity of the reservoir, but it will negatively impact the ultimate recovery factor, as the compromised thermal insulation due to heat extraction from the rock may induce more energy loss to the environment.

Additionally, grain size, flow patterns, and composition will influence the amount of heat extracted from the solid phase of the reservoir. Small grains provide a larger surface area per reservoir volume, facilitating quicker heat transfer from the rocks, while larger grains or layered strata retain heat longer. Therefore, smaller grains increase the effective storage capacity but decrease the geothermal recovery factor in a pre-charged storage zone, and vice versa. While the capacity estimation tool calculates storage capacity at varying levels of solid phase thermal recovery, only the liquid phase storage capacities are presented here. It is assumed that the GeoTES system operates under diurnal conditions with subsurface conditions that result in negligible thermal recovery from the reservoir rock.

### 3.2.3 Data Sources

Data were collected from several locations, ranging from public databases from the U.S. Geological Survey (USGS) and BRACS to private databases and industry partners. Table 2 summarizes the sources used to define the reservoir characteristics in this preliminary analysis, as well as those expected to be used in future work.

**Table 2. Summary of Data Sources Used for GeoTES Storage Capacity Analysis**

	Name	Location	Description	Reference
<b>Sources for Preliminary Analysis</b>	CalGEM Databases	California	Provides a number of tools for accessing data on O&G and geothermal wells and facilities throughout California including WellSTAR, Well Finder, and GeoSteam. These provided reservoir characteristics for potential reservoirs in California.	(CalGEM, n.d.)
	BRACS Database	Texas	Interactive database that stores well and geologic information in support of projects to characterize the brackish groundwater resources of Texas. This provided reservoir characteristics for potential reservoirs in Texas.	(Texas Water Development Board, 2023)
	USGS California Aquifers	California	A groundwater flow model that contains data on aquifers in California's Central Valley.	(Faunt, 2017)
	Nehring Associates Inc. Database	Conterminous United States	Provides reservoir characteristics for oil and gas fields across the United States.	(Nehring Associates Inc., 2012)

	Name	Location	Description	Reference
	PRM	California	Provides site-specific data from the proposed site for their GeoTES demonstration plant.	(Private Communication, 2023)
<b>Sources for Future Work</b>	USGS Aquifer Databases	Conterminous United States	Geographic Information System (GIS) data of principal and alluvial aquifers across the United States. Metadata contains reservoir characteristic data.	(Stanton et al., 2017)
	USGS CO <sub>2</sub> Storage Database	Conterminous United States	Provides data from an assessment of the technically accessible storage resources for CO <sub>2</sub> in geologic formations underlying the onshore and state waters area of the United States.	(USGS Geologic CO <sub>2</sub> Storage Resources Assessment Team, 2013)
	USGS Sedimentary Basins	Conterminous United States	GIS data and report of sedimentary basins throughout the United States. Metadata contains reservoir characteristic data.	(Coleman Jr. & Cahan, 2012)
	NATCARB Oil & Gas Database	United States and Canada	GIS data of the oil and gas fields across the United States. Metadata contains reservoir characteristic data.	(Bauer et al., 2018)
	NATCARB Saline Reservoir Database	United States and Canada	GIS data of the principal and alluvial saline aquifers across the United States. Metadata contains reservoir characteristic data.	(Bauer et al., 2018)

### 3.2.4 Results

Data were collected from the sources listed above for the four selected sites in California and Texas. The input parameters ranges (i.e., minimum, maximum, mean, standard deviation) were defined in two scenarios, All Fields and Depleted Fields, corresponding to Figure 13 and Figure 14, respectively. In the All Fields scenario, all available data for each site were used to define parameter values. In the Depleted Fields scenario, only the data points at which the resource did not produce any hydrocarbons (at which the field was depleted) were used to define values. The All Fields scenario provided significantly more data points than the Depleted Fields scenario, and assumed significantly larger volumes of each reservoir were available for GeoTES. For example, the average usable area of sites within Antelope Hills is calculated to be 1.93 km<sup>2</sup> based on 14 data points in the All Fields scenario, while the same metric is 0.19 km<sup>2</sup> based on 4 data points in the Depleted Fields Scenario. In reality, GeoTES could take advantage regions that are partially depleted of oil, producing a small amount of fossil fuel which can benefit early project economics (Berger et al., 2023). So, while it is unrealistic to expect that the entire formation is developed for GeoTES, the usable volume of a reservoir will likely extend beyond the fully depleted regions.

The Monte Carlo simulation was run 1,000 times for each site and scenario, providing statistical probabilities of thermal and electrical capacities. The P90 value can be thought of as a 90% probability that the capacity will be at least that value, or that 90% of simulations returned a capacity of at least this value. In the All Fields scenario (see Figure 13), Antelope Hills oil field has a mean thermal capacity of 36 TWh, with P90, P50, and P10 values of 8 TWh, 29 TWh, and

75 TWh, respectively. Belridge South oil field has a mean thermal capacity of 226 TWh, and P90, P50, and P10 values of 103 TWh, 214 TWh, and 373 TWh, respectively. The Yegua-Jackson aquifer has a mean thermal capacity of 44 TWh, and statistical ranges of 6 TWh, 29 TWh, and 99 TWh. And the Carrizo-Wilcox aquifer has an average thermal capacity of 554 TWh, and statistical ranges of 51 TWh, 346 TWh, 1,375 TWh. Reservoir characteristics beyond the total size significantly affect average capacity estimates and probability ranges. The thermal capacities are consistently larger by about one order of magnitude than electrical capacities, reflecting the application of the thermal-to-electric conversion efficiency factor.

The Depleted Fields scenario (see Figure 14) calculated lower capacities at all sites. As explained above, this reflects the smaller available volume that is considered available. Antelope Hills had an average thermal capacity of 0.11 TWh, and Belridge South, Yegua-Jackson, and Carrizo-Wilcox had 0.32 TWh, 41 TWh, and 32 TWh, respectively. At all sites and in all cases, there is a significant range between the P90 and P10 estimates, which reflects the uncertainty a developer should expect in utilizing complex and varied subsurface systems.

It should be noted once again that the results seen here reflect the storage capacity of undefined volumes within the target reservoirs. Each of these reservoirs are extremely large and contain many separate and often independent hydraulic and geologic systems. Nonetheless, the results suggest truly immense storage capacities available at each site. A single TWh can fully power 70,000 average US homes for a year (Duke Energy, 2016), attesting to the immense potential GeoTES can tap into. The vast storage capacities of the subsurface coupled with the low marginal cost of expansion, sparse heat losses to the subsurface, and minimal costs of managing the storage volume relative to other technologies (McTigue et al., 2023; Raade, 2022) suggest that GeoTES could be a truly grid-scale, seasonal storage solution.

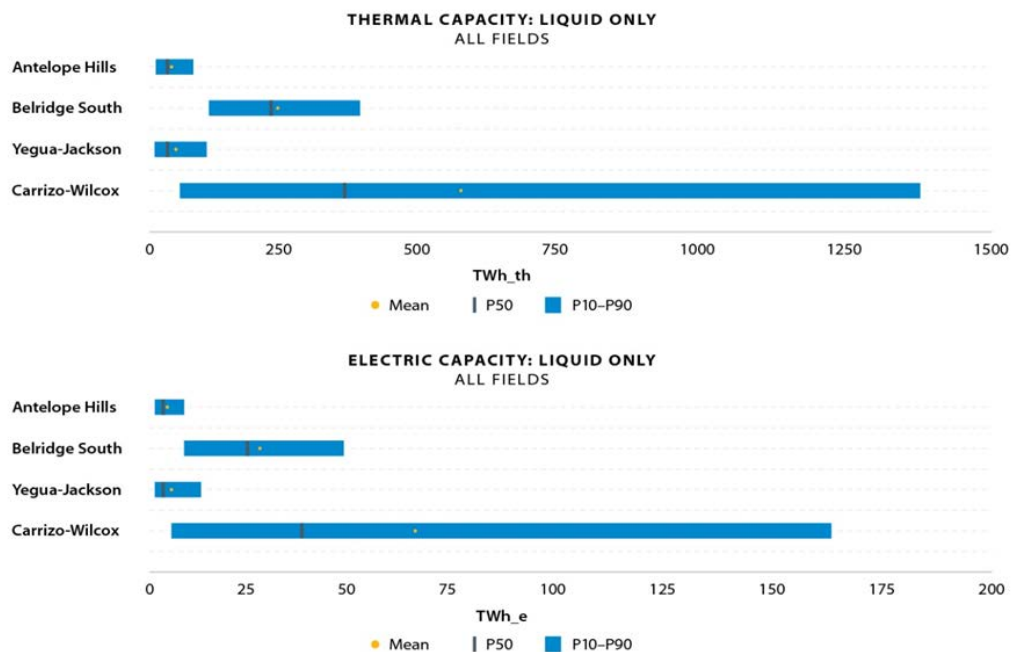


**Figure 13. (Top) Thermal storage capacity results with inputs reflecting all fields. (Bottom) Electrical storage capacity results with inputs reflecting all fields.**

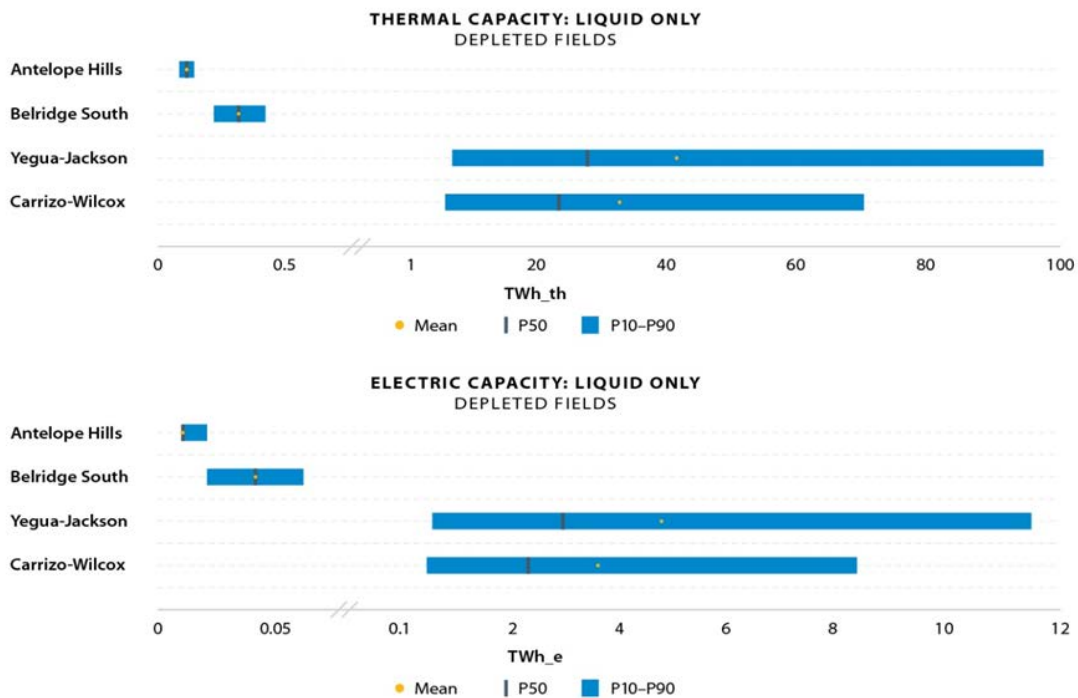


**Figure 14. (Top) Thermal storage capacity results with inputs reflecting only depleted fields. (Bottom) Electrical storage capacity results with inputs reflecting only depleted fields.**

### 3.2.5 Future Work

Ongoing efforts focus on improving the GeoTES capacity estimation tool and applying it to high-potential formations across the United States. High-level analysis will provide storage capacity estimates for prospective formations and could guide future developers. GIS data have been collected for formations across the United States, as seen in Table 2, and further effort will be made to find additional sources of applicable data. Filters can be applied to these data to select zones with the highest favorability. Figure 15 shows a preliminary down-selection of saline reservoirs across the United States based on thickness (>150 ft) and porosity (>10%) cut-off values. Feedback from industry and research experts will guide further refinement of cut-off values, and additional down-selection will be applied to the data.

With thorough, site-specific data, an in-depth analysis of a site’s storage capacity can be conducted. Collaboration with existing GeoTES projects could provide detailed data and allow calculation of more accurate storage estimates. Additionally, sites identified as highly favorable in preliminary screenings can be selected for detailed characterization or case studies. Applying the machine-learning framework from Jin et al. (2022), used for HT-ATES site identification, to potential GeoTES formations could streamline and enhance the preliminary selection of favorable sites.



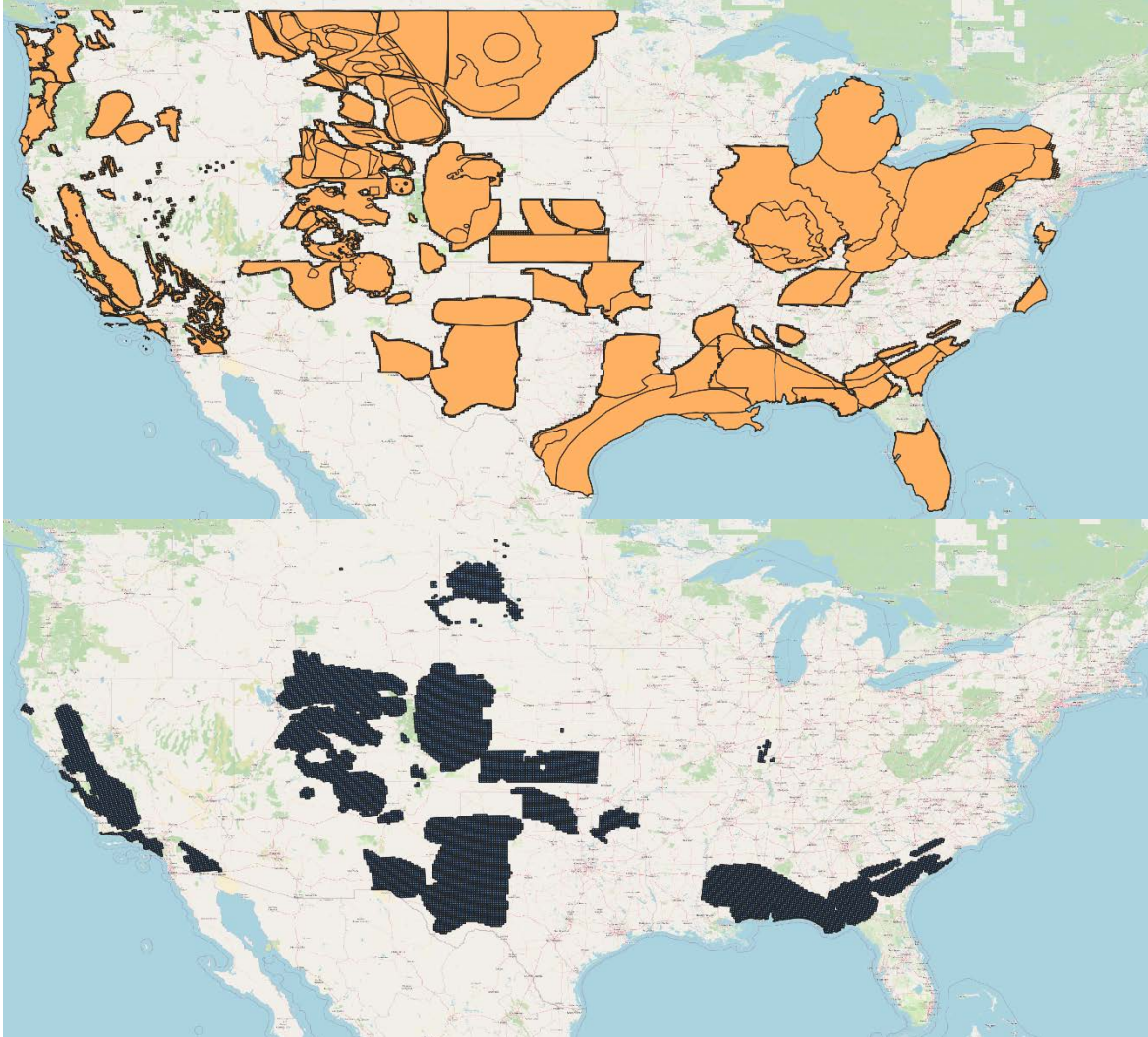


**Figure 15. (Top) Contiguous U.S. saline reservoirs from NATCARB database (Bauer et al., 2018). (Bottom) Favorable down-selection of saline reservoirs based on thickness and porosity.**

Various modifications to the capacity estimation model could better address the complex interaction between the geothermal recovery factor and solid-phase storage, as discussed in previous sections. Parini & Riedel (2000) propose a method for enhancing geothermal resource estimations by establishing the dependency of the geothermal recovery factor on several key reservoir parameters, including fracture spacing, porosity, and permeability. Similarly, Bloemendal & Hartog (2018) investigate the effects of groundwater flow and storage volume geometry on the geothermal recovery factor in ATEs systems. By treating the recovery factor as a dependent variable, storage capacity estimates would become more closely linked to the reservoir’s key geologic and hydraulic features, allowing the model to more accurately reflect GeoTES’ operational flexibility and dispatch capabilities. Additionally, the conversion efficiency could be explicitly tied to the expected power cycle and reservoir temperature or enthalpy, as demonstrated in Zarrouk & Moon (2014). Future research to identify and evaluate thermal energy storage reservoirs will inform the evolution of this model, its assumptions, and methodology.

## 4 Premier Resource Management CST-GeoTES Demonstration

### 4.1 Project Overview

Premier Resource Management (PRM) is a California-based energy company that comprises experts with decades of experience in oil and gas resource exploration and field development as well as power plant design and optimization. PRM aims to be the first-to-market player in California for thermal energy storage in low-oil-saturation reservoirs. The company is actively looking for ways to transition oil and gas assets, skills, jobs, and communities to clean and renewable energy in line with California's clean energy goals (CPUC, 2021). To do this PRM will develop a GeoTES system that will be tied to a surface CSP plant. CST technology harnesses the radiative thermal energy from the sun through (a) parabolic solar troughs, (b) linear Fresnel mirrors, (c) parabolic mirrors, or (d) heliostats, which concentrate this energy to flow lines rich in low-boiling point organic fluids (a and b), heat-engine receivers (c only), or power towers (d only). CST power cycles can attain high-temperature cycles just like those of natural gas and coal-fired power plants that harness both high-temperature thermal energy to generate electricity in a topping cycle and a lower-temperature bottoming cycle that generate electricity via a steam turbine. PRM's CST-GeoTES design shown in Figure 16 comprises parabolic trough solar collectors that use silicone as a working fluid to exchange heat with subsurface fluids for energy storage and discharge. Apart from the solar collectors, the surface system consists of heat exchangers, fluid separators, and a steam turbine-generator set.

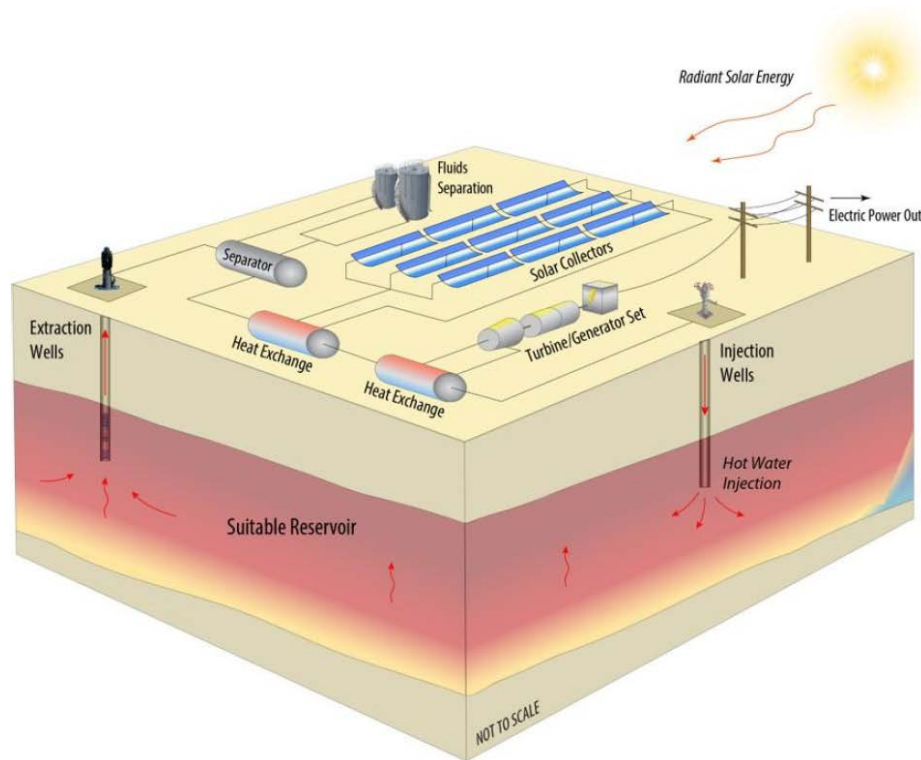


Figure 16. PRM's proposed CSP-GeoTES design

PRM holds leases with Aera Energy and E&B Natural Resources, totaling about 560 acres, on an area that connects the North Antelope and Antelope Hills oilfields in Kern County, California. The two leases are termed the Opaque and Hopkins Leases. Multiple wells have been drilled both within and just outside the lease area for oil and gas exploration and production. However, for this project, PRM will drill new wells within the Opaque Lease area. To initiate the drilling process, PRM has submitted an Underground Injection Control permit to the California Geologic Energy Management Division (CalGEM). This permit application is for drilling water injection wells down to the Point of Rocks (POR) reservoir unit in the Kreyenhagen Formation located in the North Antelope Hills oilfield. As of the time of this publication, the Underground Injection Control application has been reviewed by CalGEM and PRM is working on an addendum.

## 4.2 Subsurface Reservoir

PRM is targeting the POR member of the Kreyenhagen Formation for its GeoTES demonstration and the eventual commercial development. The formation comprises the hard, brown, and calcareous Kreyenhagen shale with an 810-ft thickness and serves as the seal for the POR reservoir. The younger Tulare clay sediments also form a secondary confining seal above the target reservoir. The Eocene POR sandstone is a light gray to tan, argillaceous, fine-grained sandstone interbedded with some thin gray-brown calcareous shale. These thin (<10 ft) shale beds form vertical reservoir seals in local hydrocarbon accumulations. Within PRM's lease area, the POR sandstone is over 3,000 ft thick, as shown in Figure 17. However, PRM's GeoTES project will utilize the upper 200–300 feet. Figure 17 also shows a cross section of the sedimentary lithofacies that describe the formation. The depositional environment is a deep-water turbidite sandstone facies with significant hydrocarbon accumulation (Scheirer, 2007).

As shown in Figure 17, the POR member of the Kreyenhagen Formation has been displaced throughout the project area by thrust fault activity. It forms the core of an Eocene structural high in the westernmost part of the expansion area, and dips steeply downward to the east into a deep synclinal trough (greater than 10,000 ft) between the expansion area and North Belridge. These structural features create a system with multiple oil traps, especially at the uppermost layers of the POR member, with overlying impermeable shale seals and lateral seals created by the offset faults.



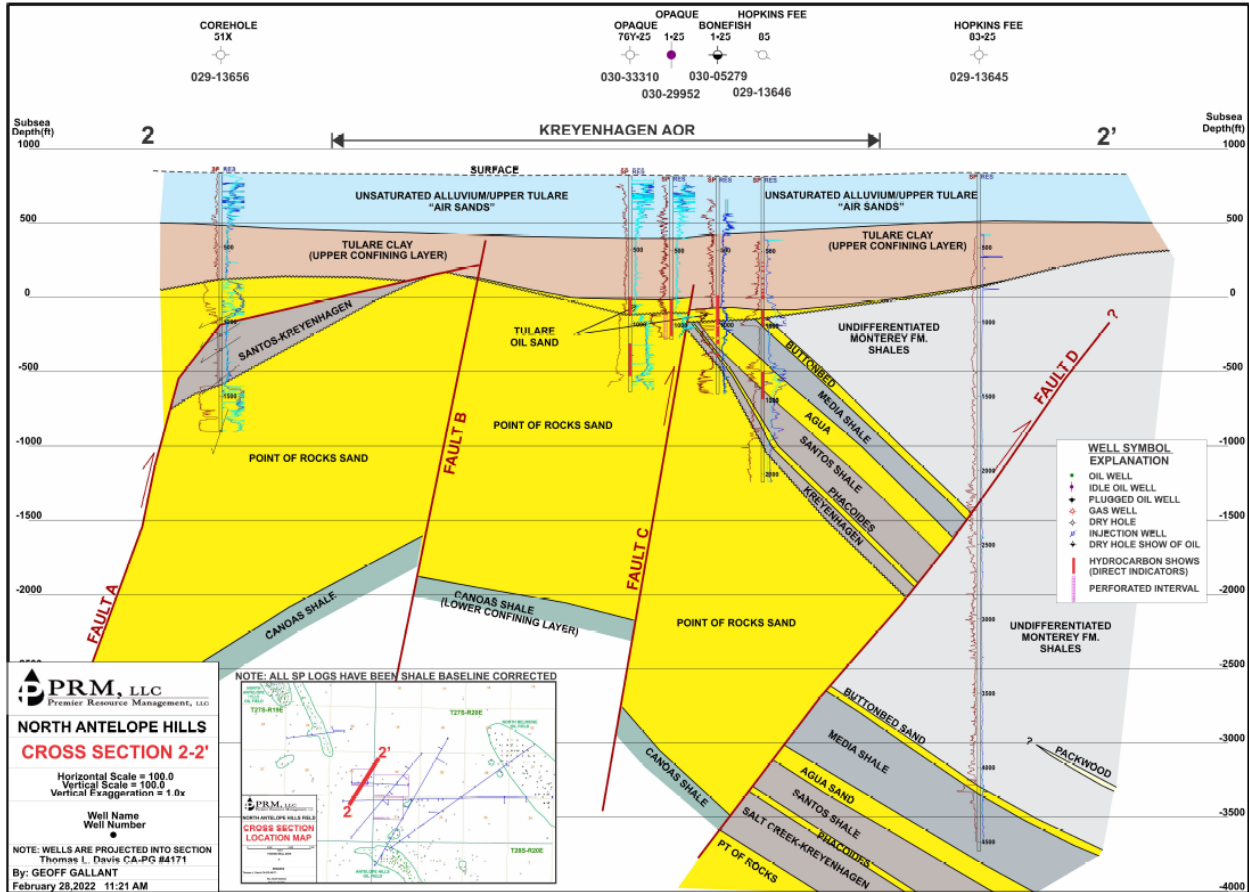


**Figure 17. The geological section of the Kreyenhagen Formation showing the structural features and lithologies within PRM's lease area. The POR sandstone is up to 3,000 ft thick and has a shale-type top (Kreyenhagen shale and Tulare clay) and bottom (Canoas shale) confining layers.**

Figure from PRM

The upper POR reservoir is the intended injection interval for PRM's CSP-GeoTES project. It is characterized by an average porosity of 32% and an average permeability of 676 mD, based on side wall core sample analyses. These primary properties make it a feasible reservoir candidate for fluid injection, storage, and production. Other reservoir properties are listed in Table 3. Although POR has some oil accumulation, it has a significant brine saturation (>90%). The POR brine is brackish with produced water total dissolved solids (TDS) from multiple wells measured 14,791–18,000 mg/L (average TDS is 16,075 mg/L).

**Table 3. Physical Properties of the Reservoir Rock and Fluid Within the POR Reservoir**

Parameter	Value
PRM Project Area (acres)	231
Porosity (%)	32
Permeability (mD)	676
Average Net Thickness (ft)	170
Average Depth to Top of POR (ft)	1,310
Reservoir Pressure (psi)	593
TDS (mg/L)	16,705

PRM plans to implement its CSP-GeoTES project in phases with an initial demonstration project followed by four additional developmental projects. The schedule and well patterns are shown in Table 4. The demonstration project will be implemented within 17.5 acres of the lease area. At this stage, 7 injection and 24 production wells will be drilled to a target depth within the POR reservoir. The demonstration project will be followed by four expansion projects averaging 26 injection wells per expansion. When fully developed, the entire project area will cover 213.8 acres with 98 injection and 207 production wells drilled from a total of 23 well pads. The well completions will be near-vertical to slanted, depending on the bottomhole location distance from their prospective well pads. The well arrangement will follow an inverted seven-spot pattern, as illustrated in Figure 18, which by project completion after year 6 will have an ultimate ratio of about two producers to one injector (Berger et al., 2023). PRM will also drill observation wells based on reservoir management requirements, and they are planned to be at an average of 3 per project phase. To ensure volumetric flow balance and reservoir pressure maintenance, each injection well flow will be about 6,000 barrels of water per day (BWPD) (~11 L/s) and production wells will flow at an average of 3,000 BWPD (~5.6 L/s) per well. All produced water will be treated and reused in-field as the main source of injection fluid.

**Table 4. Field Development and Expansion Plan for Wells in PRM's Lease Area**

Year	Area Name	Size (Acres)	Injectors	Producers	Observation Wells
1	Demo	17.5	7	24	3
3	1	46.5	19	48	3
4	2	41.1	23	42	3
5	3	56.1	25	38	4
6	4	52.6	24	55	3
	<b>Total</b>	213.8	98	207	16
	<b>Average per Project</b>	42.8	23	46	3
	<b>Average per Pattern</b>		1	2.11	0.16
	<b>Average Spacing, Acre</b>		2.2	1.0	13.4

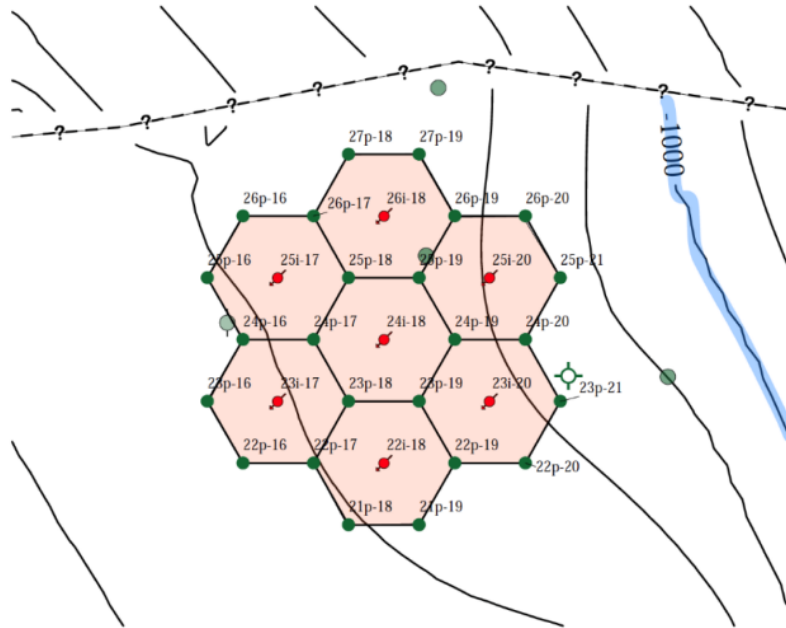


**Figure 18. Example of seven-spot well arrangement with producers shown in green and injectors shown in red**

### 4.3 Surface Plant

The surface of PRM’s GeoTES project area is owned by Aera/E&B Natural Resources. The area averages less than 5 in. of rainfall per year. The project location is unsuitable for agricultural purposes and becoming less suitable for cattle or sheep pasture as there is limited grass growth in drought years. It is also in a region with high solar irradiance, with average global horizontal irradiance of more than 6.5 kWh/m<sup>2</sup> per day. These, among other reasons, make it a prime location for siting CST systems. PRM’s CST field will comprise an array of automatically aimed parabolic mirrors that concentrate radiative thermal energy to horizontal tubes filled with silicone as the working fluid. These mirrors will be manufactured with reflector dimensions of about 6 m wide by 20 m long. The total count will be based on project size requirements. For the initial demonstration project these mirror arrays will cover an area of roughly 50–75 acres to generate 49–75 MW<sub>th</sub> of heat. The mirrors will be mounted on steel-reinforced concrete pedestal stands, typically three such stands per mirror. The pedestals will require relatively deep (~20 ft) reinforced concrete foundations to meet Kern County Planning design requirements for 110 mph winds. The mirrors will be spaced to support drive-through servicing, with about 10 feet of clearance when the mirrors are in the “service” mode, i.e., downward-aimed to allow their automatic washing, using demineralized water and biodegradable surfactants (when needed). The reflector field will be wind-fenced to assist in the wind velocity design configurations.

The surface plant will also comprise a water treatment unit for treating in-field produced water, before reinjecting into the reservoir as makeup water. PRM has determined that the makeup water will be needed depending on the GeoTES system maturity and will fall between 0% and 3% of total daily field production rates. This water will be sourced from oil reservoirs and aquifers containing brackish or saline brine at other intervals outside PRM’s project area or from wells that have been drilled to other fault blocks within the North Antelope complex. These

brines (including in-field produced water) will be separated (removing suspended solids and oil) and filtered within the water treatment unit. In addition to the solar field and the produced water treatment facility, the surface equipment will also comprise oilfield process equipment such as a three-phase (oil, water, and gas) separation unit (including a gas flotation and free-water knockout drum), manifolds and gathering lines, a custody transfer unit for oil flow measurement before off taking, and multiple fluid storage tanks.

#### **4.4 System Operation**

PRM plans to operate its CST-GeoTES system as an energy storage facility that primarily supplies electric power diurnally and seasonally, and secondarily as a load-following system that compensates for shortfall on the grid during peak times. Specifically, the demonstration project is designed to provide 15 MW of power to the grid for 5 to 8 hours on a nightly basis. In this operational schedule, the reservoir will undergo daily charging and discharge cycles to meet this demand. For seasonal operations, the CST-GeoTES system will be configured to provide power continually for up to 42 days (over 1,000 hours). In this situation, the reservoir will need to undergo about 18 months of an initial full charge and storage (to attain equilibrium) before the 42-day discharge, and it will also require months of recharge afterwards to operate efficiently (Berger et al., 2023). PRM will coordinate the power sales and interconnection contract with Pacific Gas and Electric (PG&E) and the California Independent System Operator (CAISO).

#### **4.5 PRM Pilot Demonstration Techno-Economic Analysis**

PRM plans to first execute a demonstration project before developing the full POR field in four phases. The company is looking at both debt and equity investments as well as grants to finance these projects. PRM has developed a proprietary Excel-based financial modeling tool for its CST-GeoTES that covers both costs and revenues over the life of the project. The model follows a discounted cashflow approach to estimating project life cycle costs, including in-field capital expenditures (CAPEX; engineering, construction, and equipment, excluding exploration costs) and operational expenses (OPEX), and revenues from both power and oil sales. The model assumes a project lifetime of 50 years. Table 5 summarizes the financial metrics that were derived from the model. It consists of values for energy (electricity and oil) generation/production, cost, and revenue metrics during the demonstration and full field projects within the POR development. Hence, the GeoTES team has confirmed with PRM on the cost items that pertain only to the CST-GeoTES installation and operation without any attributes to oil sales (see Table 6).

**Table 5. PRM’s Financial Model Output Parameters**

Note NPV = net present value; BOPD = barrels of oil per day; BOEPD = barrels of oil equivalents per day; MMBOE = million barrels of oil equivalents; BWPD = barrels of water per day; BOE = barrel of oil equivalents.

<b>Parameter</b>	<b>Unit</b>	<b>Demonstration</b>	<b>Full Development</b>
Year Installed	Year	2025	2029–2035
Project Area	Acres	18	232
Estimated Oil Resources	MMBO	1.4	19
<b>CAPEX</b>	<b>\$MM</b>	<b>82</b>	<b>974</b>
Cash Returned	\$MM	164	2,094
<b>NPV<sub>10</sub> to 2024</b>	<b>\$MM</b>	<b>30</b>	<b>212</b>
Peak Oil Production	BOPD	1,050	9,675
Peak Oil Production per Well	BOPD/well	44	43
Average Energy Produced	kWh/year	17,519,639	407,090,164
Average Energy Produced	BOEPD	128	2,978
Peak Oil Production per Well	BOEPD/well	49	57
Total Energy Produced	kWh	889,121,697	20,659,825,805
Estimated Oil Resources + Energy	MMBOE	4	74
Well Count Producers	count	24	223
Well Count Injectors	count	7	96
Max. Water Injection Rate	BWPD	50,069	662,942
OPEX per BOE	\$/BOE	12.94	5.68
Power Plant Size	MW	15	199
Rate of Return	%	23%	18%
<b>OPEX Total</b>	<b>\$</b>	<b>49,273,426</b>	<b>420,924,703</b>

## 4.6 PRM Demo TEA Case Study Validation

We use the system design and financial details provided by PRM as inputs to the TEA model with the objective of validating the model. The TEA model is then used to explore potential avenues for improved performance and cost.

### 4.6.1 TEA Validation

The PRM case study is evaluated for both the Demonstration (15-MW) and Full Development (199-MW) scenarios shown in Table 5. The number of injection wells is given by the thermal power requirement of the power cycle, which in turn depends on the efficiency and temperature. Table 6 shows that the TEA model calculates a similar number of injection wells to the PRM design.

**Table 6. Techno-Economic Results for Two CSP-GeoTES Case Studies**

Data were provided by PRM and correspond to Table 5. TEA-PRM corresponds to results generated by the TEA model using a fixed well cost. TEA-GETEM corresponds to results generated by the TEA model using sedimentary drilling corrected well costs from GETEM.

	Demonstration			Full Development		
	PRM	TEA-PRM	TEA-GETEM	PRM	TEA-PRM	TEA-GETEM
<b>Injection Wells</b>	7	8	8	98	97	97
<b>Solar Multiple</b>	-	1.0	1.0	-	1.25	1.25
<b>Power Block Rating, MW<sub>e</sub></b>	15	15	15	199	199	199
<b>Hours per Day</b>	3	5	5	8	6	6
<b>Electricity, GWh<sub>e</sub></b>	17.5	27.2	27.2	407.1	390.0	390.0
<b>CAPEX, M\$</b>	82	86.4	117.4	974	1132.2	1561.0
<b>OPEX, M\$</b>	1.0	0.8	2.2	8.4	10.8	28.7
<b>LCOE, \$/kWh<sub>e</sub></b>	0.18	0.14	0.23	0.10	0.14	0.22
<b>GeoTES LCOS, \$/kWh<sub>e</sub></b>	-	0.06	0.12	-	0.06	0.11
<b>GeoTES Capital Cost, \$/kWh<sub>th</sub></b>	-	0.69	1.0	-	0.59	0.90

The total energy output of the system depends on the power cycle rating, solar field size and location, and the charge-discharge dispatch schedule. The solar field size is characterized by the “solar multiple.” A solar multiple of 1 corresponds to a CSP field that delivers the design thermal power for the power cycle under ideal solar conditions and an irradiance of 950 W/m<sup>2</sup>. Larger solar fields generate proportionally more thermal energy over the course of the year. However, larger solar fields do not necessarily lead to proportionally more energy stored in the GeoTES. The maximum heat that can be added to the GeoTES is limited by the number of wells. In this example, the number of wells for charging the system equals the number of wells to discharge it—and is therefore fixed by the system power output. Therefore, the maximum thermal power that can be added to the subsurface equals the power requirement of the power cycle—and also equals the power output of a solar field with a solar multiple of 1 in ideal conditions. Larger solar fields can generate more power throughout the day, but if this power exceeds what can be absorbed by the GeoTES, it is curtailed. A dispatch schedule is chosen whereby the system does not deliver power before 5 p.m. PST; therefore, power is only delivered at peak electricity demand. When solar energy is available before 5 p.m., it is used to charge the GeoTES, and excess solar energy is curtailed. After 5 p.m., solar energy is converted to electricity, with any deficit made up by the GeoTES. The system dispatches electricity for the same number of hours each day of the year, and this number is chosen so that the net change in GeoTES energy capacity is zero—i.e., energy is neither added nor removed from the GeoTES on an annual basis.

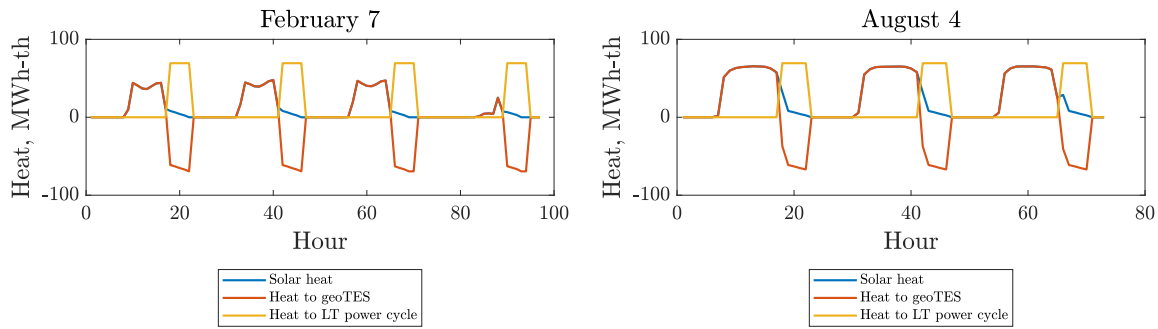


**Figure 19. Thermal energy flows for the 15-MW demonstration PRM CSP-GeoTES system**

In this study, the minimum solar field considered has a solar multiple of 1, and the energy flows in February and August are shown in Figure 18. These curves demonstrate how solar thermal energy is generated during daylight hours and this energy is added to the GeoTES. During afternoon hours, energy is extracted from the GeoTES (shown as negative heat) and used to drive the heat engine. In February, solar heat is generated over shorter timeframes and at lower magnitude than in August. Figure 19 shows the quantity of energy stored in the GeoTES throughout the year and indicates that energy is withdrawn during the winter months and added during the summer months. These graphs illustrate how the GeoTES is operated with both daily cycling and seasonal cycling. The system can reliably deliver 5 hours of power generation throughout the year, independent of the variable solar generation. Figure 19 also shows that the maximum energy capacity of the GeoTES is 48 GWh<sub>th</sub>, which is sufficient to deliver the design power output for 696 hours. Therefore, while this case study concentrates on daily power delivery, it is clear that the CSP-GeoTES system could also be used to dispatch for longer periods if required instead. For the 15 MW demonstration case, the TEA model calculates a larger electricity output than the PRM case study, see Table 6: note, the PRM electricity output of 17.5 GWh<sub>e</sub> per year, corresponds to an average discharge of 3 hours per day.

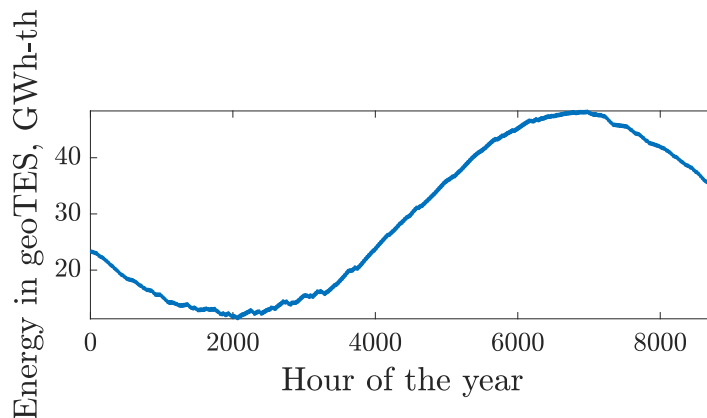


**Figure 20. Quantity of energy stored in the GeoTES throughout the year for the Demonstration 15-MW system**



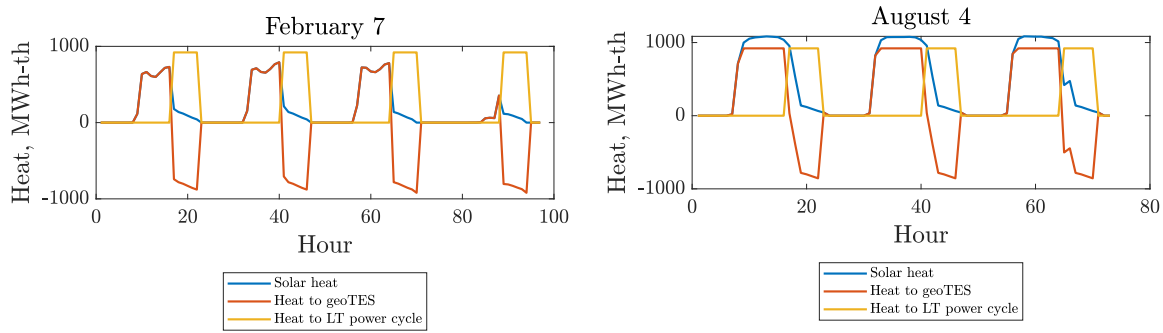


**Figure 21. Thermal energy flows for the 199-MW demonstration PRM CSP-GeoTES system**

Note LT = low-temperature

For the full demonstration (199-MW) system, a solar multiple of 1.25 is chosen, as this provides a balance between achieving a similar electricity output to the PRM calculations (see Table 6), while minimizing curtailment. Energy flows are shown in Figure 21, which indicates the system delivers power for 6 hours per day. The August power flows show that solar heat exceeds the heat that is sent to the GeoTES, and the difference between these curves corresponds to the curtailed energy. Like the 15-MW system, the larger system is also used for daily and seasonal storage. The maximum GeoTES capacity is 664 GWh<sub>th</sub>, which could power the 199-MW<sub>e</sub> heat engine for 722 hours if required.

Economic results are calculated using two approaches, as shown in Table 6. Firstly, a fixed cost of \$850,000 for each well is assumed using insight from PRM. This leads to similar cost results to those provided by PRM. Secondly, GETEM was used to calculate the well costs as a function of depth and fluid properties. GETEM estimates higher costs for the wells because it accounts for drilling inefficiencies that lead to additional time and material costs. This leads to a 35% increase in capital cost. Operational costs also increase (since these are proportional to capital costs) and as a result, the LCOE and GeoTES-LCOS increase by over 60%.

#### **4.6.2 Improving CST-GeoTES Performance and Cost Using Insights From the TEA Model**

The full 199-MW<sub>e</sub> demonstration case study as evaluated using GETEM is used as a base case scenario. Sensitivity to major design parameters is explored by varying the parameters one at a time over a wide range of feasible values. The nominal value, as well as the upper and lower bounds is shown in Table 7. The sensitivity of the LCOE to these parameters is illustrated in the tornado chart of Figure 22, which indicates which parameters have the greatest influence over system performance.

For the nominal design, the main contributions to the total capital cost are the CSP field, power block, and well drilling, which have large and similar values. Therefore, reducing the costs of these components have similar impact on the LCOS—see the top three bars. The LCOE can also be reduced by increasing the solar multiple, which increases the annual electricity generation, despite increased curtailment of solar heat (from 5.7% in the nominal case, to 24.9% in the high solar multiple case).

The most significant changes in LCOE are achieved by modifying parameters that strongly control the number of wells. Increasing the flow rate per well to 100 L/s reduces the total number of wells (and also pumps) from 644 to 74, therefore significantly reducing the capital cost, O&M, and LCOS. Increasing the maximum temperature of the GeoTES similarly reduces the LCOS. Higher temperatures lead to more efficient conversion of heat to electricity—therefore reducing the required size of the solar field and reducing the number of wells. The value of these parameters depends on the properties of the subsurface, which will determine achievable flow rates per well and upper temperature limits.

The tornado chart also illustrates the impact of altering several parameters simultaneously. The “multiple improvements” bar represents a CSP cost of 125 \$/m<sup>2</sup>, power block cost of 750 \$/kW<sub>e</sub>, solar multiple of 1.75, and a well flow rate of 80 L/s. This results in the LCOE having reducing in value from 0.22 \$/kWh<sub>e</sub> to 0.11 \$/kWh<sub>e</sub>.

The pathway to achieving these reduced values of LCOE is illustrated in the bar chart in Figure 23, which shows how the LCOE is distributed between different cost components. The first two columns represent the nominal design evaluated using either fixed well costs or GETEM, and therefore correspond to the results in Table 6. The third column shows results for a case where the well flow rate is increased to 80 L/s, which leads to a significant reduction in subsurface capital costs and O&M. The final column includes additional cost reductions that correspond to the “multiple improvements” bar on the tornado chart, which leads to reduced CSP and power block cost, as well as increased electricity generation.

**Table 7. Sensitivity Parameters for CSP-GeoTES Analysis**

Parameter	Unit	Nominal Value	Lower Value	Upper Value
Power Block Cost	\$/kW <sub>e</sub>	1000	500	1500
CSP Cost	\$/m <sup>2</sup>	170	100	250
Well Depth	m	500	200	1000
Solar Multiple	-	1.25	1.0	2.0
Well Flow Rate	L/s	11	5	100
Max. Temperature	°C	250	200	300

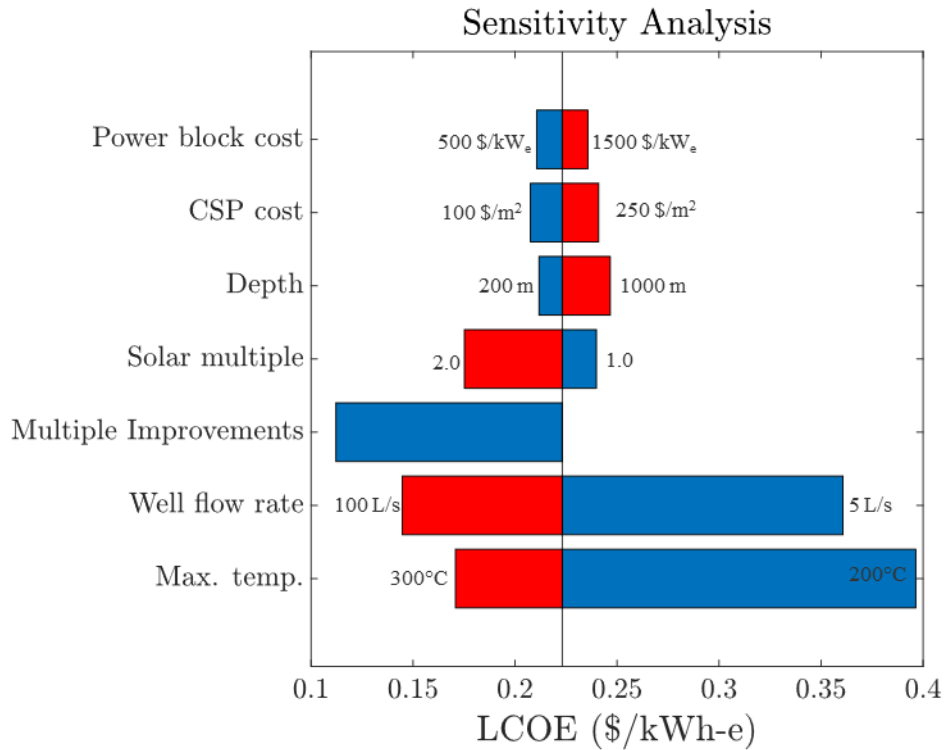


Figure 22. Tornado chart illustrating sensitivity of CSP-GeoTES LCOE to design parameters

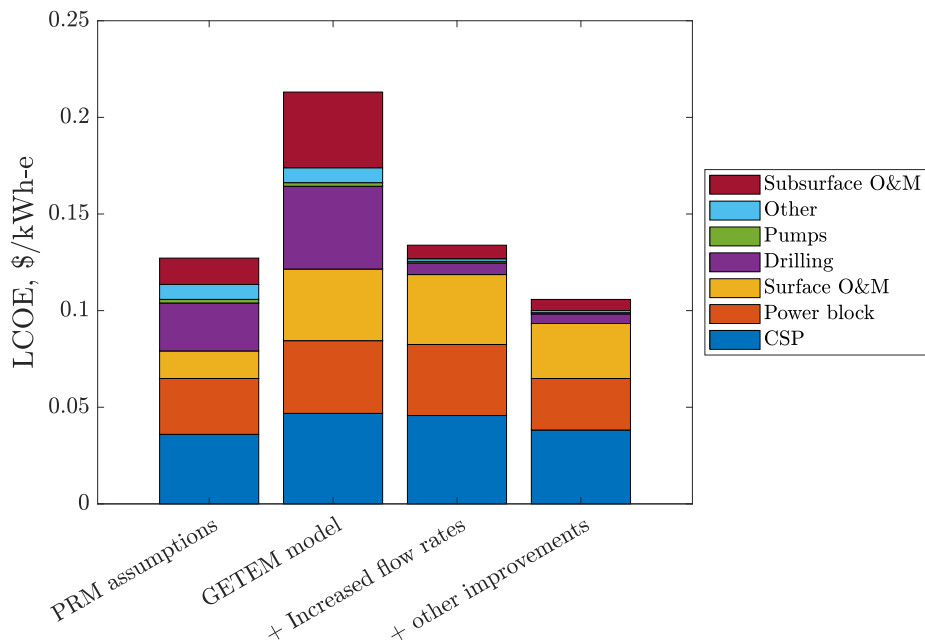
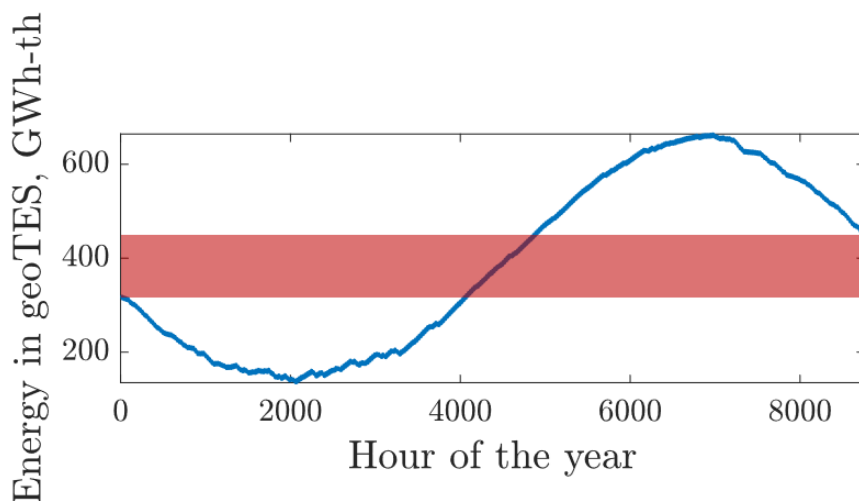


Figure 23. Bar chart showing path to reduced LCOE for CSP-GeoTES

The above results illustrate the influence that design parameters and component costs have on the lifetime system cost. Another important consideration is the value the system can provide by dispatching electricity reliably and flexibly. For example, the nominal 199-MW<sub>e</sub> case with a solar multiple of 1.25 is designed to dispatch power 6 hours per day each day of the year. The simple dispatch scheme delivers this electricity to meet the late-afternoon/evening peak in electricity demand that occurs in California, as shown in Figure 21. In this particular design, the energy capacity of the GeoTES at the end of the year is larger than at the start—as shown in Figure 24. This means that each year, there is a net increase in the energy capacity of the GeoTES. In this example, this “spare capacity” is enough to drive the power cycle for 147 hours. The net energy addition could be reduced to zero by increasing the daily dispatch by 24 minutes. Alternatively, the spare capacity could be used in the event of unexpected grid events. Therefore, each year, the GeoTES is able to provide 6 days’ worth of support to the grid in addition to the daily dispatch, which indicates that CSP-GeoTES can provide multiple services to the grid.



**Figure 24. CSP-GeoTES energy capacity for the 199-MW nominal case with 6 hours dispatch per day. The red area indicates the net increase in energy capacity over the course of 1 year.**

The GeoTES spare capacity could be increased by (1) accumulating it over several years, (2) reducing the number of dispatch hours each day, or (3) increasing the solar field size. The current system design is limited by the constraint that the number of wells is fixed by the size of the power block. Therefore, energy can only be added to the GeoTES at the same rate that it can be withdrawn for the power block. (For the PRM design, this enables the use of inverted seven-spot well layouts). Increasing the solar field size therefore leads to increased curtailment of solar heat, since power is not dispatched during daylight hours (when the demand for additional solar energy is low). Figure 25 shows the thermal energy flows for two solar multiples in August, and illustrates the large quantities of solar energy that cannot be absorbed by the GeoTES in the middle of the day. Despite this, more energy is stored at the “edges” of the day, so the total energy stored and electricity delivered does increase. Results in Table 8 show that increasing the solar multiple to 2.5 allows the system to deliver power for 8 hours per day, while also slightly increasing the spare capacity from 147 hours to 166 hours. However, curtailment increases from 5.7% to 37.8%. Despite this, the LCOE reduces slightly from 0.18 \$/kWh<sub>e</sub> to 0.16 \$/kWh<sub>e</sub>.

(Note, this LCOE calculation includes the potential electricity generated from the spare capacity, as though that capacity was used up each year).

**Table 8. Effect of Increasing Solar Multiple on Dispatch Hours, Spare Capacity, and System Cost**

Parameter	Base Case	Increase Solar Multiple	Increased Solar Multiple and Charging Wells
Solar Multiple	1.25	2.5	2.5
Dispatch Hours per Day	6	8	11
Electricity Generated, GWh <sub>e</sub>	437	588	810
Spare Generation Capacity, h	147	166	933
Total Number of Wells	644	644	1134
Curtailment, %	5.7	37.8	0.0
LCOE, \$/kWh <sub>e</sub>	0.18	0.16	0.15

A third scenario is considered in Table 8 whereby additional wells are drilled to enable all the available solar heat to be stored in the GeoTES. Thermal energy flows are illustrated in Figure 26, which shows large quantities of heat being stored in the middle of the day. This mode of operation significantly increases the GeoTES energy capacity, and therefore enables an increased number of hours of daily dispatch. In this case, the daily dispatch is 11 hours, which is distributed over the morning and evening peaks in electricity demand. In addition, the spare capacity in the GeoTES increases to 933 hours per year, meaning that each year, the GeoTES could provide grid support for 39 days. This design requires a large number of additional wells, increasing from 644 to 1134. While this substantially increases the capital cost, the LCOE reduces slightly to 0.15 \$/kWh<sub>e</sub>. Further work is required to understand the optimal design to minimize the LCOS and to quantify the value to the grid of a system that can reliably provide daily dispatch and large quantities of energy capacity.

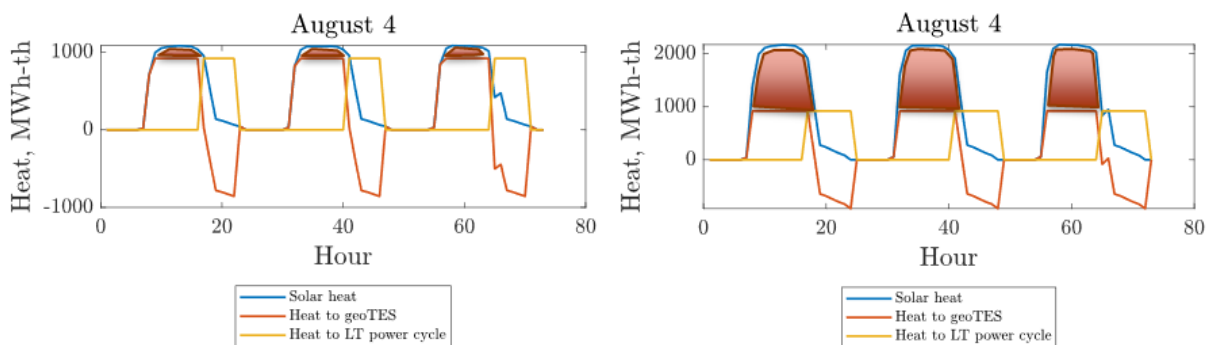


**Figure 25. Thermal energy flows in August with solar curtailment illustrated in red areas. Left: Solar multiple = 1.25. Right: Solar multiple = 2.5.**

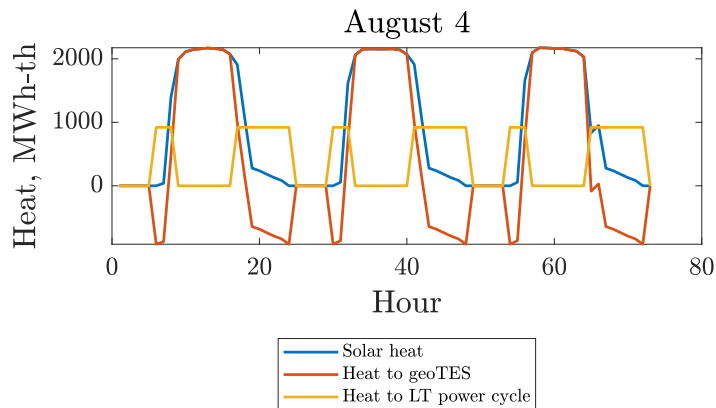


**Figure 26. Thermal energy flows in August for a solar multiple of 2.5 for a system with additional charging wells to reduce curtailment**

Another design modification for CSP-GeoTES was introduced in Figure 3b. CSP can generate temperatures higher than those that can be stored in the GeoTES,<sup>1</sup> and higher temperatures enable more efficient power cycles and reduced solar field sizes. Therefore, a combined cycle design is proposed to integrate the benefits of high-temperature solar heat and low-cost GeoTES. The solar collectors are designed to generate heat at around 350°C, and this heat is either stored in high-temperature storage tanks on the surface using thermal oils or converted to electricity in a back-pressure steam turbine. The high-temperature cycle and storage is therefore suitable for providing short-duration peaking power at relatively good efficiency.

Once the high-temperature storage is fully charged, solar heat is delivered to the back-pressure steam turbine, which generates electricity and medium-grade thermal energy at the turbine exit. The turbine exit temperature is chosen to match the GeoTES temperature and is therefore used to charge the GeoTES. When peaking power is required, the high-temperature storage is dispatched, which powers the high-temperature steam cycle. The steam turbine exit heat is then used to power the low-temperature power cycle. Once the high-temperature storage is depleted, the low-temperature power cycle is driven by discharging the GeoTES.

Thermal energy flows for this system are shown in Figure 27 for February and August. The dispatch of this system is considerably more complex than the simple CSP-GeoTES system, and the scheme described above is just one example to illustrate how this system could behave. Improved dispatch schemes would consider hourly demand for electricity. Figure 27 shows how the combined cycle provides electricity to the grid in both the morning and afternoon at the expected peaks in electricity demand. The high-temperature storage is primarily dispatched to meet the afternoon peak when electricity has the highest value. In August, the GeoTES is then dispatched later in the evening and in the morning. In February, solar availability is lower, so less power is produced from the high-temperature system, and the GeoTES provides more

<sup>1</sup> The GeoTES systems considered here use liquid water as the heat transfer fluid. Keeping water in the liquid phase requires high pressures at high temperature, which ultimately limits the maximum temperature that can be stored.



energy throughout the day. The GeoTES is also available to provide energy capacity as described above, although that capability has not been explored for the combined system.

**Table 9. Techno-Economic Results for a Combined CST-GeoTES System With High-Temperature Storage and Power Cycle**

Parameter	Combined CST-GeoTES
Solar multiple	2.5
Topping cycle power, MW <sub>e</sub>	100
Bottoming cycle power, MW <sub>e</sub>	137
CAPEX, \$/kW <sub>e</sub>	9,135
LCOE, \$/kWh <sub>e</sub>	0.14

Techno-economic results are shown in Table 9. This system does not provide a direct comparison with the simple CSP-GeoTES results as the power rating of the bottoming cycle differs. However, the results are still informative. The combined CSP-GeoTES is more complex leading to higher CAPEX (9135 \$/kW<sub>e</sub> compared to 7842 \$/kW<sub>e</sub> for the 199 MW<sub>e</sub> simple CSP-GeoTES evaluated with GETEM in Table 6). Despite this, the LCOE is reduced from 0.22 \$/kWh<sub>e</sub> to 0.14 \$/kWh<sub>e</sub>, suggesting that the high-temperature components are a good investment. Further investigation is required to quantify the value and benefit that higher-efficiency, high-temperature storage may provide to the system in terms of dispatch flexibility. Other system configurations are also possible and may be worth exploring.

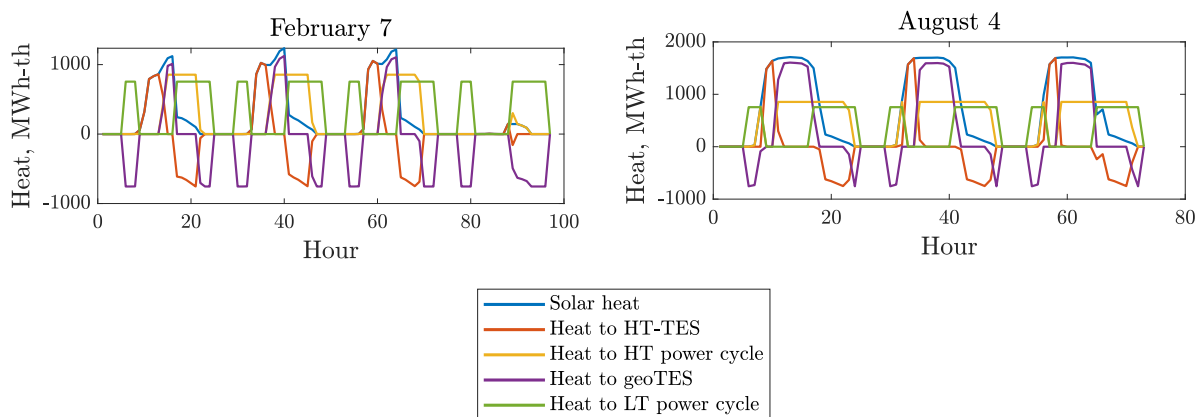


**Figure 27. Thermal energy flows for a combined CST-GeoTES system with high-temperature storage and power cycle**

This system is intended for electricity generation but could also be used to deliver industrial process heat, a significant proportion of which requires temperatures less than 200°C (Kurup & Turchi, 2015; Mcmillan et al., 2021). Here, the LCOH is calculated by considering the total thermal energy deployed by the system and not counting the power cycle capital cost. Two heat delivery options are considered: 12 hours per day or 24 hours per day. The solar multiple is

adjusted to deliver this quantity of heat each day of the year, and results are shown in Table 10. To deliver base load heat (24h per day) a large solar field with more charging wells is required, which leads to a higher LCOH than the 12h use case. The 12h LCOH of 0.018 \$/kWh<sub>th</sub> is competitive with the average industrial price of natural gas in California in 2022–2024 which ranged on average from 0.041–0.047 \$/kWh<sub>th</sub> (U.S. Energy Information Administration, 2023). However, the Henry Hub natural gas price is lower, at 0.007–0.022 \$/kWh<sub>th</sub> over the same timeframe.

**Table 10. LCOH of CSP-GeoTES Systems Delivering Either 12h or 24h Heat per Day**

Parameter	12 Hours	24 Hours
Solar Multiple	2.5	4.4
LCOH, \$/kWh <sub>th</sub>	0.018	0.023
Curtailment	5.7%	0%

Further options to be explored include using CST-GeoTES to deliver combined heat and power. This could help avoid the curtailment of solar heat that is shown in Table 8 if the solar heat can be used in an industrial process during the day.

#### 4.6.3 CST-GeoTES LCOS as a Function of Storage Duration

The results presented so far inextricably link solar thermal generation with energy storage and electricity delivery. The combined design parameters of solar field size, number of wells, power block rating, and dispatch decisions determine the quantity of energy stored, the quantity of electricity delivered, and the storage (or dispatch) duration. In the above cases, storage duration itself is difficult to define. The GeoTES may dispatch electricity for 6 hours per day, but some of this energy will have been stored for hours and some for months. The CST-GeoTES system is most simply thought of as an electricity generation system and thus, the LCOE is the most straightforward metric to use.

GeoTES plays an integral role in facilitating the daily and seasonal dispatch of electricity from CST-GeoTES, which may also be thought of as an energy storage facility, which stores heat to later convert to electricity. From this point of view, evaluating the system using the LCOS seems more appropriate, and enables a comparison with alternative energy storage technologies, such as lithium-ion batteries and molten-salt thermal energy storage. Energy storage technologies are typically described by their storage duration without considering nuanced details of their dispatch profile which may include numerous shorter cycles as well as longer ones—as typified by GeoTES systems. Other important characteristics include the round-trip efficiency and the “idle” period; that is, the duration for which energy is stored in system while not charging or discharging. Different combinations of these characteristics will lend a technology to providing different services such as seasonal storage, transmission/distribution investment deferral, renewables integration, power reliability, and energy arbitrage. The LCOS of CSP-GeoTES is calculated for a range of different storage durations and efficiency and compared to lithium-ion batteries and molten-salt thermal energy storage (MS-TES), as shown in Figure 28. These technologies are chosen to provide an update to a similar graph previously published in Sharan et al. (2021).

CSP-GeoTES LCOS is calculated for the system with improved flow rates (this design is a 199-MW<sub>e</sub> system using PRM's base case except with improved well flow rates of 80 L/s). Those results are used to calculate the GeoTES capital cost  $C_{cap}$  and O&M, where the only contributions to capital cost are from the wells, pumps, other subsurface equipment, and the power cycle. For a full LCOS appraisal, the required solar heat input  $\dot{Q}_{in}$  is procured at an average price of heat  $p_{heat}$  and electricity may also be purchased from the grid to power the pumps  $\dot{W}_{in}$  at an average price  $p_{elec}$ . Here, these prices are set to 0 \$/kWh, so that the resulting curves simply show the contribution of the GeoTES system to the full LCOS and do not consider uncertain externalities. The LCOS may then be calculated for any feasible combination of discharge duration  $\tau_{dis}$  and annual cycle frequency  $N_{cyc}$  with the following formula:

$$LCOS = \frac{C_{cap} \cdot FCR + O\&M + p_{heat}\dot{Q}_{in}\tau_{chg}N_{cyc} + p_{elec}\dot{W}_{in}\tau_{chg}N_{cyc}}{\dot{W}_{out}\tau_{dis}N_{cyc}} \quad (6)$$

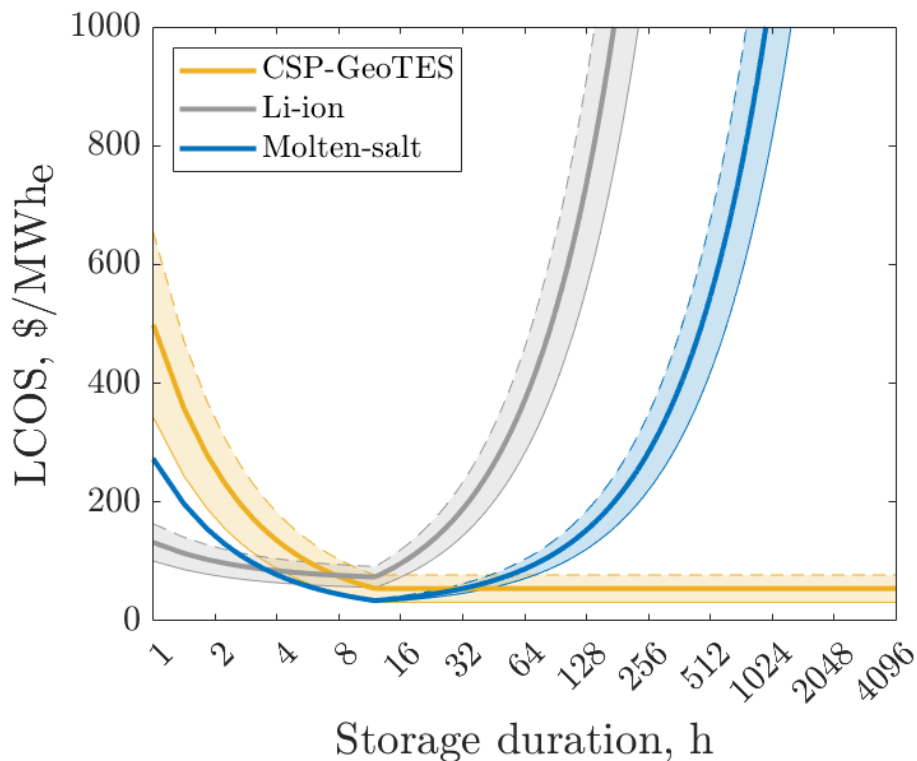
Where  $\dot{W}_{out}$  is the discharging power output and  $\tau_{chg}$  is the charge duration, which here is assumed to equal  $\tau_{dis}$ . For Figure 28, it is assumed that the storage system cycles as many times as feasible per year, with a maximum number of cycles of 365.

Figure 28 shows that the CSP-GeoTES LCOS decreases as the storage duration increases to 12 hours, as the annual electricity output increases while the cost remains the same. System capital cost does not vary as a function of discharge duration—once the wells are drilled, additional energy capacity is simply added to the GeoTES without requiring the procurement of more storage capacity. Increasing the storage duration further leads to a constant value of LCOS, as the annual energy output remains constant. The figure shows a shaded band that represents the impact of efficiency on the LCOS: lower efficiency leads to higher LCOS. The low efficiency case uses a GeoTES storage temperature of 200°C (which reduces conversion efficiency in the power cycle) and a GeoTES recovery efficiency of 75%. The high-efficiency case uses a storage temperature of 300°C and recovery efficiency of 95%.

Results are also shown for lithium-ion batteries and molten-salt thermal energy storage. Costs are taken from the 2024 Annual Technology Baseline and are expressed in terms of a cost of power capacity,  $c_P$  (\$/kW) and a cost of energy capacity,  $c_E$  (\$/kWh), where the total capital cost is  $c = (c_P + c_E\tau_{dis})\dot{W}_{out}$ . For Li-ion batteries,  $c_P = 233$  \$ / kW<sub>e</sub> and  $c_E = 252$  \$/kWh<sub>e</sub>, while for MS-TES,  $c_P = 1701$  \$/kW<sub>e</sub> and  $c_E = 25$  \$/kWh<sub>th</sub>. Shaded bands on Figure 28 indicate the influence of efficiency. Li-ion round-trip efficiency is assumed to vary between 70% and 95%, while the thermal-to-electric power block efficiency for MS-TES varies between 25% and 41.2% and effectively depends on the storage temperature.

For short storage durations, Li-ion and MS-TES have lower LCOS than CSP-GeoTES. However, Figure 28 demonstrates that the LCOS of Li-ion and MS-TES increase for storage durations over 12 hours, as the system cost increases while the energy output remains constant. Although there is considerable uncertainty in the plotted results, the figure suggests that CSP-GeoTES becomes competitive with Li-ion for storage durations over 12 hours and outperforms MS-TES for storage

durations over 32 hours. For seasonal storage durations (e.g., >500 hours), CSP-GeoTES LCOS is considerably lower than these other technologies. Further work is required to quantify the uncertainty, investigate the impact of heat and electricity prices (and their interaction effect with efficiency), and consider the time-value of dispatched power.



**Figure 28. LCOS of CSP-GeoTES, Li-ion and molten-salt thermal energy storage as a function of storage duration. Shaded areas indicate the effect of efficiency on the LCOS.**

#### 4.7 Non-Technical Hurdles to PRM’s GeoTES Demonstration

Based on PRM’s experience so far, regulatory uncertainty is the most significant non-technical risk to GeoTES development in California. California agencies, specifically CalGEM and the Central Valley Regional Water Quality Control Board, have not demonstrated a willingness to consider GeoTES as a novel geothermal opportunity. This is based on old Underground Injection Control rules for Class II injectors from the U.S. Environmental Protection Agency, which states that if there is any oil, no matter how insignificant in a production steam, the injectors are for oil and gas enhanced or improved oil recovery. Geothermal injection wells are Class V, and carbon capture and storage wells are Class VI. These agencies have processed PRM’s GeoTES project along traditional oil and gas permit pathways of Class II. In order to move forward with certainty, PRM’s GeoTES project would require dedicated legislation or agency acceptance that GeoTES provides clean power, without being classified as oil and gas. GeoTES could provide an opportunity for the State of California to unlock tremendous clean geothermal technology, yet regulations designed to protect the environment remain an obstacle for GeoTES to overcome. PRM has worked to gain support from a long list of significant stakeholders, such as Westside Water Authority, and seeks qualification under AB 1373, among other recent initiatives to streamline permitting and access to geothermal power.

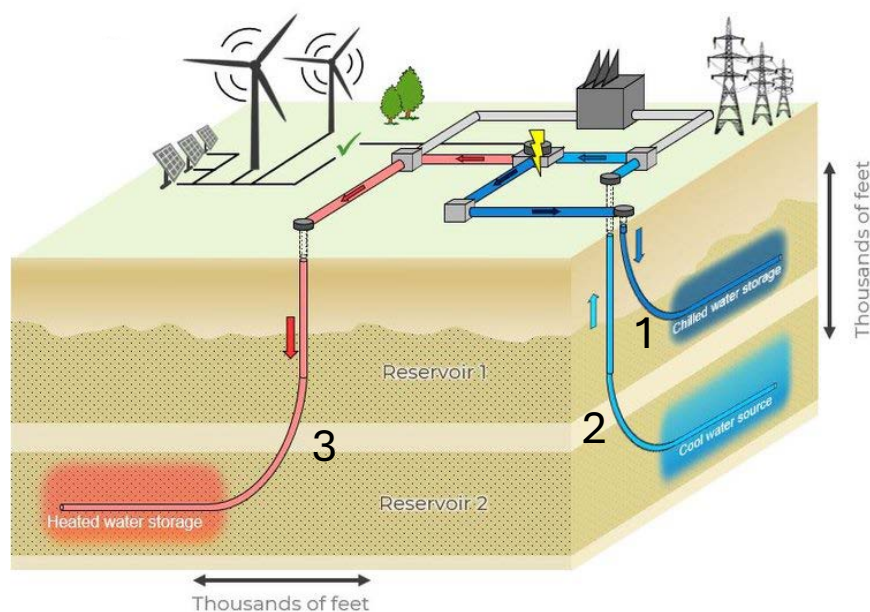
## 5 EarthBridge Energy CB-GeoTES Demonstration

### 5.1 Project Overview

EarthBridge Energy aims to provide flexible and sustainable long-duration GeoTES to their customers. Their GeoTES concept is based on harnessing the potentially excess and wasted solar and wind energy at off-peak and low-price periods using a Carnot battery system (CB-GeoTES). EarthBridge plans to demonstrate and commercially deploy CB-GeoTES systems at multiple sites in the United States. Initially, they plan to perform a pilot demonstration with one of their partners in Texas to confirm their model outputs and prototype designs for CB-GeoTES. EarthBridge has also secured land rights for acreage in West Texas where they intend to deploy a commercial-scale project.

An illustration of EarthBridge’s CB-GeoTES system design is shown in Figure 29. The subsurface system consists of a shallow reservoir for cold storage (Reservoir 1), a deeper reservoir for hot storage (Reservoir 2), and a set of three wells for: (1) chilled, (2) cool, and (3) heated water. Well 1 is drilled into a shallow reservoir, and Wells 2 and 3 are completed in a deeper reservoir. The shallower reservoir is assumed to be at a lower temperature compared to the deeper reservoir (as depicted in Figure 29), but the system design can utilize the same reservoir for source water and hot and cold storage. Any temperature difference between these reservoirs will depend on the site-based pre-GeoTES subsurface thermal gradient. The surface design consists of an industrial-scale water-source heat pump and a similar-scale heat engine. Both power cycles use a working fluid such as CO<sub>2</sub>, isopentane, or R125 in a closed loop.

(a) Charge



### (b) Discharge

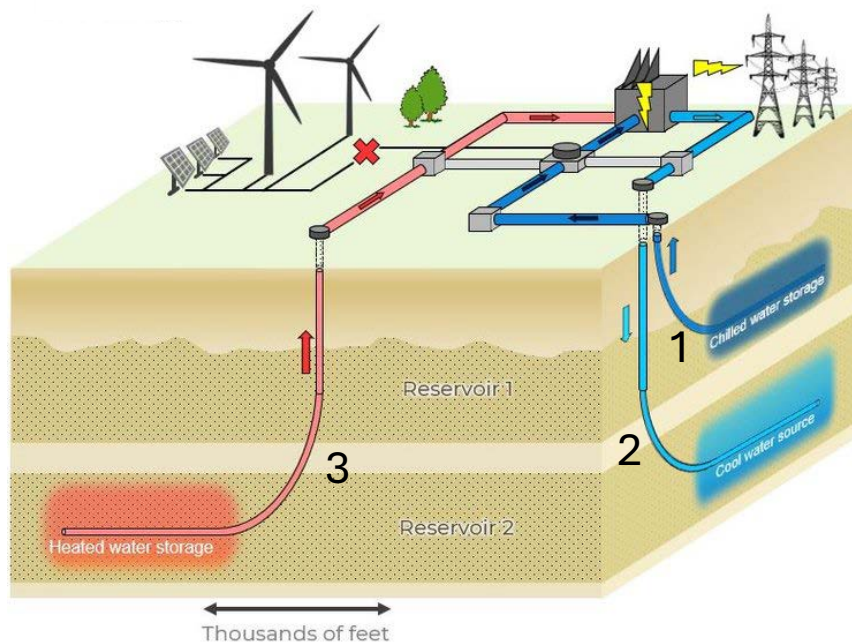


**Figure 29. EarthBridge Energy’s CB-GeoTES concept. Showing a subsurface system with three wells connected to surface system that mainly consists of a heat pump and heat engine**

Figures from (EarthBridge Energy, n.d.).

During the charging process, cool water is withdrawn from Reservoir 2, via Well 2, to the heat pump. The heat pump utilizes the thermal energy provided by both fluids in its compression-evaporation cycle. The thermal energy from cool water is exchanged with the working fluid to preheat it before it enters the compressor. The resulting chilled water is injected through Well 1 into Reservoir 1 for cold storage. After the working fluid is compressed to a supercritical state, its thermal energy is exchanged with the Reservoir 2 fluid, raising it to a higher temperature. This hot fluid is then reinjected into Reservoir 2 via Well 3 for heated water storage. The working fluid is then expanded to a subcritical state to restart the heat pump cycle.

When power is needed by the grid, the heated water stored in Reservoir 2 is produced via Well 3 to the surface and exchanges thermal energy with the high-pressure working fluid within the closed power cycle of the heat engine to a supercritical state. The supercritical working fluid is used to drive a turbine-generator set to generate electricity that is transmitted to the grid. The cool water is reinjected into another section of Reservoir 2 through Well 2. To increase the heat engine efficiency, the chilled water from Reservoir 1 is used to cool the working fluid exiting the turbine-generator set before it is recycled within the loop to begin another compression-evaporation cycle.

## 5.2 Subsurface Reservoir

EarthBridge is targeting multiple sandstone bearing reservoirs between the 2450 ft and 4500 ft depth interval at their test site. These zones are interbedded with shale and dolomite minerals. For the current collaboration with the GeoTES team, EarthBridge has provided information



about a 100-ft thick layer of sandstone at an initial temperature of 50°C. The average permeability and porosity of 1 Darcy and 30 p.u., respectively, makes it a very suitable volumetric storage candidate. The reservoir is saturated with brackish water with an average total dissolved solids (TDS) of 1,215 mg/l (see Table 11). The thermal properties of the reservoir rock and fluid are shown in Table 12. The one order of magnitude difference in specific heat capacity and thermal conductivity between the reservoir rock and the reservoir fluid shows good thermal storage capabilities. We assume that the caprock and bedrock of the reservoir mostly comprise shale based on information from well logs at the site.

**Table 11. Reservoir Brine Composition, Total Dissolved Solids, Hardness, and Specific Conductivity**

Solute composition and total dissolved solids (TDS) are in mg/l.

Well	SiO <sub>2</sub>	Ca	Mg	Na	K	HCO <sub>3</sub>	CO <sub>3</sub>	SO <sub>4</sub>	Cl	NO <sub>3</sub>	TDS	Hardness as CaCO <sub>3</sub>	% Na	Specific Conductivity (micro-mhos at 25°C)
E-82	46	77	7.1	327	327	164		293	348	2.2	1180	221	76	1850
E-83	42	17	1.8	470	470	522	28	1.2	435	7.5	1250	50	95	2170

**Table 12. Physical and Thermal Properties of the Reservoir Rock and Fluid**

Parameter	Value
Fluid viscosity and fluid density at 150°C	0.1864 cP; 0.918 g/cm <sup>3</sup>
Thermal conductivity, rock	2.0 W/(m·K)
Thermal conductivity, fluid	0.685 W/(m·K)
Thermal diffusivity, fluid	0.174 mm <sup>2</sup> /s
Thermal diffusivity, rock	1.127 mm <sup>2</sup> /s
Specific heat capacity, fluid	4.3 J/(g·K)
Specific heat capacity, rock	0.71 J/(g·K)
Thermal expansion, fluid	0.1 K <sup>-1</sup>
Thermal expansion, rock	11 × 10 <sup>-6</sup> K <sup>-1</sup>

At the demonstration scale, the development will consist of a well doublet (i.e., single well pair)—Wells 2 and 3 in Figure 29—with a discharge flow rate of 25 L/s that is equivalent to discharging 10 MW<sub>th</sub> of thermal energy. The wells will be operated in a complementary push-pull cycle, such that during the charge cycle, cool water produced from Well 2 will be injected (after heating) into the reservoir using Well 3 and then during the discharge cycle, hot water produced from Well 3 will return to the reservoir via Well 2, thereby maintaining reservoir pressure. The full-scale system will integrate Well 1 for cold storage.

The commercial-scale facilities are anticipated to initially discharge 20 MW<sub>e</sub> during Phase 1 of the projects with plans to expand up to 200 MW<sub>e</sub> once fully developed. Phase 1 will consist of 8 well doublets with a per well flow rate of 60 L/s. The bottomhole of each well will be located at

sufficient separation to prevent major fluid and thermal interference at the longest storage cycle frequencies. All wells will have a 1,000-foot lateral production/injection interval at their respective target depths. At this interval, the drilled 9-5/8-inch hole will be completed with a 7-inch casing.

### 5.3 Surface Plant

The surface unit design, shown in Figure 30, will primarily consist of a heat pump and heat engine connected to the wells via surface gathering lines. The former will convert grid or behind-the-meter electricity to thermal energy, while the latter will convert the stored thermal energy from the storage reservoirs back to electricity during hours of grid demand. The heat pump unit comprises a compressor, turbo expander, and two heat exchangers. EarthBridge is also researching other working fluids suitable for this application. For the demonstration project, the heat pump will be rated at 10 MW<sub>th</sub>, corresponding to flow rate of 25 L/s for a 100°C temperature lift (i.e., the difference between the evaporator/source and condenser/sink temperature). The commercial-scale design will accommodate a total thermal capacity of 200 MW<sub>th</sub> (400 L/s). The proposed CB-GeoTES system will be designed for a hot storage temperature of 150°–200°C; with a goal of increasing this to 250°C for greater heat engine efficiency depending on reservoir geochemical and geomechanical constraints. The heat engine unit will consist of a turbine-generator set, a turbo pump, and two heat exchangers. The unit will be designed to deliver >1 MW<sub>e</sub> gross power output for the demo project (20 MW<sub>e</sub> for the full development). So far, EarthBridge's model estimates that a minimum hot storage temperature of 140°C will be economical. A sensitivity analysis around the impact of hot and cold storage temperatures among other factors on the project feasibility is discussed in Section 5.6.

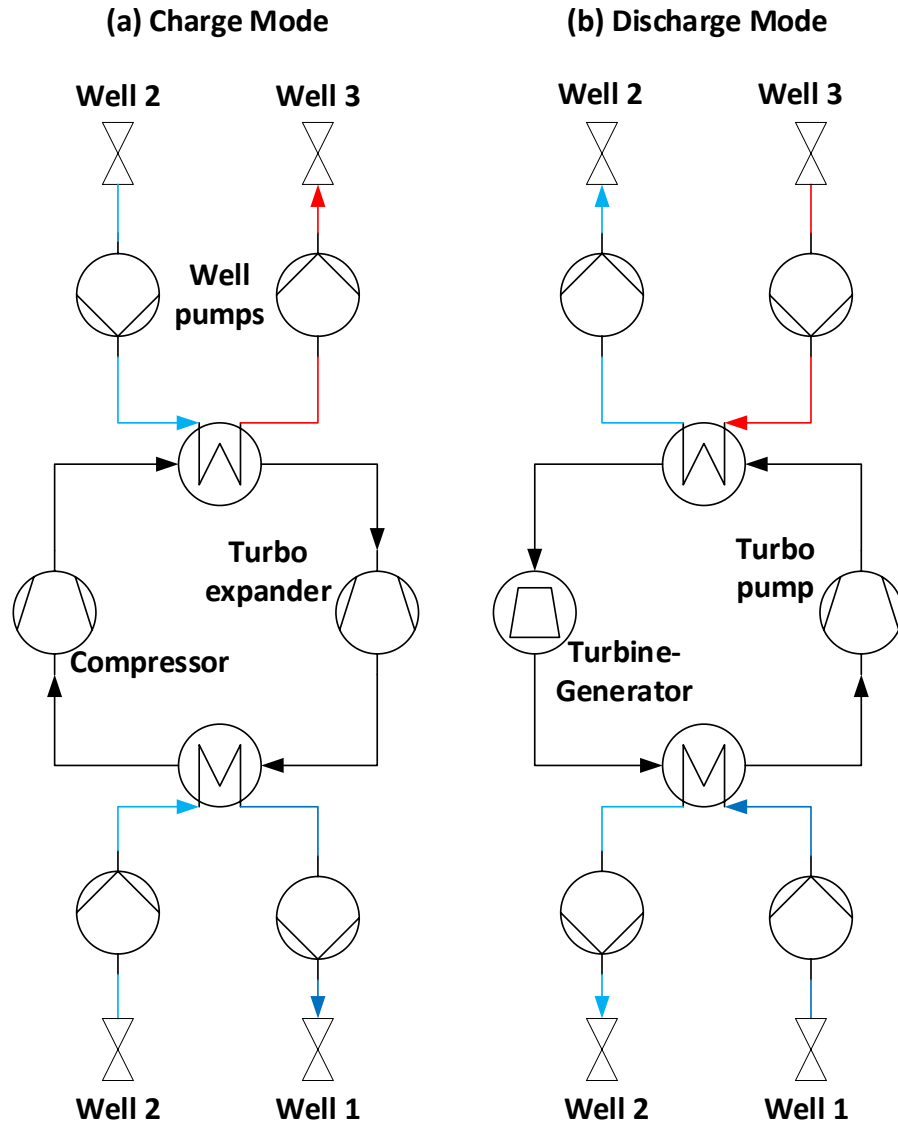


Figure 30. Line diagram of the surface unit showing the components in the heat pump (left) and the heat engine (right). The heat pump consists of a compressor, turbo expander, and two heat exchangers. The heat engine comprises a turbo pump, turbine-generator, and heat exchangers. The black flow line represents working fluid flow in the closed loop. The dark blue, light blue, and red lines represent chilled, cooled, and heated water, respectively.

### 5.4 System Operation

EarthBridge plans to operate the CB-GeoTES as a long-duration energy storage system capable of a minimum of 12-hour constant power discharge. As a base case, the system will be operated diurnally, with 12-hour charge and discharge daily cycles. At full field-scale, with available reservoir volume, the system will be designed for seasonal storage and discharge of up to 60 days (timescale >1,000 hours).

## 5.5 EarthBridge Pilot Demonstration Techno-Economic Assessment

EarthBridge has developed a TEA model that is based on the pumped thermal energy storage module in NREL’s StoreFAST model. This model follows a simplified approach to estimate the CAPEX, O&M cost, and LCOE for a specified discharged power output. The model uses a discounted cash flow approach to determine the present values of costs and payback period. In the model, EarthBridge’s revenue is derived from participating in both arbitrage (80%) and fixed capacity payments pricing (20%). Table 13 summarizes the model inputs, financial assumptions, and model results.

**Table 13. EarthBridge's TEA Model Input and Output Parameters**

Parameter	Unit	Value
<b>Input</b>		
Power output	MW	10
Storage duration	h	504
Electricity pricing	\$/kWh, average	0.086
Project lifetime	year	30
Interest rates	%	5.6
Tax rate	%	29.84
Insurance rate	% of CAPEX	0.65
<b>Output</b>		
CAPEX	\$	42,960,000
O&M	\$	1,761,337
Payback period	year	6
<b>LCOE</b>	<b>\$/MWh</b>	<b>68</b>

## 5.6 EarthBridge Demo Techno-Economic Analysis Case Study Validation

We use the system design and financial details provided by EarthBridge as inputs to the TEA model with the objective of validating the model. The TEA model is then used to explore potential avenues for improved performance and cost.

### 5.6.1 TEA Validation

A key decision for the CB-GeoTES system is the design of the CB. These devices have not been commercialized so far, meaning a wide variety of heat pump and heat engine configurations may be chosen, and many have been proposed (Olympios et al., 2021) and have started development (Novotny et al., 2022). A further decision is whether the CB will create both hot and cold thermal energy storage. Previous work indicated that the cold storage would require a larger number of wells than the hot storage, while only contributing slightly to the round-trip efficiency. An alternative design could use the environment as the “cold storage”—i.e., using the air as the heat source for the heat pump and the heat sink for the heat engine. Doing so would reduce the cost at the expense of lower efficiency. A number of different CB designs were

considered for CB-GeoTES, including some that used supercritical CO<sub>2</sub> as the working fluid (based on earlier work (McTigue et al., 2020; Morandin et al., 2011)). Ultimately, R125 was found to be a suitable fluid, as its properties enabled better integration with the cold geological fluid.

Three options are explored here and applied to the EarthBridge case study: (1) a CB design using R125 working fluid with both hot and cold storage; (2) a CB design using R125 working fluid with only hot storage; and (3) a CB using a commercially available heat pump developed by MAN Energy Solutions with CO<sub>2</sub> working fluid and hot storage only. The heat engine cycle uses a design similar to that used in geothermal binary cycles. The first two concepts use novel heat pump and heat engine designs specifically developed for this application and have not been demonstrated. The third option is a design that feasibly could be procured off-the-shelf by using heat pump and heat engine units that are commercially available.

A temperature-entropy diagram of the R125 heat pump is illustrated in Figure 31; this is a recuperated transcritical cycle. This heat pump creates both hot thermal storage and cold thermal storage. Cool fluids are drawn from a reservoir at 25°C and used as the heat source for the heat pump and are thus cooled as energy is extracted from them. The cold fluids are then reinjected to the reservoir at 5°C. Simultaneously, warm fluids are drawn from a reservoir at 50°C and used as the heat pump heat sink, thereby being heated to 162°C before being reinjected. This system requires a relatively large number of cold wells compared to hot wells, and this is predominantly because the cold fluid goes through a small temperature change compared to the hot fluid. The second CB concept considered does not use cold storage. Instead, the atmosphere is used as the heat source for the heat pump and the heat sink for the heat engine. A recuperated, transcritical R125 cycle is again used (as in Figure 31), although the heat pump evaporator is at a slightly higher temperature.

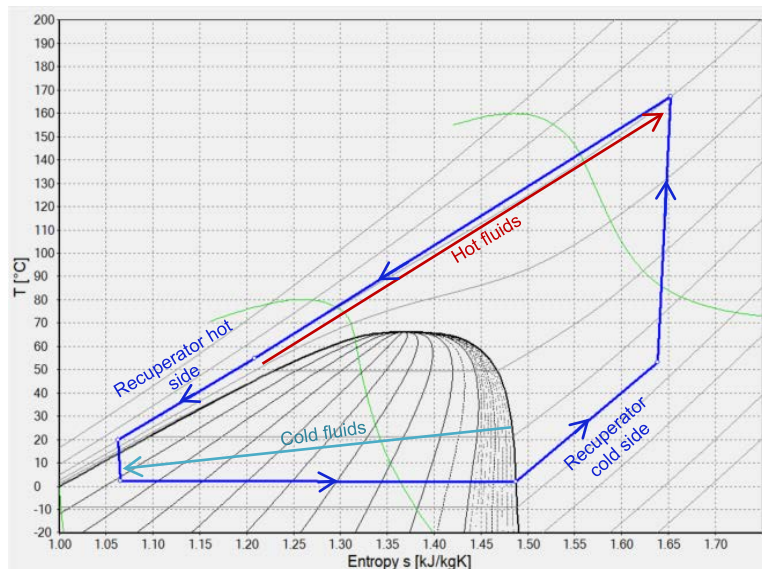


**Figure 31. Temperature-entropy diagram of a recuperated heat pump using R125 working fluid. The heat pump heats one set of production fluids up to 162°C and another set of fluids are cooled to 5°C. The hot and cold fluid streams are then reinjected to separate regions of the GeoTES to create hot and cold storage.**

These three CB designs are compared in Table 14, and are designed to operate with the 10-MW<sub>e</sub> EarthBridge case study. The design that uses cold storage requires 10 cold wells (and pumps) in addition to the four wells for the hot storage system. The round-trip efficiency is the electricity output of the heat engine divided by the electricity input to the heat pump, and it is apparent that CB with cold storage only has a slight advantage over the system without. This is because the cold storage is limited by the freezing point of water, so the cold storage is not much colder than the environment. The system using commercially available technologies is the least efficient—partly because different cycles are used in the heat pump and heat engine, which leads to some inefficiencies. These cycles have round-trip efficiencies in the region of 40% which is typical of CBs of this design (Mercangöz et al., 2012). The table also shows a “real” round-trip efficiency that incorporates the parasitic energy consumption in well pumping and air-cooled evaporators/condensers. In this case, the system with cold storage has a clear superior efficiency. This is due to the large energy consumption that is required to move large amounts of air through the heat pump evaporator and heat engine condenser, compared to the pumping requirements for cold geothermal water to provide the same function.

**Table 14. Technical Performance of Three Carnot Batteries Considered for the 10-MW EarthBridge Case Study**

Parameter	Cold Storage	No Cold Storage	Currently Available
Charge cycle	Transcritical R125	Transcritical R125	MAN CO <sub>2</sub>
Discharge cycle	Transcritical R125	Transcritical R125	“Geothermal binary”
Hot wells	4	4	4
Cold wells	10	0	0
Round-trip efficiency, %	43.4	42.8	36.7
Real round-trip efficiency, %	38.3	31.5	26.8

System costs are evaluated using two methods: (1) a fixed well cost of \$850,000 and fixed pump costs of \$300,000 based on expertise from EarthBridge. It should be noted that the EarthBridge techno-economic results in Table 13 do not include the cost of the charging electricity, so this factor is not included in these results; (2) using assumptions from GETEM to evaluate well and pump costs and assuming an electricity price of 0.05 \$/kWh<sub>e</sub>.

The LCOS for the three CB designs and two economic metrics are compared in Figure 32, which also illustrates the distribution of LCOS between different components. The first bar illustrates the LCOS for a system using fixed well and pump costs and the same efficiency (50%) as the EarthBridge system in Table 13. The LCOS (roundly 0.1 \$/kWh<sub>e</sub>) is slightly higher than the value evaluated by EarthBridge (0.068 \$/kWh<sub>e</sub>). The LCOS is slightly higher when lower round-trip efficiencies are used. The LCOS calculated using GETEM is higher than when fixed costs are used: well costs tend to be larger, but pump costs are lower. However, including the cost of charging electricity substantially increases the LCOS. This is mainly a result of the low round-trip efficiency, which means that over 60% of the procured electricity is lost. Including the electricity cost leads to LCOS around 0.25 \$/kWh<sub>e</sub>. The LCOS of the systems with and without cold storage are very similar, with the cold storage system having a lower LCOS by 0.01 \$/kWh<sub>e</sub>.



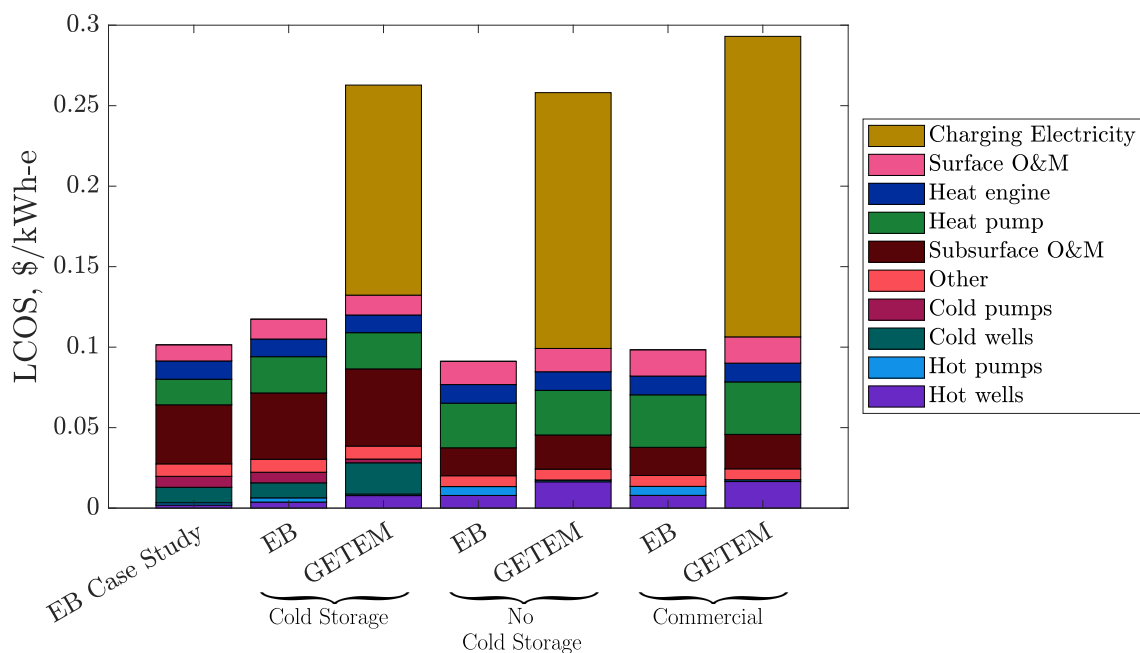


**Figure 32. Bar chart showing three Carnot battery designs applied to the EarthBridge 10-MW case study. Results are evaluated using fixed costs suggested by EarthBridge (marked “EB”) and also by using GETEM.**

### 5.6.2 Improving CB-GeoTES Performance and Cost Using Insights From the TEA Model

The CB-GeoTES system using commercially available heat pumps/engines and evaluated with GETEM is used as a base case scenario. (This design was chosen since it is the most likely to be demonstrated in the near term). Sensitivity to major design parameters is explored by varying the parameters one at a time over a wide range of feasible values. The nominal value, as well as the upper and lower bounds are shown in Table 15. The sensitivity of the LCOS to these parameters is illustrated in the tornado chart of Figure 33, and indicates which parameters have the greatest influence over system performance.

**Table 15. Sensitivity Parameters for the CB-GeoTES Analysis**

Parameter	Low	Nominal	High
Depth, m	500	1000	1500
Heat engine cost, \$/kW <sub>e</sub>	500	1000	1500
Heat pump temp, °C	120	150	170
Heat pump Cost, \$/kW	500	1000	1500
Heat pump rate	2x	1x	2x-lo elec.
Well flow rate	10	60	125
Electricity price, \$/kWh <sub>e</sub>	0.01	0.05	0.10

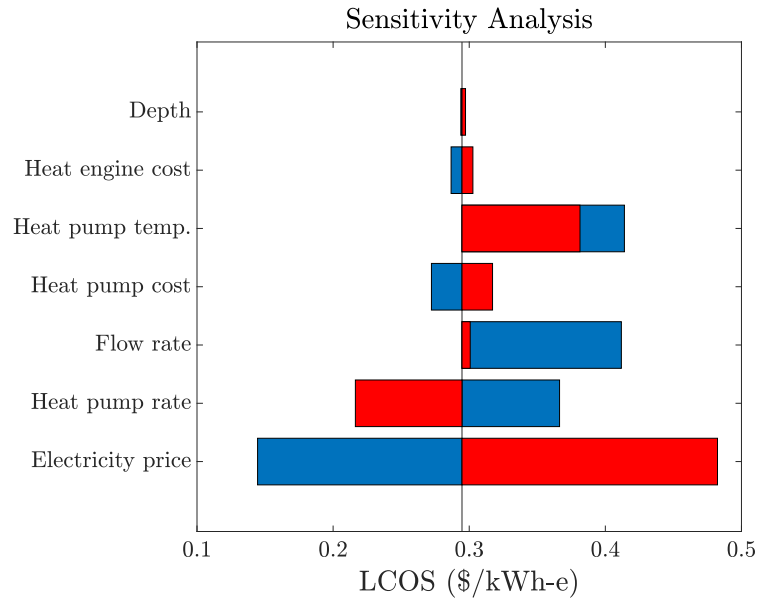


**Figure 33. Tornado chart illustrating sensitivity of CB-GeoTES LCOS to design parameters**

The electricity price has the largest influence over LCOS and the choice of electricity market, charging strategy, and possibly use of behind-the-meter electricity generation will have an important role in the commercialization of this technology. Similar to the CSP-GeoTES design, the well flow rates also have a significant effect on the LCOS with larger flow rates leading to fewer wells and lower costs. The cost of the heat pump and heat engine are also important considerations, with the system being more sensitive to the heat pump cost since it has a larger power rating (due to the inefficiencies).

Two alternative maximum temperatures are considered: 120°C and 170°C, and details of commercial heat pumps that operate at these temperatures are shown in Table 16. Both designs lead to higher LCOS than the base case design at 150°C. Unlike CST-GeoTES, higher maximum temperatures do not clearly lead to better performance: although higher temperatures improve heat engine efficiency, they lead to reduced heat pump performance (of the coefficient of performance [COP]) due to the increased temperature lift required. Therefore, a balance must be struck between heat pump and heat engine performance. The system at 120°C has a reasonable COP but compromises heat engine performance (and also increases the number of wells due to low power densities), whereas the system at 170°C reduces efficiency by using a low heat pump COP.

**Table 16. Performance Details of Three Available Heat Pumps**Data from <https://heatpumpingtechnologies.org/annex58/task1/>

Parameter	Heat Pump 1	Heat Pump 2	Heat Pump 3
Manufacturer	MAN	Siemens	Turboden
Fluid	CO <sub>2</sub>	R1233zd(E)	R1233zd
COP	2.85	2.7	2.0
T <sub>sink, in</sub> , °C	50	60	104
T <sub>sink, out</sub> , °C	150	120	170

Another important consideration is the relative power rating of the heat pump compared to the heat engine. In the base case, the heat pump charging phase has the same duration as the heat engine discharging phase. Previous analysis has suggested that there are fewer low-price electricity hours available than high price (Martinek et al., 2022). Therefore, it may be advantageous to increase the power rating of the heat pump so that it can charge the system in less time and take advantage of reduced electricity prices. Figure 33 shows that doubling the heat pump power rating leads to a higher LCOS, which is due to higher heat pump costs and more wells to put the increased thermal power into the GeoTES. The figure also illustrates a scenario where the heat pump rate is doubled but the charging electricity cost is reduced to 0.01 \$/kWh<sub>e</sub> as a result of being able to charge more frequently at low-price times. In this case, the LCOS reduces substantially. This further emphasizes the need for detailed market analysis to understand the spread of available prices—and how they may change in future years. This is particularly important if arbitrage is intended as a major source of revenue.

An alternative CB-GeoTES system could deliver industrial process heat rather than electricity. Due to the use of a heat pump, this concept is more efficient than converting excess grid electricity to heat using an electric heater. The LCOH is calculated using the same system costs as previously used, although without the heat engine cost, and considering the thermal energy extracted from the GeoTES rather than its conversion to electricity. A tornado plot showing sensitivity to the system design is shown in Figure 34, which shows similar trends to the LCOS tornado chart. LCOH in the range of 0.01–0.03 \$/kWh<sub>th</sub> are achieved depending on the average electricity purchase price. For reference, the average annual price of natural gas in Texas in 2022–2024 ranged from 0.009–0.022 \$/kWh<sub>th</sub>, while the Henry Hub price was 0.007–0.022 \$/kWh<sub>th</sub> (U.S. Energy Information Administration, 2023).

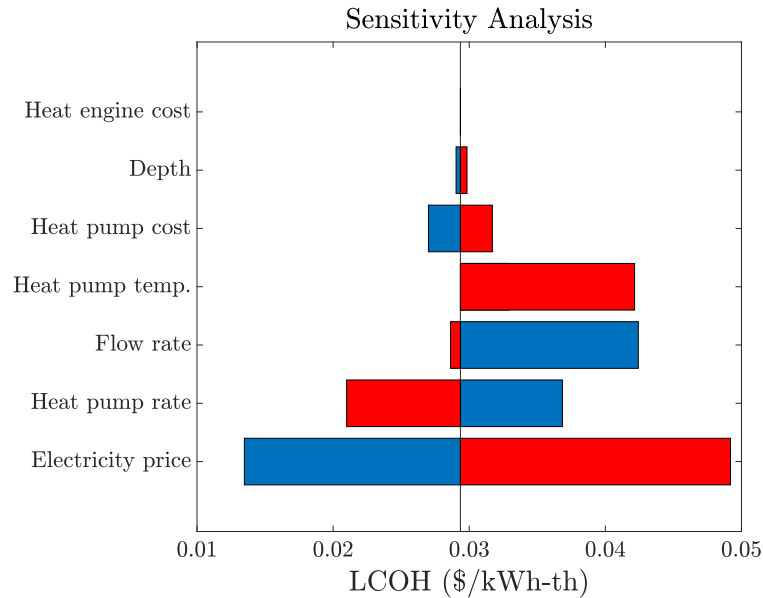


**Figure 34. Tornado chart illustrating sensitivity of CB-GeoTES LCOH to design parameters**

### 5.6.3 CB-GeoTES LCOS as a Function of Discharge Duration

Following the work described in Section 4.6.3, the LCOS of CB-GeoTES may also be calculated as a function of storage duration and efficiency. In this case, the CB design using hot and cold storage is considered, and results are shown in Figure 35. The LCOS of Li-ion batteries and MS- TES are also shown, as described in Section 4.6.3. Shaded areas indicate the effect of efficiency, with lower efficiency leading to higher LCOS. For CB-GeoTES, the round-trip efficiency is varied between 20.0% and 54.8% to generate these curves. The curves follow the same shape as those in Section 4.6.3, whereby the LCOS reduces up to storage durations of 12 hours. For CB-GeoTES, the LCOS then remains constant for longer storage durations, indicating that the capital cost does not increase with discharge duration. However, the LCOS of Li-ion and MS- TES increases rapidly, and CB-GeoTES is considerably more competitive for seasonal storage applications. The uncertainty and assumptions behind these plots require further investigation.

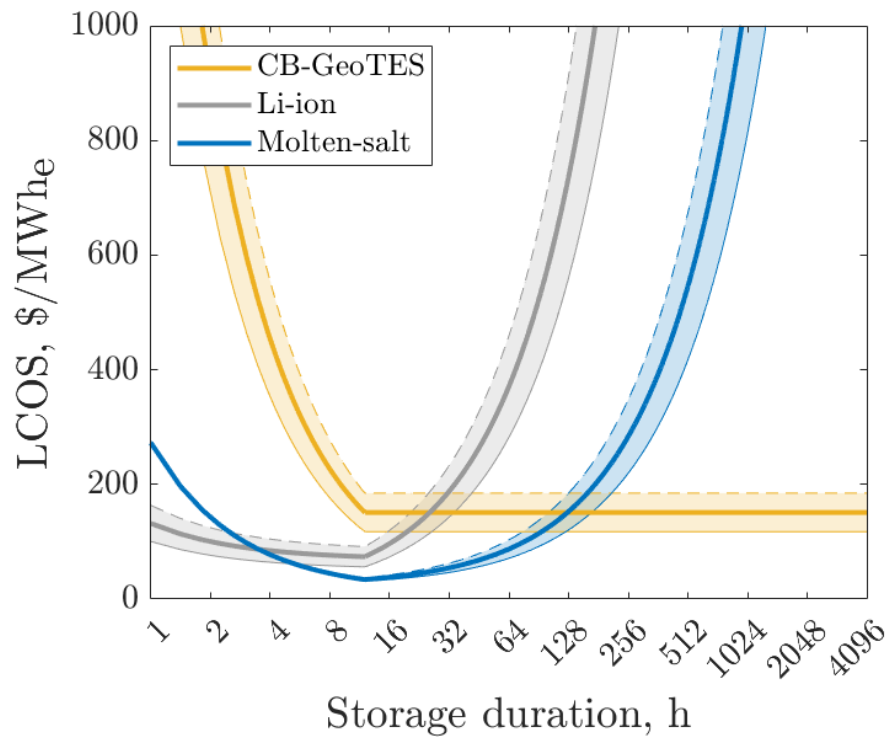


Figure 35. LCOS as a function of storage duration and efficiency for CB-GeoTES, Li-ion batteries, and MS-TES

## 6 Project Outcomes and Plan for Future Work

The GeoTES project involved extensive national lab and industry partnerships that facilitated the development of a TEA model that can predict GeoTES performance and cost for multiple system configurations and dispatch scenarios. In this section, we discuss the major outcomes of this project relative to project objectives and outline plans for future work.

### 6.1 Project Outcomes

We have developed an integrated TEA model that can be used to evaluate the initial viability of a proposed GeoTES design. The MATLAB-based model comprises several distinct subsystems (such as the reservoir, wells, power cycle, and solar field) that each require detailed modeling to capture their distinct characteristics. The model is capable of simulating GeoTES storage and dispatch operations for durations ranging from hourly to seasonal.

The TEA model outputs—such as thermal and electrical power/energy inflow and outflow, capital costs, and levelized costs of energy (i.e., electricity and heat) and storage—were validated against those of proposed industry demonstration projects for both CST-GeoTES and CB-GeoTES. For CST-GeoTES, the model was validated against the proposed system designed by PRM. It showed good agreement with PRM's estimations when well and pump costs derived from PRM's estimations were used. When GETEM-based costs were used, there was a slight overprediction due to GETEM's project/site agnostic assumption of these costs. From a sensitivity analysis perspective, the LCOE of the CST-GeoTES case is most sensitive to well flow rate and the charging temperature. An optimal design scenario was proposed with a CSP cost of 125 \$/m<sup>2</sup>, power block cost of 750 \$/kW<sub>e</sub>, solar multiple of 1.75, and a well flow rate of 80 L/s. This results in the LCOE reducing from a base case value of 0.22 \$/kWh<sub>e</sub> to 0.11 \$/kWh<sub>e</sub>. With 12-hour and 24-hour LCOH of 0.018 \$/kWh<sub>th</sub> and 0.022 \$/kWh<sub>th</sub>, respectively, CST-GeoTES could be competitive in the California market with an average industrial price of natural gas in California of 0.041–0.047 \$/kWh<sub>th</sub>. The LCOS for CST-GeoTES depends on the energy storage duration. Although the LCOS is relatively higher for shorter durations (e.g., ~0.50 \$/kWh<sub>e</sub> for 1 hour of storage), it is an order of magnitude lower (0.06 \$/kWh<sub>e</sub>) for longer storage durations and competitive with lithium-ion batteries (beyond 12 hours of storage) and MS-TES (beyond 32 hours).

The CB-GeoTES model was validated against the proposed design developed by EarthBridge Energy. Three options were explored and applied to the EarthBridge case study: (1) a CB design using R125 working fluid with both hot and cold storage; (2) a CB design using R125 working fluid with only hot storage; and (3) a CB using a commercially available heat pump with CO<sub>2</sub> working fluid and hot storage only. The CB-GeoTES with cold storage only had a slight (round-trip) efficiency advantage over the system without (43.4% vs. 42.8%). This is because the cold storage is limited by the freezing point of water, so the cold storage is not much colder than the environment. The system using commercially available technologies was the least efficient—partly because different cycles were used in the heat pump (CO<sub>2</sub>) and heat engine (binary cycle) which leads to some inefficiencies. Using the commercially available design, the LCOS from the model was higher than that estimated by EarthBridge (0.10 \$/kWh<sub>e</sub> vs 0.068 \$/kWh<sub>e</sub>). This is because of the low round-trip (38.7%) efficiency of the commercially available design. Sensitivity analysis reveals that the model is most sensitive to electricity price. Including



electricity price in the TEA for CB-GeoTES leads to an increase in LCOS from the base value to 0.25 \$/kWh<sub>e</sub>.

To determine storage sites suitable for GeoTES, we gathered and analyzed geological, petrophysical, and geophysical data of oil and gas reservoirs and aquifers in California and Texas. Our primary focus was on depleted oil and gas fields that have surpassed their economic life and shallow brackish aquifers unsuitable for potable water use. We down-selected possible sites based on cut-off values for site characteristics (e.g., reservoir temperature, formation thickness, permeability, porosity, depth, and brine salinity) and preliminary costs. Using this approach, the Carrizo-Wilcox, Yegua-Jackson, and Dockum brackish aquifers in Texas were identified as having the highest suitability. Similarly, in the central California region, the White Wolf, Belridge South Tulare, and Belridge South Reef Ridge were the most suitable. We went a step further to evaluate the storage potential in the selected sites. The Carrizo-Wilcox aquifer had the highest storage potential with a mean capacity of 554 TWh<sub>th</sub> (i.e., 63 TWh<sub>e</sub>). The estimated capacity serves as an upper limit of storage potential given that not all fields in the basin will be developed.

Over the course of the project, the team was involved in multiple outreach activities including conference presentations, panel discussions, and the facilitation of a GeoTES workshop. These forums were used as platforms to gauge industry knowledge and perspectives on the technical and commercial aspects of developing GeoTES and share our ongoing work on GeoTES technology assessment. Overall, the team received helpful questions and feedback from experts within the geothermal and oil and gas industries. The feedback has shaped our analysis and also provided potential areas for future research.

## 6.2 Suggestions for Future Work

Although this project covered both TEA and resource potential estimation of GeoTES, follow-on work would be beneficial to industry and exploration of multiple use cases (electricity and industrial heat). The suggestions, although not exhaustive, are geared toward efficiency improvements and life cycle cost savings. The following opportunities have been discussed.

1. Risk mitigation for commercial deployment of GeoTES systems. The deployment barriers of GeoTES may include not only technical challenges, but also non-technical issues such as local state policies. To address this, the mitigation strategies would include developing demonstration projects, compiling lessons learned and best practices, and disseminating information to the public.
2. Justify the value of GeoTES to future decarbonized grids and other energy sectors in various scenarios that may have different combination of renewable technologies and storage technologies for different regions in the United States. Right now, the value of GeoTES with respect to its flexible dispatching capabilities up to seasonal scale has not been properly recognized.
3. Assess the potential of GeoTES to future energy decarbonization. GeoTES can be a pure storage technology and a dispatchable technology combining generation and storage. The effort may include initial screening and exploration of suitable reservoirs for GeoTES deployment and assessing its value to the national grid and local economy.

4. Address technical barriers of GeoTES with innovative RD efforts:
- a) **Alternative power cycle for CB-GeoTES:** This includes alternative Brayton cycles (supercritical versus transcritical CO<sub>2</sub>), working fluids that have better thermal properties than CO<sub>2</sub> to improve heat withdrawal and rejection. The selection of the cycle and working fluid may be temperature dependent (e.g., transcritical cycles are more suitable for low-temperature applications). Additional process equipment within the power cycle have also been discussed including an adsorption chiller to further cool down the warm brine exiting the heat engine during discharge operations.
  - b) **Value of cold storage:** Cold storage is necessary to maximize energy conversion efficiencies. However, it introduces the need for an additional subsurface reservoir (or, at best, an enormous single reservoir) and additional well pairs. On the other hand, cold storage could have a value in district cooling applications during summer months. At the industrial scale, cold storage could also find essential value in decarbonizing data center operations requiring MW-scale cooling demand per site as reported by Zhang et al. (2024). These benefits relative to additional field development costs should be evaluated.
  - c) **Number of well pairs:** The team has discussed two and three well pairs to save on drilling costs. EarthBridge’s original design has a three-well system with a co-mingled flow of the warm and tepid brine going into a water sourcing reservoir (the far side of the deep reservoir). Suggested design scenarios include:
    - Three-well cold storage with mixing of heat engine output of hot and cold to arrive back at starting source (original reservoir) temperature.
    - Three-well cold storage with air cooling to maintain injection temperature at starting temperature.
    - Hot only system (with heat engine).
    - Cold only system (without heat engine).
  - d) **Higher-temperature storage:** The team has discussed the ability to charge the hot reservoir to higher temperatures (>200°C). This needs to be evaluated from a reservoir property and materials perspective. Since the native reservoirs are usually less than 100°C before GeoTES, charging sedimentary formations to these higher temperatures may result in significant changes in the mechanical properties of the rock grains as well as alteration of brine geochemical properties. These issues would need to be verified by further experimentation and coupled thermal-hydrologic-mechanical-chemical reservoir modeling of the system.
  - e) **Reduction in parasitic pumping:** Due to the very high flow rates needed for charge and discharge operations, pumping costs are a significant part of the GeoTES cost profile. Savings could be derived from the use of regenerative turbine pumps that harness the high-pressure discharge capabilities of positive displacement pumps and the flexibility of centrifugal pumps. These will be appropriate as injection pumps to take advantage of the additional potential energy.

- f) **Power cycle efficiency consideration:** Consideration of double flash system like in conventional geothermal if temperatures are above 200°C. This could lead to some efficiency gain; however, evaporative water loss during cooling (depending on whether it is wet or dry cooled) before reinjection could also arise. Another design consideration, suggested by Kevin Kitz from geothermal engineering consulting company Kitworks, is the recovery of cooling tower water for reinjection.
  
- g) **Geochemical analysis:** There is a need to experimentally determine the geochemical interaction of chemical species that are exchanged between the rock matrix and the fluids in the pores and fractures during GeoTES. This analysis can help determine the influence of GeoTES-induced temperature cycling on the chemical and mechanical properties of the storage formation and the overlying/underlying formations. It will also help in predicting the onset of performance inhibiting phenomena such as precipitation-induced plugging, souring, scaling, and subsidence.

## References

- Atkinson, T., Ginosar, D., Adhikari, B., Toman, J., & Podgorney, J. (2023). *Reservoir Thermal Energy Storage Benchmarking* (Technical Report 22–69373). Idaho National Laboratory. <https://doi.org/10.2172/1997222>
- Bauer, J., Rowan, C., Barkhurst, A., Digiulio, J., Jones, K., Sabbatino, M., Rose, K., & Wingo, P. (2018). *NATCARB* [Dataset]. National Energy Technology Laboratory - Energy Data eXchange; NETL. <https://doi.org/10.18141/1474110>
- Berger, E., Lawrence, F., Umbro, M., Harness, P., & Lederhos, J. (2023, August 15). *Geothermal Energy Storage (Geo-TES) Using Traditional Oil Reservoirs*. SPE Energy Transition Symposium. <https://doi.org/10.2118/215726-MS>
- Bloemendal, M., & Hartog, N. (2018). Analysis of the impact of storage conditions on the thermal recovery efficiency of low-temperature ATEs systems. *Geothermics*, *71*, 306–319. <https://doi.org/10.1016/j.geothermics.2017.10.009>
- Bradley, H. B. (1987). Properties of Produced Waters. In *Petroleum engineering handbook*. Society of Petroleum Engineers, Richardson, TX. <https://www.osti.gov/biblio/5929149>
- Burns, E. R., Bershaw, J., Williams, C. F., Wells, R., Uddenberg, M., Scanlon, D., Cladouhos, T., & van Houten, B. (2020). Using saline or brackish aquifers as reservoirs for thermal energy storage, with example calculations for direct-use heating in the Portland Basin, Oregon, USA. *Geothermics*, *88*, 101877. <https://doi.org/10.1016/j.geothermics.2020.101877>
- CalGEM. (n.d.). *WellSTAR* (Version R5.1.12.1) [Computer software]. California Geologic Energy Management Division. <https://wellstar-public.conservation.ca.gov/General/Home/PublicLanding>

California Department of Conservation & Division of Oil, Gas, and Geothermal Resources. (1998). *California Oil & Gas Fields—Central California* (CD-1; p. 499). California Department of Oil and Gas Division of Oil, Gas, and Geothermal Resources.

California ISO. (2020). *What the duck curve tells us about managing a green grid*. California ISO. [https://www.caiso.com/documents/flexibleresourceshelprenewables\\_fastfacts.pdf](https://www.caiso.com/documents/flexibleresourceshelprenewables_fastfacts.pdf)

Charpentier, R. R., & Klett, T. R. (2005). Guiding Principles of USGS Methodology for Assessment of Undiscovered Conventional Oil and Gas Resources. *Natural Resources Research*, 14(3), 175–186. <https://doi.org/10.1007/s11053-005-8075-1>

Coleman Jr., J. L., & Cahan, S. M. (2012). *Preliminary catalog of the sedimentary basins of the United States* (Report 2012–1111; Open-File Report, p. 31). USGS Publications Warehouse. <https://doi.org/10.3133/ofr20121111>

CPUC. (2021, June 24). *CPUC Orders Clean Energy Procurement To Ensure Electric Grid Reliability*. California Public Utilities Commission - Press Release. <https://www.cpuc.ca.gov/news-and-updates/all-news/cpuc-orders-clean-energy-procurement-to-ensure-electric-grid-reliability>

Daniilidis, A., Mindel, J. E., De Oliveira Filho, F., & Guglielmetti, L. (2022). Techno-economic assessment and operational CO<sub>2</sub> emissions of High-Temperature Aquifer Thermal Energy Storage (HT-ATES) using demand-driven and subsurface-constrained dimensioning. *Energy*, 249, 123682. <https://doi.org/10.1016/j.energy.2022.123682>

DOE. (2024). *FY23 Solar-thermal Fuels and Thermal Energy Storage Via Concentrated Solar-thermal Energy Funding Program*. Energy.Gov. <https://www.energy.gov/eere/solar/fy23-solar-thermal-fuels-and-thermal-energy-storage-concentrated-solar-thermal-energy>

- Duke Energy. (2016). *Duke Energy customers surpass 1 terawatt-hour of energy savings through My Home Energy Report Program*. Duke Energy | News Center. <https://news.duke-energy.com/releases/duke-energy-customers-surpass-1-terawatt-of-energy-savings-through-my-home-energy-report-program>
- EarthBridge Energy. (n.d.). *Our Technology—The GeoBattery*. EarthBridge Energy. Retrieved June 6, 2024, from <https://www.earthbridgeenergy.com/ourtechnology>
- EIA. (2023, June 21). *As solar capacity grows, duck curves are getting deeper in California—U.S. Energy Information Administration (EIA)*. Today in Energy. <https://www.eia.gov/todayinenergy/detail.php?id=56880>
- Esposito, A., Porro, C., Augustine, C., & Roberts, B. (2012). *Estimate of the Geothermal Energy Resource in the Major Sedimentary Basins in the United States (Presentation)* (NREL/PR-6A20-56444). National Renewable Energy Lab. (NREL), Golden, CO (United States). <https://www.osti.gov/biblio/1052899>
- Faunt, C. C. (2017). *Groundwater Availability of the Central Valley Aquifer, California*. U.S. Geological Survey. <https://doi.org/10.5066/F79S1PX3>
- Fleuchaus, P., Godschalk, B., Stober, I., & Blum, P. (2018). Worldwide application of aquifer thermal energy storage – A review. *Renewable and Sustainable Energy Reviews*, 94, 861–876. <https://doi.org/10.1016/j.rser.2018.06.057>
- Glassley, W., Brown, E., Asquith, A., Lance, T., & Perez, G. (2013). Geothermal energy potential from oil fields in the Los Angeles Basin and co-located renewable resources. *Transactions - Geothermal Resources Council*, 37, 715–720.
- IPSEpro: Process Simulation and Heat Balance Software*. (2022). [Computer software]. SimTech. <https://www.simtechnology.com/cms/>



- Islam, M. T., Huda, N., Abdullah, A. B., & Saidur, R. (2018). A comprehensive review of state-of-the-art concentrating solar power (CSP) technologies: Current status and research trends. *Renewable and Sustainable Energy Reviews*, *91*, 987–1018.  
<https://doi.org/10.1016/j.rser.2018.04.097>
- Jin, W., Atkinson, T. A., Doughty, C., Neupane, G., Spycher, N., McLing, T. L., Dobson, P. F., Smith, R., & Podgorney, R. (2022). Machine-learning-assisted high-temperature reservoir thermal energy storage optimization. *Renewable Energy*, *197*, 384–397.  
<https://doi.org/10.1016/j.renene.2022.07.118>
- Kurup, P., & Turchi, C. (2015). Initial Investigation into the Potential of CSP Industrial Process Heat for the Southwest United States. *NREL Technical Report - NREL/TP-6A20-64709*.
- Martinek, J., Jorgenson, J., & McTigue, J. D. (2022). On the operational characteristics and economic value of pumped thermal energy storage. *Journal of Energy Storage*, *52*, 105005. <https://doi.org/10.1016/j.est.2022.105005>
- McMillan, C., Schoeneberger, C., Zhang, J., Kurup, P., Masanet, E., Margolis, R., Meyers, S., Bannister, M., Rosenlieb, E., & Xi, W. (2021). Opportunities for Solar Industrial Process Heat in the United States Opportunities for Solar Industrial Process Heat in the United States. *NREL Technical Report - NREL/TP-6A20-77760, January*.
- McTigue, J. D., Farres-Antunez, P., Neises, T., & White, A. (2020). Supercritical CO<sub>2</sub> Heat Pumps and Power Cycles for Concentrating Solar Power. *SolarPACES, December*.
- McTigue, J. D., Farres-Antunez, P., Sundarnath J, K., Markides, C. N., & White, A. J. (2022). Techno-economic analysis of recuperated Joule-Brayton pumped thermal energy storage. *Energy Conversion and Management*, *252*(115016).  
<https://doi.org/10.1016/j.enconman.2021.115016>

- McTigue, J. D., Zhu, G., Akindipe, D., & Wendt, D. (2023, October). *Geological Thermal Energy Storage Using Solar Thermal and Carnot Batteries: Techno-Economic Analysis*. GRC Transactions, Reno, Nevada.
- Mercangöz, M., Hemrle, J., Kaufmann, L., Z'Graggen, A., & Ohler, C. (2012). Electrothermal energy storage with transcritical CO<sub>2</sub> cycles. *Energy*, *45*(1), 407–415.  
<https://doi.org/10.1016/j.energy.2012.03.013>
- Meyer, J., Croskrey, A., Suydam, A., & Oort, N. (2020). *Brackish Groundwater in Aquifers of the Upper Coastal Plains, Central Texas* (385). Texas Water Development Board.  
[https://www.twdb.texas.gov/publications/reports/numbered\\_reports/doc/R385/R385\\_UCPC.pdf](https://www.twdb.texas.gov/publications/reports/numbered_reports/doc/R385/R385_UCPC.pdf)
- Morandin, M., Henchoz, S., & Mercangöz, M. (2011). Thermoelectric energy storage: A new type of large scale energy storage based on thermodynamic cycles. *World Engineers' Convention*.
- Nehring Associates Inc. (2012). *The significant oil and gas fields of the United States* [Dataset]. database available from Nehring Associates, Inc.
- Novotny, V., Basta, V., Smola, P., & Spale, J. (2022). Review of Carnot Battery Technology Commercial Development. *Energies*, *15*(2), 647. <https://doi.org/10.3390/en15020647>
- Olympios, A. V., McTigue, J. D., Farres-Antunez, P., Tafone, A., Romagnoli, A., Li, Y., Ding, Y., Steinmann, W.-D., Wang, L., Chen, H., & Markides, C. N. (2021). Progress and prospects of thermo-mechanical energy storage—A critical review. *Progress in Energy*, *3*(2), 022001. <https://doi.org/10.1088/2516-1083/abdbba>
- Parini, M., & Riedel, K. (2000). *Combining Probabilistic Volumetric and Numerical Simulation Approaches to Improve Estimates of Geothermal Resource Capacity* (World Geothermal

- Congress). Unocal Corp., Geothermal Technologies and Services.  
<https://www.geothermal-energy.org/pdf/IGAstandard/WGC/2000/R0891.PDF>
- Pepin, J. D., Burns, E. R., Dickinson, J. E., Duncan, L. L., Kuniandy, E. L., & Reeves, H. W. (2021). *National-Scale Reservoir Thermal Energy Storage Pre-Assessment for the United States*.
- Raade, J. (2022). *Seasonal Energy Storage: A Technical and Economic Framework*.
- Rothleder, M. (2022, March 16). *Our evolving grid | California ISO*. Energy Matters.  
<https://www.caiso.com/about/news/our-evolving-grid>
- Rubin, R., Kolker, A., Witter, E., & Levine, A. (2022). *GeoRePORT Protocol Volume VI: Resource Size Assessment Tool* (NREL/TP-5700-81820). National Renewable Energy Laboratory (NREL), Golden, CO (United States). <https://doi.org/10.2172/1864530>
- Scheirer, A. H. (2007). *Petroleum Systems and Geologic Assessment of Oil and Gas in the San Joaquin Basin Province, California*. U.S. Geological Survey.  
<https://pubs.usgs.gov/pp/pp1713/>
- Schill, E., Knauth, R., Xheni, G., & Bauer, F. (2024). DeepStor—Heat Cycling in the Deep and Medium-Deep Subsurface. *Proceedings, 49th Workshop on Geothermal Reservoir Engineering, 49*.  
<https://pangea.stanford.edu/ERE/db/GeoConf/papers/SGW/2024/Schill.pdf>
- Schmidt, O., Melchior, S., Hawkes, A., & Staffell, I. (2019). Projecting the Future Levelized Cost of Electricity Storage Technologies. *Joule*, 3(1), 81–100.  
<https://doi.org/10.1016/j.joule.2018.12.008>
- Sharan, P., Kitz, K., Wendt, D., McTigue, J., & Zhu, G. (2021). Using Concentrating Solar Power to Create a Geological Thermal Energy Reservoir for Seasonal Storage and

- Flexible Power Plant Operation. *Journal of Energy Resources Technology*, 143(1), 010906. <https://doi.org/10.1115/1.4047970>
- Short, W., & Packey, D. J. (1995). A Manual for the Economic Evaluation of Energy Efficiency and Renewable Energy Technologies. *NREL Technical Report NREL/TP-462-5173*, March.
- Stanton, J., Anning, D., Brown, C., Moore, R., McGuire, V., Qi, S., Harris, A., Dennehy, K., McMahon, P., Degnan, J., & Bohlke, J. (2017). *Brackish Groundwater in the United States* (Professional Paper 1833). U.S. Geological Survey. <https://doi.org/10.3133/pp1833>
- Stricker, K., Grimmer, J. C., Egert, R., Bremer, J., Korzani, M. G., Schill, E., & Kohl, T. (2020). The Potential of Depleted Oil Reservoirs for High-Temperature Storage Systems. *Energies*, 13(24), Article 24. <https://doi.org/10.3390/en13246510>
- System Advisor Model (SAM)* (Version Version 2022.11.21). (2022). [Computer software]. National Renewable Energy Laboratory. [sam.nrel.gov](http://sam.nrel.gov)
- Texas Water Development Board. (2023). *BRACS Database* [Dataset]. <https://www.twdb.texas.gov/groundwater/bracs/database.asp>
- U.S. Energy Information Administration. (2023). *California Natural Gas Industrial Price*. <https://www.eia.gov/dnav/ng/hist/n3035ca3m.htm>
- USGS Geologic CO2 Storage Resources Assessment Team. (2013). *National assessment of geologic carbon dioxide storage resources—Results* (Version 1.1) [Dataset]. <http://pubs.usgs.gov/circ/1386/>
- Williams, C., Reed, M., & Manner, R. (2008). *A Review of Methods Applied by the U.S. Geological Survey in the Assessment of Identified Geothermal Resources* (1296). U.S. Geological Survey.

Zarrouk, S. J., & Moon, H. (2014). Efficiency of geothermal power plants: A worldwide review.

*Geothermics*, 51, 142–153. <https://doi.org/10.1016/j.geothermics.2013.11.001>

Zhang, Y., Peng, P., Sartor, D., Dobson, P., Jin, W., Atkinson, T., Oh, H., Sickinger, D.,

Beckers, K., & Acero-Allard, D. (2024). *Data Centers and Subsurface Thermal Energy*

*Storage – Matching Data Center Cooling Needs with Recharging of Subsurface Thermal*

*Energy Storage* (Internal Technical Project Report Internal Technical Project Report).

## Appendix A. Outreach Activities for GeoTES

During this project, the GeoTES team has participated in several outreach activities within and outside the geothermal community. This has created better awareness of this technology. During these events, the team has also received notable feedback from both geothermal and oil and gas stakeholders on implementation challenges and areas for further research. This section discusses the six outreach events in which the team participated.

### A.1 Geothermal Transition Summit—May 2023

The team attended the maiden Geothermal Transition Summit held in Houston, Texas, from May 23, 2023, to May 24, 2023. Dayo Akindipe (NREL), Trevor Atkinson (INL), and Derek Adams (EarthBridge Energy) represented the GeoTES team. During the summit, Akindipe and Atkinson connected with oil and gas and geothermal experts and service providers to gauge their awareness of GeoTES as an energy transition technology. Awareness was generally low, as most of the conference was focused on next-generation geothermal power technologies. Although there were three sessions on oil and gas well repurposing, the use case was for geothermal power and heat production. Adams was a panelist in a session tagged “Service Provider Led Collaboration.” Adams and co-panelists discussed how service providers can encourage cooperation with both geothermal and oil and gas operators to bridge supply chain challenges and ultimately capitalize on geothermal potential. They also discussed solutions for tackling supply chain gaps in the geothermal industry.

### A.2 Society of Petroleum Engineers Energy Transition Symposium—August 2023

Our team presented two papers at the inaugural Society of Petroleum Engineers Energy Transition Symposium in Houston, Texas (Aug. 22–23, 2023), and one of our industrial partners gave a lightning presentation describing their project. Pat Dobson (LBNL) gave a talk titled “Hybrid Uses of High-Temperature Reservoir Thermal Energy Storage: Lessons Learned From Previous Projects.” Following his presentation, the audience posed the following questions:

- What type of site characterization is needed?
- What are the thermal energy storage efficiencies?
- How can you characterize the heat loss of the system?
- Do national labs collaborate with industry and academia?

Guangdong Zhu (NREL) gave the next talk, “Techno-economic Analysis and Market Potential of Geologic Thermal Energy Storage (GeoTES) Charged With Solar Thermal and Heat Pumps Into Depleted Oil/Gas Reservoirs and Shallow Reservoirs: A Technology Overview.” He received the following questions from the audience following his presentation:

- Why are depleted oil reservoirs preferable to aquifers? Existing wells may pose problems as leaks to the system. Aquifers may have fewer geochemical issues.



- What is the experience of sulfur-reducing bacteria at elevated temperature? Depleted oil reservoirs often have sulfur-reducing bacteria. What could be done to mitigate this?
- Are there any benefits to using a closed loop system? What are the trade-offs in terms of cost, capacity, water treatment, etc.?

During one of the breaks, the PRM team gave a lightning presentation on their project titled “Geothermal Energy Storage (GeoTES) Using Traditional Oil Reservoirs.” The main question posed to PRM was whether they have considered deploying their technology in states with lower permitting hurdles outside California.

Our team members had informal discussions with other attendees during the meeting, most of whom were from the oil and gas industry.

### **A.3 Geothermal Rising Conference—October 2023**

The team was well represented at the 2023 Geothermal Rising Conference in Reno, Nevada (Oct. 1–4, 2023). Attendees included national lab researchers from NREL (Guangdong Zhu, Dayo Akindipe, and Joshua McTigue) and LBNL (Ram Kumar, now INL), and our industry partners PRM (Mike Umbro and Jim Lederhos) and EarthBridge Energy (Derek Adams). Umbro was a panelist at the open plenary of the conference, where he discussed GeoTES as one of the mainstream “energy transition solutions.” Members of the team gave oral presentations on the completed GeoTES project research at the time. A total of four papers were presented by the team, including:

- “Geological Thermal Energy Storage Using Solar Thermal and Carnot Batteries: Techno-Economic Analysis” (presented by McTigue)
- “Thermo-Hydrological Modeling of Thermal Energy Storage in a Depleted Oil Reservoir” (presented by Kumar)
- “Geologic Thermal Energy Storage (GeoTES) Using Shallow Subsurface Aquifers” (presented by Kumar)
- “Geological/Geo Thermal Energy Storage (GeoTES) Using Traditional Oil Reservoirs” (presented by Umbro).

McTigue’s session fielded lots of questions from the audience. These questions are broadly classified into the following:

- Coupling GeoTES with an existing geothermal plant for flexible plant operation
- Reservoir dynamics during the early years of operation before attaining a steady state
- Intermediate power cycle option for CST-GeoTES to increase overall plant efficiency.

The major discussion points during Mike’s presentation were around the issue of delayed Underground Injection Control permitting in California for GeoTES projects due to an embargo on oil and gas production in the state.

#### **A.4 Stanford Geothermal Workshop—February 2024**

The 49th Stanford Geothermal Workshop was held at Stanford University, California from February 12, 2024, to February 14, 2024. At the workshop, Guangdong Zhu (NREL) presented a paper titled “Geological Thermal Energy Storage (GeoTES) Charged with Solar Thermal Technology Using Depleted Oil/Gas Reservoirs and Carnot-Battery Technique Using Shallow Reservoirs.” He described GeoTES as using depleted oil and gas reservoirs and shallow reservoirs as locations where hot water can be stored in the subsurface, providing high-capacity and long-duration energy storage systems. Our team evaluated two concepts: one involving using water heated by concentrated solar, and the other using a CB heat pump system to convert surplus electrical energy into hot water, and then to reconvert the stored hot water back into electricity when needed.

One of the questions raised by the audience related to how much stored heat would be lost to the surroundings during charging and storage. Guangdong noted that the heat loss would be proportional to the surface area of the reservoir, and for larger systems, this should be fairly small once the reservoir has been thermally charged and the neighboring wall rocks have been heated. An important recommendation made during the session was that it will be important for the project to secure the water rights associated with the reservoir, because this could be a significant economic barrier to success.

#### **A.5 NREL GeoTES Workshop—April 2024**

The team organized a [2-day workshop on GeoTES](#) at the NREL Golden, Colorado, campus from April 29, 2024, to April 30, 2024. At this workshop, attendees from industry, the U.S. Department of Energy Geothermal Technologies Office (DOE-GTO), and national labs converged to discuss progress on the GeoTES project and other underground energy storage projects funded by the U.S. Department of Energy (DOE).

##### **Day 1**

On the first day of the workshop, participants listened to presentations by Jeff Winick (DOE-GTO), Guangdong Zhu (NREL), Mike Umbro (PRM), Jim Lederhos (PRM), Derek Adams (EarthBridge), and Joshua McTigue (NREL). Their presentation slides can be found [here](#). The following important discussion points and questions were raised during each session:

##### ***GTO Vision and Portfolio on GeoTES and Geothermal Hybridization—Jeff Winick***

- Has the team looked at the distribution of storage durations that would be optimal? What kind of distribution of storage options are you looking at or think are necessary? How many kilowatt-hours can you store?
- What is the carbon profile of the grid at the time GeoTES is being used?
- At what scale will GeoTES operate?

### ***Initial Evaluation of the Needs of Seasonal Storage Towards 100% Grid Decarbonization—Guangdong Zhu***

- Transmission cost is a factor that we have not considered in the GeoTES project.
- Is there a state that has a better solution for this outside of California?
- Are you looking at future demand curves?
  - The main point here is that whatever technology you look into, you should meet that demand.
  - Wind and solar photovoltaics (PV) cannot dominate energy generation.
- I have wondered if California is already oversaturated with PV? Based on the current prices
- We keep hearing about how data centers are going to become bigger impact on the grid. What does that future demand look like?
  - Look at the competing problem from the demand side.

### ***Daily and Long-Duration Storage for CST Using Geological Thermal Energy Storage: Pilot Plant and Techno-economic Analysis—Mike Umbro and Jim Lederhos***

- Have you thought about coupling this with a water sourcing technology?
  - We have thought about this but have not done anything about it yet; it is definitely on the radar.
- Have you looked at other options to monetize the project? Citing a data center?
- Has anyone modeled thermal expansion and potential for subsidence or uplift?
- Once you reach the temperature, will the well be self-flowing?
  - Yes, but they are closed loop. We want 600 psi at the bottom and at the surface.
  - Turbine pumps tend to be a lot cheaper and last longer, so that is probably what we will go with, but electric submersible pumps are also being looked into.
- What's the power purchase agreement price?
  - It can range, depending on how much you finance.
- How do you justify to the public that this is a renewable project instead of an oil and gas project?

### ***GeoTES Hybridized With CSP—Joshua McTigue***

- Have you factored how the value of the systems will change with time?
  - We only looked at the electricity prices for a single year to look at the value and how it will compare to similar technologies.
- You end with more storage than you start with. Was that a buffer?
  - This is a dispatch decision; you would run the model and entirely compete against GeoTES.
  - The decision was to choose which hours or how many hours of the day for each season of the year, then run for multiple years to understand long-term effects.
  - This will produce two numbers: how much energy you did produce based on the price, or how much energy you could produce.
- Could you see how robust your system is based on specific data—such as rainy or cloudy days?

- Ramsgate (PRM’s project partner) has 20 years irradiance daily timeseries data that is integrated into the model.
- What were the range of depths you used?
  - 200–1000 meters
  - The target depth was 500 meters
  - Comes down to not only the drilling cost but also the pumping power
  - As you go deeper, permeability goes down.
- Do you know the permeability of your reservoir?
- Rate of 11 L per second that was based on the data that PRM provided—6,000 barrels per day. Do you see similar rates on production?
  - Yes, we will see similar rates on production.

***GeoBattery—Derek Adams***

- The apparently cheapest power in the world is utility scale. Does this tie with dedicated PV?
- What kind of inputs are you using for models?
- Where do you get your data from?
  - Most of it comes from the Texas Railroad Commission.

***Update on GeoTES Techno-Economic Analysis: Model and Results—Joshua McTigue***

- Why does the LCOS not include the energy discharged?
- What is the value of zero carbon power, delivered on demand when nothing else is available? No one will build more solar in California. Then in theory you create headroom that allows for more PV to be built. This is a very rich area for additional study.
- Have you compared this to storing other fuels such as natural gas?
- Maintaining supply delivery
  - Capacity payments, making sure you can deliver on the energy promised. However, you are not rewarded to the extent that you would think
  - Maybe there needs to be a real evaluation of resilience.
- Transmission congestion—You could look at deferring transmission.
- How do we figure out the value of very long-duration energy storage to the grid?

***Day 2***

On the second day of the workshop, participants discussed GeoTES reservoir characterization and site selection, challenges of GeoTES, GeoTES for data center heat recovery, and other NREL projects addressing subsurface thermal energy storage for heating and cooling applications. Presentation slides for Day 2 can be found [here](#). The presenters were: Trevor Atkinson (INL), Erik Witter (NREL), and Pat Dobson (LBNL). At the end of the day, all participants shared their reflections, takeaways, and recommendations for future work.

***Characterization Approach and Database for Oil/Gas Reservoirs and Brackish Aquifers in California and Texas—Trevor Atkinson and Erik Witter***

- When you did your down-selection, were there any sort of key parameters for selecting those fields?
  - The depth was a large component—as far as a cut-off on depth, we did not establish that.
- Did you ever look into regeneration of heat loss?
- What were the typical thicknesses of these basins?
  - 200–300 meters
- In terms of the usable area around the surface, do you see a limit on that and any issues?
  - This was very high level; we assumed that, up to the edges, these were full thickness.
- Groundwater flows is [are] the biggest risk when it comes to losing your heat.
- Is there concern with trying to use an old reservoir?

### ***Review of Past Challenges Encountered With High-Temperature GeoTES projects—Pat Dobson***

- Is there a way you can characterize the barriers into categories?
- It is a challenge to get everyone feeling comfortable that you have successfully de-risked your project.
  - You need to use data and modeling so that you can defend your project accurately.
- Has there been any work for or examples for other technologies that have subsurface-related things for this work? Have they looked at what the carbon storage looks like, or the permitting issues related to that?
  - DOE is funding a project related to this, but we have not seen a GeoTES project related to this.
- Has there been any attempt in setting up a testing site for this? Would DOE be interested in setting up a location for real pilot scale testing?

## **A.6 Geothermal Transition Summit—May 2024**

At the Geothermal Transition Summit in Houston, Texas (May 21–22, 2024), our team participated in a panel discussion titled “Geological Thermal Energy Storage (GeoTES) Technology Integration with Renewables for Transforming Oil and Gas Reservoirs.” The panelists were Guangdong Zhu (NREL), Trevor Atkinson (INL), Tatiana Pyatina (Brookhaven National Laboratory), Derek Adams (EarthBridge Energy), and Mike Umbro (PRM), and the panel was moderated by Patrick Dobson (LBNL). Guangdong Zhu kicked off the panel with a short description of GeoTES, which was then followed by a lively discussion. Here are some of the questions that were addressed by the panelists:

- Depleted oil and gas fields are potential targets for GeoTES development, given the abundant subsurface information available, the existing infrastructure, and the need to provide an energy and employment transition to those communities. What stakeholders need to be integrated to make these types of projects happen?
- For GeoTES to work, there needs to be three components of the project—a source of heat that can be stored, an underground reservoir to store the heat, and an offtaker who will

purchase the stored energy (either as thermal energy or electricity). What can be done to build these partnerships?

- Are there different drilling and well completion methods that could be used for GeoTES that could lower costs and make sure that the wells are resilient to thermal cycling? Would new well completion methods and cements help?
- What are the most important selection criteria for identifying a potential reservoir for GeoTES? What are the potential issues that might rule out a project? Would a site screening tool be helpful?
- What types of regulatory and permitting issues need to be addressed to facilitate GeoTES projects? Would it be helpful to educate regulatory agencies about GeoTES, given that it falls into multiple categories (geothermal, oil and gas, underground injection, etc.)?
- Would a pilot GeoTES demonstration project help in mitigating potential issues and demonstrating the commercial viability of this concept?
- Use of LCOS alone doesn't seem to capture all of the value of GeoTES (e.g., decarbonization, long-term storage, resilience, etc.) What additional ways could be used to make sure that the full value of GeoTES is realized when comparing it to other energy storage options?

The audience also posed some questions for the panel. These included:

- What are the risks associated with GeoTES?
- Where can GeoTES be deployed?